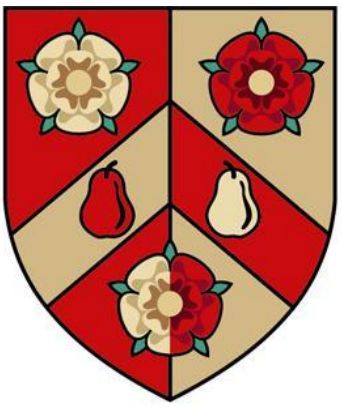
Engineering of a Third-Generation Chimeric Antigen Receptor with Specificity for HLA-A2 for Use in Regulatory T Cell Therapy



Sabrina Wright

Wolfson College

&

Transplant Research Immunology Group

Nuffield Department of Surgical Sciences

University of Oxford

Supervisors: Dr. Joanna Hester and Dr. Fadi Issa

Thesis submitted for M.Res. in Surgical Sciences in Michaelmas Term 2022

Abstract

Background

Current pharmacologic regimens of immunosuppression for allogeneic transplant recipients increase vulnerability to cancers and infections due to their systemic mode of action, in addition to side effects such as organ toxicity. Furthermore, daily medication regimens pose a significant burden to the patient. Cellular therapy has been proposed as an alternative, and clinical trials have shown promising results for the efficacy of regulatory T cells – a naturally-occurring subset of T cells responsible for maintaining immune homeostasis – for preventing graft rejection in kidney patients. Genetic engineering has led to the development of Chimeric Antigen Receptors (CARs); these are customizable receptors that can be expressed in therapeutic cells to confer specificity for an antigen of choice. Pre-clinical models have shown the superiority of CAR-expressing Tregs over polyclonal Tregs at preventing allograft rejection, as well as their preferential homing towards the target antigen, and it is envisaged that CAR-Tregs could replace standard drugs in the clinic.

Objectives

1. To critically review current applications of Green Fluorescent Protein (GFP) expression induction in cell therapies, with a focus on Tregs.
2. To evaluate induction of Green Fluorescent Protein expression in human Tregs on their function and molecular phenotype.
3. To critically review current approaches and outcomes of CAR-Treg adoptive therapy in pre-clinical and clinical studies.
4. To design and create a third-generation CAR with specificity for Human Leukocyte Antigen HLA-A2.

Findings

CRISPR-Cas9 mediated genome editing was used to insert a GFP homology-directed repair template into the RAB11A locus of sorted and *ex vivo*-expanded human Tregs, and proof-of-concept experiments with bulk $CD4^+$ T cells illustrated the longevity of GFP expression using this method. Editing efficiency was between 30 and 40%, and GFP-expressing Tregs were capable of suppressing effector $CD8^+$ T cells almost completely when delivered in ratios of 1:2 or 1:4. In addition, their gene expression and cytokine production (notably the anti-inflammatory cytokine IL-10) was comparable to that of unmodified Tregs.

Simultaneously, a Chimeric Antigen Receptor construct was designed and synthesized with an antigen-binding region specific to HLA-A2, then inserted into a pIRES2-eGFP expression vector.

Conclusion

Human Tregs do not lose their suppressive function upon the induction of GFP expression, and CARs hold potential for preventing allograft rejection in allogeneic transplantation.

Contents

1. Introduction 6

1.1. Regulatory T cells 6

1.1.1. Regulatory T cells in solid organ transplantation 7

1.2. Chimeric antigen receptors 10

1.3. Genetic manipulation of cells to improve function or *in vivo* tracking 11

1.4. Aims 12

2. Materials and methods 14

2.1. Isolation of BB7.2 scFv DNA from hybridoma monoclonal antibodies 14

2.1.1. Expansion of hybridomas 14

2.1.2. Thawing and culturing hybridomas 14

2.1.3. RNA extraction of hybridomas 15

2.1.4. Reverse transcription of BB7.2 RNA 15

2.2. PCR amplification of light and heavy scFv chains 15

2.2.1. BB7.2 heavy chain 16

2.2.2. BB7.2 light chain 17

2.2.3. PCR with high fidelity polymerase 17

2.3. TOPO® cloning to amplify heavy and light BB7.2 chains 18

2.4. Construction of the CAR sequence 20

2.5. Generation of GFP^+ human $CD4^+$ cells using CRISPR-Cas9 technology 22

2.5.1. Amplification of GFP-containing HDRT 22

2.5.2. Production of GFP^+ $CD4^+$ T cells using CRISPR-Cas9 24

2.5.3. Production of GFP^+ Tregs using CRISPR-Cas9 25

2.5.4. Suppression assay with GFP^+ Tregs: VPD analysis 27

2.5.5. Suppression assay with GFP^+ Tregs: gene and cytokine analysis 27

3. Green Fluorescent Protein: a literature review 30

3.1. Fluorescent proteins 30

3.2. Green Fluorescent Protein 30

3.3. Applications of GFP^+ cells 31

3.4. Sources of GFP^+ cells 32

3.4.1. Transgenic rodent strains 32

3.4.2. Electroporation 34

3.4.3. Viral delivery 35

3.4.4. Genome editing with CRISPR-Cas9 35

3.5. Risks of GFP expression in mammalian cells 36

3.6. GFP expression in regulatory T cells 37

4. Generation of GFP^+ human regulatory T cells 43

4.1. Generation of GFP^+ $CD4^+$ T cells as a proof of concept 43

4.2. Generation of GFP^+ human Tregs 45

4.3. Suppressive function of GFP^+ human Tregs 47

4.4. Molecular changes upon suppression by GFP^+ human Tregs 50

5. CAR-Tregs: a literature review 63

5.1. The clinical need for novel therapeutics in transplantation 63

5.2. Regulatory T cells as novel therapeutic agents 64

5.3. Engineered specificity for Tregs 65

5.4. Chimeric Antigen Receptors for engineered specificity 66

6. Construction of a third-generation CAR specific for HLA-A2 73

6.1. Isolation of BB7.2 scFv sequence from hybridomas 74

6.2. Construction of the HLA-A2-specific CAR 75

6.3. Insertion of the CAR into a pIRES2-eGFP expression plasmid 76

7. Conclusions and future directions 80

7.1. GFP expression as a research tool 80

7.2. Third-generation Chimeric Antigen Receptor expression in human Tregs 81

8. Appendices 83

8.1. Complete sequence of the BB7.2-specific CD28-CD27 CAR 83

8.2. Impact of COVID-19 on this thesis 83

9. Bibliography 84

1. Introduction

1.1. Regulatory T cells

The subset of lymphocytes known today as regulatory T cells, or Tregs, was first identified in a landmark paper by Sakaguchi *et al.* in 1995, who described them as bearing the surface marker signature $CD4^+CD25^+$.(Sakaguchi et al., 1995) These cells were found to be potent suppressors of the immune system, and depletion of the Treg subset in animal models led to exacerbated immune responses and the spontaneous development of autoimmunity.(Sakaguchi et al., 1995) Tregs are responsible for limiting the proinflammatory response towards alloantigens in order to prevent collateral damage to host tissue; they also maintain immune homeostasis under non-inflammatory conditions by promoting tolerance towards self-antigens. The transcription factor Forkhead Box P3 (FOXP3) drives expression and maintenance of the Treg phenotype, and is now considered to be another definitive marker of this subset.(Hori et al., 2003)

Tregs operate through an array of contact-dependent and -independent (soluble) mechanisms to modulate the immune environment; some of the major pathways shall be described here.

In a contact-dependent manner, they may directly interfere with the activation signals of dendritic cells (DCs) by engaging with the costimulatory molecules CD80 and CD86 via the Treg surface molecule CTLA-4; this induces the downregulation of CD80/86 on the cell surface of DCs, preventing DC-mediated co-stimulation of conventional T cells (Tconvs).(Onishi et al., 2008) Binding also triggers the release of a rate-limiting enzyme called indoleamine 2,3 dioxygenase (IDO), thereby increasing the concentration of tryptophan metabolites in the microenvironment, which in turn suppress cell cycle progression in Tconvs.(Mellor et al., 2003)

Alternatively, Tregs may act upon target cells by releasing soluble cytokines or cytolytic enzymes. The cytokine IL-10 is a key regulatory molecule with the capacity to inhibit Tconvs

from releasing proinflammatory cytokines and chemokines;(Schmidt et al., 2012) furthermore, IL-10 inhibits the expression of Class II Major Histocompatibility Complexes (MHCs) – the extracellular machinery used for antigen presentation – in DCs and other professional antigen-presenting cells.(Akkaya et al., 2019)

IL-35, although not constitutively expressed on human cells, is upregulated specifically during chronic activation of Tregs and has been demonstrated to directly inhibit the proliferation of Tconvs.(Schmidt et al., 2012)

TGF-β is another cytokine deeply intertwined with Treg function, being associated with induction of FOXP3 expression and the suppression of both B and T cell activity.(Nakamura et al., 2001) Membrane-bound TGF-β on the surface of Tregs has the additional role of instigating the *de novo* generation of Tregs from naïve T cell precursors to create infectious tolerance.(Andersson et al., 2008)

Granzyme B and perforin are expressed by Tregs to mediate the direct killing of target cells; they appear to work synergistically, Granzyme B entering the cell autonomously but requiring a signal from perforin for entry into the nucleus and initiation of apoptosis.(Grossman et al., 2004; Shi et al., 1997; D. M. Zhao et al., 2006)

Tregs are also known to disrupt the metabolic processes of proinflammatory cells through competition for critical resources such as IL-2 and other cytokines. In this way, proinflammatory cells are deprived of access to molecules required for survival, resulting in apoptosis.(Pandiyan et al., 2007)

Altogether, these mechanisms allow Tregs to manipulate their local microenvironment in order to control the immune response against self- and alloantigens.

1.1.1. Regulatory T cells in solid organ transplantation

Recent investigations into the possibility of harnessing the innate suppressive capacity of Tregs for clinical application have revealed huge potential for the treatment of

autoimmune diseases, inflammatory conditions, graft-versus-host disease (GvHD), and solid organ transplantation.(Field et al., 2001; Horwitz et al., 2002; Jones et al., 2003; Piccirillo et al., 2005) It was demonstrated that *ex vivo*-expanded polyclonal Tregs could prolong skin and islet allograft survival in humanized mouse models by decreasing infiltration of $CD4^+$ and $CD8^+$ effector T cells, prompting the question of whether these results could be replicated in human patients.(Issa et al., 2010; Wu et al., 2013) In the context of allogeneic transplantation, recipients will naturally mount an immune response against the donor organ, leading to the onset of organ rejection. Currently, this is managed by administering a trio of pharmacologic drugs to suppress the body's natural rejection response. While it cannot be emphasized enough that modern immunosuppression has transformed healthcare, the toxicity of these drugs poses a significant health risk for patients, such as by promoting cardiovascular complications;(Fellström, 2001) they also dramatically increase the risk of cancer and increase susceptibility to opportunistic infections.(Fishman, 2007; Mittal & Colegio, 2017) Many examples of toxicity can be attributed to the fact that the immunomodulatory effects of these drugs are systemic and not localised to the allotransplant. It is also worth emphasizing that the burden imposed on the patient by a daily regimen of medication can result in non-adherence, opening the gate for chronic rejection processes.

There have been intense research efforts into alternative forms of immunosuppression that reduce toxicity and medication burden, through which adoptive cell transfer (ACT) has emerged as a promising candidate. Theoretically, by infusing *ex vivo* expanded Tregs into a transplant recipient, the increased ratio of Tregs to Tconvs induces suppression of the immune system and prevents allogeneic organ rejection by the patient.

After initial murine studies supported the efficacy of polyclonal Treg infusion for the prevention of allograft rejection, the first clinical trials in humans were approved.(Mathew et al., 2018; Sawitzki et al., 2020) The results of Mathew *et al.* were obtained from a trial

involving nine recipients of living donor kidney allografts who received autologous Tregs at two months post-transplantation, following lymphocyte depletion; Tregs were given in combination with mycophenolate mofetil (MMF) and sirolimus maintenance therapy. Mathew *et al.* reported no serious adverse events related to Treg infusion, and no symptoms of opportunistic infection were observed. Two years post-transplantation, the authors observed 100% graft survival. A separate investigation named The ONE Study, involving an international consortium of researchers, took a more radical approach and trialled the possibility of reducing pharmacologic suppression down to a monotherapy after Treg infusion. Recipients were initially administered with triple therapy (prednisolone, MMF, and tacrolimus) before receiving an infusion of autologous Tregs at five days post-transplantation.(Sawitzki et al., 2020) Remarkably, 15 out of the 38 patients who completed the observation period of 60 weeks had been successfully weaned onto tacrolimus monotherapy without rejection; furthermore, they experienced fewer incidents of viral infection compared to control patients on standard therapy.(Sawitzki et al., 2020) Together, these findings suggest that adoptive transfer of Tregs is not only a promising alternative for preventing organ rejection, but is also associated with reduced systemic suppression of anti-pathogen responses, resulting in fewer opportunistic infections. Previously published data suggested that polyclonal Tregs may remain detectable in the body for over one year, drastically reducing the number of required infusions and therefore the medication burden for the patient – presenting another advantage over conventional immunosuppressants.(Bluestone et al., 2015)

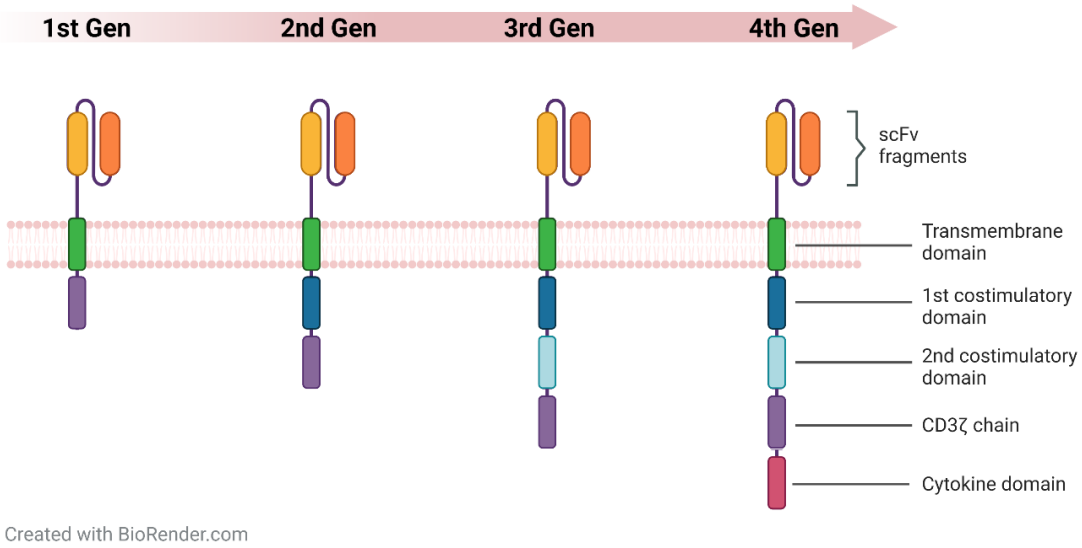
Finally, the intrinsic autonomy of cells, expressed through their ability to interact with other cell types, proliferate *in vivo*, and suppress through a variety of mechanisms depending on the context of their microenvironment, renders Tregs superior to traditional forms of immunosuppressive therapy.

1.2. Chimeric Antigen Receptors

While cellular therapy circumvents many of the toxicities associated with traditional drugs, the risk remains that polyclonal cell therapy may still restrain patients' capacity to respond to threats of pathogenic infection and cancer, owing to the presence of many T Cell receptor (TCR) specificities within the cell population. It is therefore envisaged that localised, antigen-specific therapy will one day replace systemic immunosuppression following allogeneic transplantation.

Experimentation with different techniques to confer antigen specificity to cells resulted in the first chimeric antigen receptor (CAR) in 1989 by Gross and colleagues.(Gross et al., 1989) Their synthetic receptor combined the variable and constant domains of an anti-2,4,6-trinitrophenyl antibody to a portion of either an α or β TCR chain, and the resulting construct was transfected into a T cell hybridoma line. CARs have since been engineered into a variety of cell types, including conventional $CD4^+$ T cells (Tconvs), $CD8^+$ T cells, NK cells, and Tregs.(Elinav et al., 2008; McGuinness et al., 2004; Müller et al., 2008) The "first-generation" CARs did not include a costimulatory domain and therefore showed limited persistence.(Kowolik et al., 2006) Subsequent improvements to the original design have focused on augmenting longevity and functionality by adding costimulatory domains (to allow for full cellular activation) and cytokine sequences (for additional effector function), as illustrated in Figure 1.

Figure 1. Evolution of the CAR design.



Early applications of CARs were invariably in the field of oncology, where they demonstrated exceptional efficacy in the treatment of relapsed and refractory cancer where other modes of treatment had been unsuccessful. Their therapeutic success in animal models, and later in clinical trials, led to the approval of two independent CAR-based therapies for clinical use by the US Food and Drug Administration (FDA) and the European Medicines Agency (EMA).(Hayden et al., 2019) More recently, the experimental application of CARs has been extended to their expression in Tregs for pre-clinical treatment of autoimmune and inflammatory diseases, GvHD, and solid organ transplantation. Notably, CAR-Tregs have shown superiority over their polyclonal counterparts in murine models of transplantation at suppressing disease severity and graft rejection.(Boardman et al., 2017; MacDonald et al., 2016) I will critically assess current CAR-Treg designs in Chapter 4.

1.3. Genetic manipulation of cells to improve function or *in vivo* tracking

Genetic modification of cells may be achieved through viral delivery, CRISPR, transfection, and other methods, each with their own advantages and disadvantages that will be discussed in due course.

Genetic modification may involve knocking out the gene encoding a cell product that is detrimental to therapeutic success – for example, researchers have previously generated a knockout of glucocorticoid receptor in virus-specific T cells to allow for infusion in immunosuppressed patients;(Kaeuferle et al., 2020) or knockout of MHC in adoptively transferred cells to avoid detection in an allogenic host.(Deuse et al., 2019) Alternatively, genes may be inserted to enhance or add to the existing functionality of the cell – for example, conferring cytokine expression to a cell, or redirecting the cell specificity to a target tissue.(G. P. Wright et al., 2009)

Cells may also be genetically manipulated to express a protein marker for identification and sorting, such as the peptide tag Myc. An adaptation of this technique is used for fluorescence labelling: cells can be engineered to express fluorescent protein under the control of an ubiquitous or tissue-specific promoter, meaning that the user can conveniently isolate and visualize cells using FACS and fluorescence microscopy without the need for antibody staining.

However, the possibilities of gene editing in cells are so vast that it would be impossible to summarize them succinctly; it is up to researchers to selectively apply gene editing to produce optimal cellular products for their research purpose.

1.4. Aims

This project focuses on the advancement of Treg cellular therapies by exploring their improved detection using an integrated fluorescent marker, as well as the development and critical assessment of CAR-Treg adoptive transfer therapy.

The specific aims of this research project were:

a) To critically review current applications of Green Fluorescent Protein (GFP) expression induction in cell therapies, with a focus on Tregs. (Chapter 3)

b) To evaluate induction of Green Fluorescent Protein expression in human Tregs on their function and molecular phenotype. (Chapter 4)

c) To critically review current approaches and outcomes of CAR Treg adoptive therapy in pre-clinical and clinical studies. (Chapter 5)

d) To design and create a third-generation CAR with specificity for the human leukocyte antigen HLA-A2. (Chapter 6)

Based on data from the existing literature, it was hypothesised that GFP could be efficiently induced in expanded human Tregs for fluorescence detection, and that this could be achieved using CRISPR-Cas9 technology; that gene editing efficiency could produce GFP expression in approximately 20-40% of target cells*;* and the transgenic cells could be detected for at least two weeks after *in vitro* culture.(Roth et al., 2018; Z. Zhang et al., 2018)

HLA-A2 was chosen as a suitable target partly because of its history in CAR-Treg studies in allogeneic transplantation models.(Boardman et al., 2017; MacDonald et al., 2016; Noyan et al., 2017) HLA-A2 is an allele of Class I Major Histocompatibility Complex (MHC) and is expressed in an estimated 25-41% of people worldwide.(Chen et al., 2012; Saito et al., 2016) This means that therapeutic strategies targeting HLA-A2 are applicable to a large proportion of the global population, and this renders an anti-HLA-A2 CAR design extremely relevant.

2. Materials and methods

2.1. Isolation of BB7.2 scFv DNA from hybridoma monoclonal antibodies

2.1.1. Expansion of hybridomas

Clone BB7.2 hybridomas (with antigen specificity for HLA-A2) were obtained from Alastair Waugh (Human Immunology Unit) for the purpose of isolating the DNA sequence from the variable region of its monoclonal antibody. The hybridoma culture had tested negative for mycoplasma contamination using the Lucetta and Hoescht methods. The hybridomas were cultured in 75cm^2 Corning flasks in RPMI-1640 medium supplemented with 10% FBS, 1% penicillin/streptomycin, and 1% L-glutamine. After 2 days of expansion, hybridoma cultures were split and diluted 1:5 with fresh medium as described. After 3 more days of expansion (5 days total), hybridomas were frozen at -80^{o}C in a freezing medium consisting of 10% dimethyl sulfoxide (DMSO), 90% FBS, at a cell density of 3 x 10^6 cells/mL. After 24 hours, cells were transferred from -80^{o}C to liquid nitrogen (LN) storage.

2.1.2. Thawing and culturing hybridomas

For expansion, hybridomas were thawed according to standard protocol. Hybridomas should be maintained at a density of between 1 x 10^5 and 1 x 10^6 cells per mL; therefore, cultures were established at a density of 2 x 10^5 to allow for growth. Hybridomas were expanded in 7 mL of medium inside a 25cm^2 Corning flask at 37^{o}C. This time, the medium contained 20% FBS as recommended for hybridomas immediately after thawing. The cell culture was split 1:1 on Day 3, each flask receiving fresh 20% FBS medium. Cultures were split 1:1 again on Day 5 and fed with 20% FBS medium. On Day 9, hybridomas were split 1:3, this time weaning the FBS composition of culture medium down to 10%. Hybridomas were harvested after 14 days by gentle resuspension in their growth medium by pipetting, then transferred into Falcon tubes and centrifuged for 5 minutes at 520 rcf, 4^{o}C.

Supernatant was removed and the cell pellet resuspended with fresh medium. After a cell count, 1 x 10^7 hybridomas were divided between two Eppendorf tubes, washed with PBS and centrifuged for 5 minutes at 520 rcf, 4^{o}C. The supernatant was removed with a pipette. The hybridoma pellets were immediately frozen at -80^{o}C without freezing medium in preparation for RNA isolation.

2.1.3. RNA extraction of hybridomas

Frozen hybridoma cell pellets underwent RNA extraction using the RNeasy Mini Kit (Qiagen, Cat. No. 74104) according to instructions. A final elution volume of 70 µL was obtained. RNA was then quantified with NanoDrop (Thermo Scientific).

Gel electrophoresis was performed to confirm the presence of quality hybridoma RNA (i.e. undegraded). Hybridoma RNA was run on a 1.5% agarose gel using 10x SYBR Safe DNA Gel Stain (Invitrogen, Cat. No. S33102) at 60 volts for 30 minutes. The following ladders were used:

HyperLadder^{TM} 100bp (Bioline, Cat: BIO-33056)

GeneRuler 1 kb Plus DNA Ladder (Thermo Scientific, Cat: SM1333)

A Bio-Rad Gel Doc EZ Imager was then used to visualise the RNA band within the gel, to confirm that RNA was indeed present.

2.1.4. Reverse transcription of BB7.2 RNA

Eluted RNA obtained with the RNeasy Mini Kit was processed with a High-Capacity cDNA Reverse Transcription Kit (Applied Biosystems, Cat: 4368814) according to instructions.

2.2. PCR amplification of light and heavy scFV chains

A selection of putative primers with known sequences specific for the light (VL) and heavy (VH) chains of the BB7.2 variable region were tested to identify the correct combination of candidates. The light and heavy chains of the BB7.2 variable fragment have previously been found to have a size of approximately 300 base pairs (Demin Li, personal communication). Through a Polymerase Chain Reaction (PCR), the correct primers could be identified by the presence of a strongly fluorescent band of appropriate size when PCR reactions were visualised through gel electrophoresis. Therefore, the DNA samples obtained through reverse transcription were loaded into a thermocycler with the following conditions:

Program Stage	Temperature	Duration
1. Initial denaturation	96°C	5 minutes
2. Denaturation	96°C	30 seconds
3. Annealing	67°C*	1 minute
4. Extension	72°C	1 minute
5. Cycling (repeat of steps 2-4, 29x)	-	-
6. Final extension	72°C	10 minutes
7. Cooling	4°C	∞

*67°C was determined as the optimal anneal temperature after testing the pooled primers in different temperatures.

2.2.1. BB7.2 heavy chain

Three separate reactions were created using pools of four putative forward primers each, and one known reverse primer, as follows:

1. Forward primers: DLP83, DLP84, DLP85, DLP86. Reverse primer: DLP95.
2. Forward primers: DLP87, DLP88, DLP89, DLP90. Reverse primer: DLP95.
3. Forward primers: DLP91, DLP92, DLP93, DLP94. Reverse primer: DLP95.

Primers were pooled in this manner initially to reduce the number of reactions needed. After one reaction gave a positive result, the forward primers within that reaction were

tested individually. PCR was performed using the Biotaq™ DNA Polymerase Kit (Bioline, Cat: BIO-21040) according to instructions. The PCR products of the pooled primer reactions were loaded onto a 1.5% agarose gel of 0.5x TBE and run at 60 volts for 1.5 hours to allow for greater separation of DNA fragments. Forward primer DLP85 was deemed to be the best candidate.

2.2.2. BB7.2 light chain

The PCR and gel electrophoresis protocols for identifying the correct heavy chain primers, and generating the correct DNA product for the heavy chain, were applied to the light chain. In this case, the panel of putative forward primers consisted of DLP96-DLP105 and known reverse primer DLP106. Forward primer DLP96 was deemed to be the best candidate.

2.2.3. PCR with high fidelity polymerase

Sequences for the selected forward (and reverse) primers are given below:

Primer Name	Sequence	Length (bp)
VH Forward Primer DLP85	CAGGTGCAGCTGAAGCAGTC	20
VH Reverse Primer DLP95	GCCAGTGGATAGTCAGATGGGGGTGTCGTTTTGGC	35
VL Forward Primer DLP96	GATGTTTTGATGACCCAAACT	21
VL Reverse Primer DLP106	GGATACAGTTGGTGCAGCATC	21

Once the correct primer candidates had been identified, the PCR reactions were repeated with these primers, this time using the Platinum™ Superfi™ PCR Master Mix Kit (Invitrogen, Cat: 12358-010) This kit contains high fidelity polymerase, which increases the fidelity of DNA replication during PCR and therefore creates a more accurate dsDNA

sequence from the original template of sufficient quality for sequencing and other downstream applications requiring high specificity.

PCR was performed with the same thermocycler conditions as previously, with an annealing temperature of 67°C. Template DNA was diluted from 1393.8 ng/µL to a working concentration of 100 ng/µL using nuclease-free ddH_2O. Thermocycling conditions were based on the recommendations of the Platinum™ Superfi™ kit:

Program Stage	Temperature	Duration
1. Initial denaturation	98°C	30 seconds
2. Denaturation	98°C	10 seconds
3. Annealing	67°C	30 seconds
4. Extension	72°C	30 seconds
5. Cycling (repeat of steps 2-4, 29x)	-	-
6. Final extension	72°C	5 minutes
7. Cooling	4°C	∞

The Platinum™ Superfi™ kit has a recommendation of 1.2% agarose composition; therefore, each PCR product was run on a 1.2% agarose TAE gel at 60 volts for 1.5 hours. The bands for the primer combinations DLP85/95 and DLP96/106 aligned with the correct estimated size of the heavy and light chains, and produced strong readings in the transilluminator, therefore indicating that the PCR products contained the correct DNA for the chains. These bands were subsequently excised over a transilluminator using sterile surgical scalpels and placed into separate Eppendorf tubes. The Wizard® SV Gel and PCR Clean-up System (Promega, Cat: A9281) was used to isolate the DNA from the gel.

2.3. TOPO® cloning to amplify heavy and light BB7.2 chains

Purified BB7.2 light and heavy chain DNA samples proceeded to an optimised TOPO® cloning workflow. The Zero Blunt® TOPO® PCR Cloning Kit for Sequencing (Invitrogen, Cat: 45-

0031) includes OneShot® chemically competent cells for transformation. For competent cell culture, 500 mL of LB broth without agar was prepared with 50 mg/mL kanamycin, and an additional 500 mL of LB broth containing 15g/L agar (with 50 mg/mL kanamycin) was also made. Both were sterilised by autoclaving. In a sterile hood, the stock solution of LB-agar-kanamycin was divided between three Petri dishes and left to set. Using aseptic technique, a master mix was created for TOPO® cloning – ultimately incorporating either of the BB7.2 chains into the plasmid TOPO® vector for amplification of the DNA:

TOPO® undiluted salt solution	2 µL
TOPO® vector	1 µL

This solution was divided equally between two Eppendorf tubes. To the first tube, 4.5 µL of amplified light chain DNA (Platinum™ Superfi™ PCR product) was added. To the second tube, the same volume of pre-amplified TOPO® Control DNA was added. Reactions were mixed gently via pipetting, then incubated at room temperature for 30 minutes. The reaction tubes were then immediately placed on ice. To begin bacterial transformation, two vials of OneShot® competent cells were thawed on ice. 2 µL of light chain DNA TOPO® reaction product from the previous step was added to a corresponding vial of competent cells and mixed gently by tapping; this was repeated with the Control DNA TOPO® reaction product for the second vial of cells. The reaction was incubated on ice for 30 minutes. Competent cells were then heat-shocked for 30 seconds in a heating block at 42°C, then immediately placed on ice. 250 µL of room temperature SOC medium was added to each sample. Vials were sealed and shaken horizontally at 200 rpm at 37°C for 1 hour. LB-agar plates were preheated at 37°C for 30 minutes prior to plating of bacteria. Using aseptic technique, the total volume from each incubated vial was poured into a corresponding agar plate and evenly spread using a sterile spreader. For the third agar plate, used as a sterility control, 250 µL of room temperature SOC medium was added without any

reaction product and spread evenly on the agar. Plates were left to dry upright at 37°C for 10 minutes, before being inverted and incubated for 12-16 hours at 37°C. In a sterile hood, a stock solution of LB-kanamycin was prepared by adding 30 µL of 50 mg/mL kanamycin solution to a Falcon tube and bringing the volume to 30 mL with sterile ddH_2O. The solution was aliquoted between five 50 mL-Falcon tubes and labelled from one to five. Tubes were then heated in a water bath at 37°C. Using aseptic technique, five different bacterial colonies on the light chain DNA agar plate were picked from the agar using pipette tips, each tip then being ejected into a corresponding Falcon tube. Lids were untightened, covered loosely with foil, and the cultures were placed in a shaking incubator at 37°C, 200 rpm, for 12-16 hours. Of the bacterial culture liquid, 3 mL was taken from each Falcon tube and divided between two 2 mL-Eppendorf tubes. The cultures were processed with a Qiagen Plasmid Mini Kit (Qiagen, Cat: 12123). The concentration of each plasmid DNA sample was analysed using NanoDrop before being sent for Sanger sequencing (with M13 Reverse primer). Sequences were analysed using ApE software (created by M. Wayne Davis) for verification of amplification of BB7.2 light chain. The TOPO® cloning process was then repeated as above for the heavy chain DNA.

2.4. Construction of the CAR sequence

Construction of the full CAR sequence was possible using the heavy and light chain sequences of the antigen-specific region obtained through high-fidelity amplification and cloning, and publicly available sequences of the remaining structural components. Sequences for the CD8α signal peptide and CD8α hinge sequence were obtained from (Galetto, 2015a, 2015b); the sequences for the glycine-serine linker and CD3ζ chain were obtained from (Bedoya et al., 2015); the Myc tag sequence was obtained from (Rondon et al., 2009); the CD28 transmembrane domain sequence was obtained from (Chang & Moreb, 2015); the CD28 sequence was obtained from (Forman & Wang, 2015); the CD27 sequence was obtained from (Brogdon et al., 2014). Advice on additional CAR components was kindly given by Demin Li

(NDCLS, University of Oxford). The CAR sequence was synthesised into a pMK cloning plasmid using the design and order tools available through the Invitrogen GeneArt Gene Synthesis service (available at: https://www.thermofisher.com/uk/en/home/life-science/cloning/gene-synthesis/geneart-gene-synthesis.html).

The plasmid was designed to contain two enzyme restriction sites – EcoRI and BamHI – and kanamycin resistance to enable antibiotic-based colony selection in future cloning experiments. The full BB7.2 CAR sequence can be found in the Appendices (8.1).

After receiving the synthesised CAR-pMK, the sample was diluted to 1 ng/µL concentration and amplified using the TOPO® cloning kit by pipetting 1 µL directly into a vial of competent cells; transformed cell cultures containing CAR-pMK DNA underwent plasmid isolation using the Qiagen Plasmid Mini Kit, with the final DNA being eluted into 30µL TE Buffer instead of the recommended 50 µL in order to improve concentration.

pIRES2-eGFP-ND26 mammalian expression vector was a kind gift from Demin Li (NDCLS, University of Oxford). The vector expresses eGFP constitutively, carries kanamycin resistance for selection, and allows for coexpression of a transgene and GFP as a function of its Internal Ribosome Entry Site (IRES). Bacterial transformation and plasmid isolation were repeated with the pIRES2-eGFP-ND26 plasmid to amplify the DNA sample, once again eluting into 30µL TE Buffer. A restriction digest was performed on the eluted DNA using 10x rCutSmart™ Buffer (New England Biolabs, Cat. No. B6004S), EcoRI-HF and BamHI-HF enzymes (both from New England Biolabs, Cat. No. R3101S and R3136S, respectively) in the following recipe:

10x rCutSmart™ Buffer	5 µL
Nuclease-free Water	31 µL
Plasmid DNA	10 µL (either CAR-pMK or pIRES2-eGFP-ND26)
EcoRI-HF	2 µL
BamHI-HF	2 µL
Total:	**50 µL**

The reaction was incubated at 37°C for 3 hours. The digested expression vector, pIRES-eGFP, was further incubated in 2 µL of 1 U/µL Calf Intestinal Alkaline Phosphatase for 30 minutes at 37°C to prevent self-ligation. Both digests were run on a 1.0% agarose TAE gel for 1.5 hours. The gel band was then excised and processed with the Wizard® SV Gel and PCR Clean-up System.

The excised CAR DNA was ligated into a pIRES2-GFP expression plasmid, using T4 ligase (Invitrogen, Cat. No. 15224-017) and 10x T4 Ligase Buffer (New England Biolabs, Cat. No. B0202S), using the following recipe:

10x T4 Ligase Buffer	1 µL
Digested pIRES2-eGFP	2 µL
Digested CAR	6 µL
T4 Ligase	1 µL
Total:	**10 µL**

Of note, the recipe did not follow the 1:3 molar ratio of vector:insert, but rather used a 1:3 ratio of volumes, as it was advised through personal communication that this approach produced more favourable results for ligation efficiency. The reaction was incubated at room temperature overnight (16 hrs) and proceeded directly to TOPO® cloning, performed as previously described. Bacterial cultures containing pIRES2-eGFP-CAR DNA were processed using a Qiagen Plasmid Mini Kit (eluted into 30µL TE Buffer, Invitrogen, Cat. No. 12090015) and the resulting plasmids were once again purified and visualised using gel electrophoresis.

2.5. Generation of GFP$^+$ human CD4$^+$ cells using CRISPR-Cas9 technology

2.5.1. Amplification of GFP-containing HDRT

A plasmid containing a GFP sequence flanked by RAB11A or CD4 homology arms was obtained from the Alexander Marson research group. The sequence was amplified using the Platinum™ Superfi™ PCR kit and subsequently analysed with Nanodrop. To obtain sufficient quantity of the HDRT, the PCR was performed with eight replicates, and each

replicate simultaneously purified with Agencourt AMPure XP beads (Beckmann Coulter, Cat: A63880); an optimised protocol was created for this construct to gain sufficient quantity of DNA for nucleofection. Eight PCR reactions (each with a volume of 50 µL) were performed using the Platinum™ Superfi™ kit to amplify the HDRT. In brief, AMPure XP beads were warmed to room temperature before use; each PCR reaction tube containing amplified HDRT then received beads in a ratio of 1.6 µL bead suspension to 1.0 µL PCR product (i.e. each 50 µL reaction received 80 µL of beads). The contents of each tube were mixed and incubated for 15 minutes at room temperature to allow the beads to bind the DNA. The tubes were then spun briefly before being placed on a high-strength magnetic stand for 5 minutes until the liquid became clear. With the tubes still on the magnet, the liquid was carefully removed with a 200 µL pipette without disturbing the beads. Exposed beads were then washed with 80% ethanol (200 µL per tube) and incubated on the magnet in the ethanol for 30 seconds. Ethanol was then carefully removed. The ethanol wash was repeated twice for a total of three washes. Residual ethanol in the PCR tubes was then removed with a 10 µL pipette and tubes were left to dry on the magnet for 5 minutes. After removing the tubes from the magnet, 10 µL of nuclease-free water was added to the first tube, such that the beads were washed to the bottom of the tube and allowed to resuspend in the water. The entire volume of resuspended beads was then transferred to the second tube in the same manner, washing the beads down and resuspending them at the bottom of the tube; this was serially repeated until the final tube of beads had been resuspended. The final tube with the collated contents was vortexed strongly to detach the beads from the HDRT DNA, then incubated at room temperature for 10 minutes. The tube was placed on a low-strength magnetic stand for 5 minutes to spatially separate the beads and DNA. Once clear, the liquid (containing suspended DNA) was eluted into a clean Eppendorf tube using a 20 µL pipette. This was then analysed with Nanodrop.

2.5.2. Production of GFP$^+$ CD4$^+$ T cells using CRISPR-Cas9

Initially, bulk CD4$^+$ T cells were isolated for CRISPR insertion of either a RAB11A-GFP or CD4-GFP HDRT. This was achieved through PBMC isolation from human peripheral blood samples, followed by positive isolation of CD4$^+$ cells using CD4 MicroBeads (Miltenyi, Cat. No. 130-045-101) and 3-day expansion in the presence of CD3/CD28 Dynabeads™ (Gibco, Cat. No. 11161D) prior to bead removal and electroporation using a Lonza 4D-Nucleofector™ (program EH-115) at 500 V, based on a published optimised protocol for T cells. (Zhang *et al*., 2018)

Cas9 stocks were kept at 40 pmol/µL; gRNA stocks were 100µM (100pmol/µL); and HDRT amplification with AMPure XP beads – when successful – brought the concentration of HDRT to ~1 µg/µL. For optimal editing of 1 million Tregs, 50 pmol (0.8 µL) of Cas9 and 100 pmol of gRNA (1 µL) were required.

Firstly, after CD3/CD28 bead removal, cells were collected into a Falcon tube and centrifuged for 5 minutes at 500 rcf, 4°C. Supernatant was discarded and the Tregs were washed twice with sterile PBS – with 14 mL for the first wash and 2 mL for the second wash. Supernatant was discarded and the cells were resuspended in 1 mL PBS per 1 million cells. Cells were then divided between separate cryovials depending on treatment group, in multiples of 1 million. Cryovials were centrifuged for 5 minutes at 500 rcf, 4°C, then placed on ice while assembling the RNP.

For RNP production, appropriate volumes of Cas9 and gRNA (per million cells) were pipetted into sterile PCR tubes. The tubes were vortexed and immediately placed in a preheated 25°C thermocycler for exactly 10 minutes. Meanwhile, a 24-well plate was prepared with pre-warmed antibiotic-free Complete Medium, each well receiving 1 mL. 500 U/mL of IL-2 was then added to each well. After 10 minutes at 25°C, the RNP tubes were placed on ice and taken into a sterile hood.

The centrifuged cells were retrieved from ice and taken to the sterile hood, and the supernatant was carefully removed with a pipette. 1.8 µl (50 pmol) of RNP (for 1 million cells) was transferred into each of 2 tubes, and 4 µg of HDRT was then transferred into each Eppendorf (per 50 pmol RNP) – this was equivalent to 4 µL of ~1 µg/µL HDRT. The cells in cryovials were resuspended in 20 µL of P3 buffer per treatment. 1 million cells were then transferred into their corresponding Eppendorf tube and mixed by pipetting. Cells from each Eppendorf were then transferred to a corresponding sterile well on an electroporation X-strip for nucleofection. Cells were immediately electroporated. Each group of cells on the X-strip was transferred to a 1 mL well on the prepared plate of Complete Medium (CM) and pipetted gently to mix. The cells were incubated for 24 hours at 37^{o}C before administrating penicillin/streptomycin.

2.5.3. Production of GFP^{+} Tregs using CRISPR-Cas9

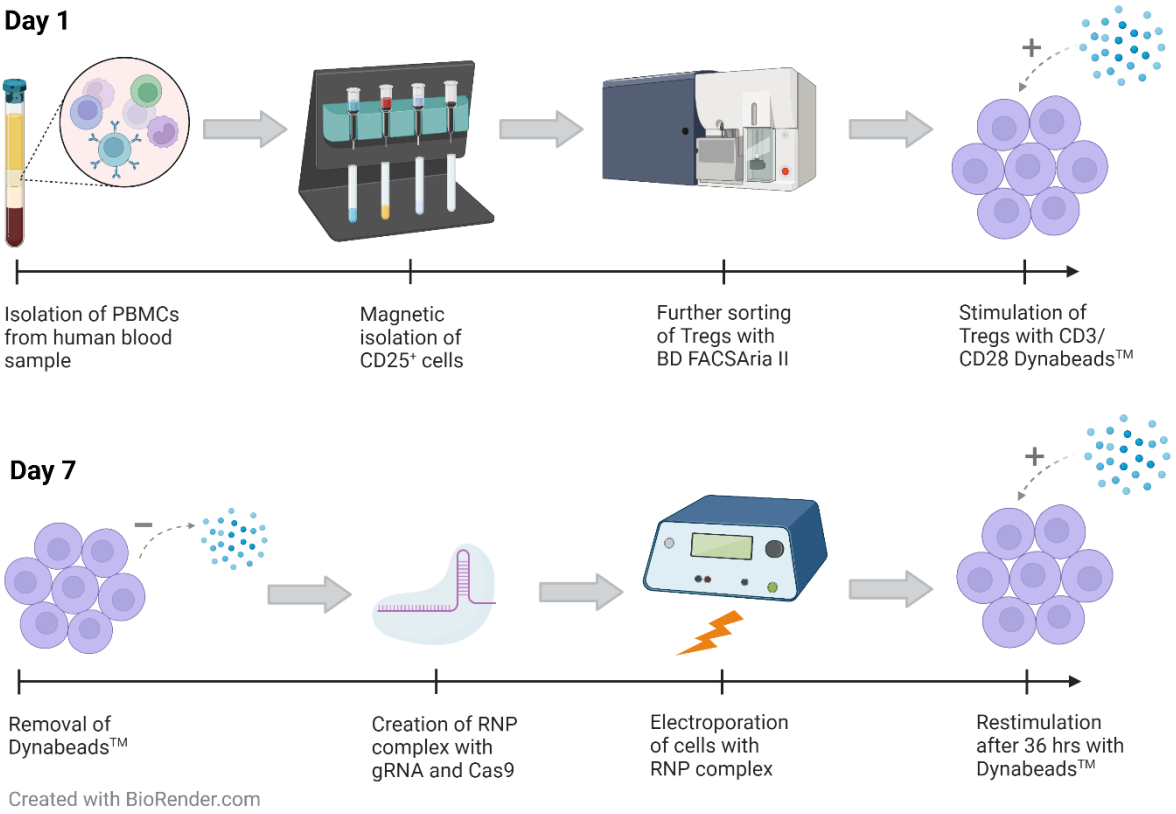
Tregs were isolated from previously frozen PBMCs using CD25 Microbeads II (Miltenyi, (Cat. No. 130-092-983), followed by further sorting with BD FACSAria™ II (Table 1). After 7 days of stimulation with CD3/CD28 Dynabeads™ and 1000 U/mL IL-2, beads were magnetically removed and Tregs were electroporated with RAB11A-GFP homology-directed repair template (HDRT) at a concentration of 4 µg HDRT per million cells. Two wells, each containing one million Tregs, were electroporated with RAB11A-GFP HDRT (GFP^{+} Tregs), and a third well of Tregs was established as a control to undergo electroporation without HDRT ("Control" Tregs). Meanwhile, an additional group of Tregs was kept in culture and did not undergo electroporation ("Normal" Tregs). Each cell group was cultured in 1 mL of CM (containing 10% human serum in place of FBS) supplemented with 500 U/mL IL-2. 24 hours after electroporation, cells were given 10 U/mL penicillin/streptomycin. Cells were then centrifuged at 420 rcf, 5 mins, 4^{o}C, and resuspended in CM (10% human serum). The cell suspensions were aliquoted across a U-bottomed 96-well plate. After an additional 12

hours, 50 µL of medium was removed from the surface of each well, leaving the pellet undisturbed, and replaced with 50 µL of fresh medium (10% human serum) containing CD3/CD28 Dynabeads™. Seven days post-electroporation, $HDRT^+$ Tregs and $HDRT^-$ (control) Tregs were washed and fixed: the contents of each well were collected into Falcon tubes, 3 mL of FACS buffer added, then the tubes were centrifuged for 5 minutes at 500 rcf, 4°C. The supernatant was discarded, and cells were resuspended in 300 µL of Fixation/Permeabilisation buffer before being stained for flow cytometry (Table 1).

Table 1. Treg Staining Panel

Target	Fluorochrome	Brand	Cat. No.
CD4	APC-Cy7	BioLegend	300518
CD27	eFluor 450 (Pacific Blue)	Invitrogen	48-0279-42
CD70	PE	BioLegend	355104
FOXP3	Alexa-Fluor 647	BioLegend	320114
Foxp3 Isotype Control (ICFC)	Alexa-Fluor 647	BioLegend	400136
7-AAD	Per-CP	Invitrogen	00-6993-50

Figure 2. The process of CRISPR-mediated gene editing of Tregs.



2.5.4. Suppression assay with GFP$^+$ Tregs: VPD analysis

GFP$^+$ Tregs that were initially expanded for 7 days prior to electroporation as previously described were cultured for another 7 days post-electroporation before, a) being sampled for flow cytometry for GFP expression, and b) the remainder seeded in cocultures with PBMCs stained with Violet Proliferation Dye (VPD) on a U-bottomed plate to observe the effects of Tregs on effector cell proliferation. Similarly, Control Tregs (electroporation, no HDRT) and Normal Tregs (no electroporation, no HDRT) were also seeded in cocultures. Tregs were added to PBMCs at the following ratios: 0:1, 1:2, 1:4, 1:8, 1:16, 1:32, and 1:64. The suppression assay was run for 3 days before VPD was analysed using flow cytometry.

2.5.5. Suppression assay with GFP$^+$ Tregs: gene and cytokine analysis

GFP$^+$ Tregs were tested for their suppressive capacity against allogeneic PBMCs, with Normal Tregs (non-electroporated, GFP$^-$) from the same donor as the GFP$^+$ Tregs used as controls. Previously frozen GFP$^+$ Tregs were tested in either a 1:1 or 1:4 ratio of Tregs:PBMCs on a U-bottomed plate. With the exception of the PBMCS Only (no beads) group, all wells received stimulation CD3/CD28 Dynabeads™. The following treatments were created on the first plate:

Treatment Group	Tregs Per Well	Dynabeads™ Per Well	PBMCs Per Well	Cell:PBMC Ratio
GFP$^+$ Tregs + PBMCs (1:1) (+ beads)	1.0 x 10^5 GFP$^+$ Tregs	2 x 10^4	1 x 10^5	1:1
Normal Tregs + PBMCs (1:1) (+ beads)	1.0 x 10^5 Normal Tregs	2 x 10^4	1 x 10^5	1:1
GFP$^+$ Tregs + PBMCs (1:4) (+ beads)	2.5 x 10^4 GFP$^+$ Tregs	2 x 10^4	1 x 10^5	1:4
Normal Tregs + PMBCs (1:4) (+ beads)	2.5 x 10^4 Normal Tregs	2 x 10^4	1 x 10^5	1:4
PBMCs only (+ beads)	0	2 x 10^4	1 x 10^5	-
PBMCs only (no beads)	0	0	1 x 10^5	-

In addition, a second plate was set up to compare the proliferation of Tregs stimulated with CD3/CD28 Dynabeads™ against unstimulated Tregs. 200 U/mL IL-2 was added to all wells to encourage Treg survival in the unstimulated treatments while ensuring only one variable (CD3/CD28 Dynabeads™). The following treatments were created on the second plate:

Treatment Group	Tregs Per Well	CD3/CD28 Beads Per Well	IL-2
GFP^+ Tregs (unstimulated)	1.0 x 10^5 GFP^+ Tregs	0	200 U/mL
GFP^+ Tregs (stimulated)	1.0 x 10^5 GFP^+ Tregs	2.0 x 10^4	200 U/mL
Normal Tregs (unstimulated)	1.0 x 10^5 Normal Tregs	0	200 U/mL
Normal Tregs (stimulated)	1.0 x 10^5 Normal Tregs	2.0 x 10^4	200 U/mL

Plates were incubated at 37°C for 4 days. After the incubation period, cells were harvested into V-bottomed plates and centrifuged at 500 rcf for 5 minutes at 5°C. The pellets were left in the V-bottomed plates, while the supernatants were transferred back to the U-bottomed plates. Cell pellets were resuspended with 200 µL of chilled PBS, and then transferred into corresponding Eppendorf tubes (one tube per well). PBS-suspended cells were vortexed briefly and counted to select the appropriate RNA extraction kit. RNA extraction was performed using the Qiagen RNeasy Plus Mini Kit (Cat. No. 74134) for the following treatments:

A) GFP^+ Tregs + beads + PBMCs

B) Normal Tregs + beads + PBMCs

C) PBMCs only + beads

D) Qiagen RNeasy Plus Micro Kit (Cat. No. 74034) was used for PBMCs only (no beads)

RNA concentrations were analysed on the NanoDrop. Then, RNA expression was quantified using the Quant-IT RNA Assay Kit (Life Technologies, Cat. No. Q33140) in combination with the Nanostring Human Organ Transplant Panel (HOT-B) and the NanoString nCounter SPRINT. Supernatant from the suppression assay was analysed with the BioLegend™ Multi-Analyte Flow Assay Kit Human Th Cytokine Panel (12-plex) (Cat. No. 741027) to quantify cytokine protein production.

3. Green Fluorescent Protein: a literature review

3.1. Fluorescent proteins

An important feature of synthetically engineered cells in biological research is the inclusion of a fluorescent protein marker to enable detection of the modified cell product. The benefits are twofold: firstly, it enables efficient sorting of correctly modified cells prior to downstream expansion and infusion; secondly, it allows for *in vivo* tracking of cells to assess their survival, localisation, and immunological dynamics with high precision and resolution. Through histological sampling, such transgenic cells can be visualised with fluorescence microscopy, providing a unique understanding of cellular localisation within target tissue.

3.2. Green Fluorescent Protein

Green Fluorescent Protein (GFP) is a member of the family of *endogenous reporters*: protein-encoding genes that can be engineered into cells of interest, resulting in fluorescent protein production and thereby a means of identification within a heterogenous sample.(Progatzky et al., 2013) GFP was originally derived from the jellyfish species *Aequorea victoria* and confers a constitutive green fluorescence when expressed.(Soboleski et al., 2005)

Unlike fluorescent dyes, endogenous reporters such as GFP are not diluted during cell division events (whereas dyes are shared between daughter cells), and protein expression is therefore consistently detectable through generations of cells.(Progatzky et al., 2013) Variations of GFP have been engineered via mutagenesis, including Yellow Fluorescent Protein (YFP) and Enhanced Green Fluorescent Protein (eGFP), each exhibiting variations in brightness, photostability, colour, and spectral values, which may be preferential for different applications or used concurrently for multiple protein tagging.(Lippincott-Schwartz & Patterson, 2003) Many different fluorescent reporters are commercially available for research use, yet GFP and its variations undoubtedly constitute the most widely used fluorescent labels for *in vitro* studies and animal models. Their popularity might be attributed to the extensive research and

knowledge of the GFP family, as well as their high fluorescence, stability *in vivo*, and robustness against laboratory chemicals used in the cell-fixing process such as ethanol and paraformaldehyde.(Yu et al., 2003) Furthermore, GFP requires no additional coenzymes or exogenous substrates in order to function.(Lippincott-Schwartz & Patterson, 2003)

In genetic engineering procedures, the GFP sequence is placed under the control of an appropriate promoter region which may be tissue-specific (for example, the CD34 promoter region for exclusive GFP expression in $CD34^+$ stem cells) or constitutive (for example, any of the cytomegalovirus, elongation factor-1α, human ubiquitin-C, or chicken β-actin promoters).(Mothe et al., 2005; Norrman et al., 2010; Schaefer et al., 2001; Ye et al., 2004)

3.3. Applications of GFP^+ cells

Despite the valuable information provided by *in vitro* experiments, they do not give insight into the behaviour of cell products once they enter the body. Before any therapy can progress to clinical trials, it is critical to understand the dynamics of migration, tissue localisation, and persistence *in vivo*. GFP labelling provides a means of monitoring these factors in animal models in order to assess the suitability of cellular therapy for human use. With the aid of imaging techniques such as wide-field fluorescence microscopy, single-photon laser confocal fluorescence microscopy (LSCM), and two-photon LSCM (TPLSM), GFP-tagged cells are easily identifiable within tissue samples in combination with a suitable fluorescence filter.(Hadjantonakis & Nagy, 2000; Yu et al., 2003) Moreover, GFP^+ cells do not require additional staining in order to be detected with microscopy or FACS systems.

For the ultimate insight into cell fate, GFP-tagged cells can be used for whole-organism live imaging. Hoffman and colleagues pioneered this field using rodent models into which GFP-expressing cancer cell lines were transplanted, allowing cancer metastasis to be monitored over time *in situ*.(Hoffman, 2018; Yang et al., 2000) As a result of its real-time and high-resolution insight into cell dynamics, GFP live imaging is also a useful tool for novel drug

screening (and has been proposed for assessing chemotherapeutic drugs due to its efficacy at visualising tumour development).(Hoffman, 2018; Yang et al., 2007)

The stability of GFP expression, and the generational transfer of GFP-encoding genes from parent to daughter cells, lends itself particularly well to the fields of cell fate mapping, adoptive cell transfer, and spatial-temporal analysis of immunological processes. GFP has been induced in umbilical cord-derived mesenchymal stem cells to observe skin localisation and later identify the differentiated progeny of the original stem cells, confirming their differentiation into skin epithelial cells and supporting cord-derived stem cells as a treatment for skin injuries.(Dai et al., 2007) In the field of transplantation, GFP^+ allospecific T cells have not only illustrated the recruitment of T cells to corneal allografts, but have also allowed researchers to identify a distinct phenotype of T cells associated with high motility and cell activation within a rejecting allograft.(Tan et al., 2013) Overall, GFP labelling is an invaluable tool for studying the differentiation, migration, and fate of cell subsets.

3.4. Sources of GFP^+ cells

3.4.1. Transgenic rodent strains

GFP^+ reporter rodent strains, generated by embryonic injection or viral transduction of the developing embryos, are extremely common as a source of fluorescent cells for *in vitro* and *in vivo* studies.(Okabe et al., 1997; Tischner et al., 2006) Using myelin-specific encephalitogenic T cells obtained from $eGFP^+$ transgenic rats, Tischner *et al.* were able to illustrate the migration patterns and spinal cord infiltration associated with experimental autoimmune encephalomyelitis in GFP^- Lewis rats (a model of multiple sclerosis).(Tischner et al., 2006) By infusing $eGFP^+$ Tregs and Tconvs into the same rodent line, they demonstrated the preferential expansion and infiltration of Tregs into spinal cord tissue when treated with anti-CD28 antibody, and were thus able to support polyclonal Treg

activation as an effective treatment for multiple sclerosis. Many other examples of adoptive cell transfer studies using GFP as a tracking method have been published, providing unique insights into the behaviour of therapeutic cells. Some have also extended the potential of GFP labelling to whole-organ transplantation, as seen in the rat model developed by Hakamata *et al.*, and to bone marrow transplantation, such as the GFP-labelled haematopoietic cells derived from the Vav-GFP mouse line by Perez-Cunningham and colleagues.(Hakamata et al., 2001; Perez-Cunningham et al., 2016) Collectively, these studies demonstrate the versatility of animal-derived GFP^+ cells across a range of medical contexts.

The type of gene knock-in also has noticeable impacts on cell functionality, which should always be considered when designing fluorescent therapeutic cells. Chang and colleagues described differential efficacy of GFP^+ Tregs on lupus disease symptoms based on the method used to knock-in the GFP sequence, comparing the Tregs from B6.*Sle1*.fGFP-FoxP3 mice (expressing GFP via FoxP3 N-terminal insertion) with those from B6.*Sle1*.iGFP-FoxP3 (expressing GFP via an internal ribosomal entry site); they found that lupus disease symptoms were more severe in mice bearing B6.*Sle1*.fGFP-FoxP3 Tregs with N-terminal insertion GFP, including thinner glomerular basement membranes, higher incidence of nephrophilic autoantibodies, and more complement component 3.(Chang et al., 2019) The total number of splenic GFP^+ Tregs from both GFP^+ knock-in mice was also significantly reduced compared to B6.*Sle1* (GFP^-) mice, indicating that GFP insertion played some role in the reduction of Treg proliferation. The authors postulated that Foxp3 N-terminal insertion of GFP may lead to transcriptional changes in the Foxp3 gene which ultimately affect the activity of Tregs. This raises the question of whether targeting GFP to the Foxp3 gene is the most suitable strategy for generating GFP^+ Tregs if it affects the functionality of the resulting

cells, and one might argue that a better strategy might rely on targeting GFP to a non-essential or housekeeping gene.

3.4.2. Electroporation

The GFP sequence (or one of its mutated variants) in the form of mRNA or DNA may be transferred directly to a cell population *in vitro* using electroporation to create transient pores in the target cell membrane to facilitate its uptake. This approach represents a more versatile method of GFP labelling as it can be used when animal models are unavailable for a specific research interest, and it circumvents the biosafety risks associated with viral transduction. It is a common belief that electroporation yields low percentages of transduced cells, but evidence for this is variable. Boissel and colleagues found the efficiency of mRNA electroporation to be consistently below 10% for peripheral blood cells.(Boissel et al., 2012) Yet others have reported high-efficiency methods of electroporation; Zhao *et al.* achieved over 90% efficiency in activated primary human and murine T cells receiving *in vitro*-transcribed GFP mRNA and 95% efficiency for unstimulated human peripheral blood cells.(Y. Zhao et al., 2006)

The major disadvantage of this method of gene insertion is the transient expression of protein, which makes electroporation less suitable for *in vivo* applications and long-term expansion of transgenic cells. Indeed, Zhao *et al.* reported that GFP expression in T cells peaked between 24 and 72 hours post-electroporation, and disappeared to background levels by Day 14.(Y. Zhao et al., 2006) Similarly, in their efforts to optimise T cell electroporation with pmaxGFP plasmid, Zhang and colleagues reported peak GFP expression until Day 3, after which it declined to 6-7% by Day 21.(Z. Zhang et al., 2018) Of interest, Zhang's study investigated the possibility of cell activation affecting transfection efficiency: it was found that unstimulated T cells could show as little as <5% efficiency, with similar results for T cells activated for only one day (using anti-CD3/CD28 beads).(Z. Zhang

et al., 2018) Efficiency peaked at over 40% for cells activated over 3 days, but quickly fell to 20% for cells activated continuously over a 5-day period. Of further note, higher electrical voltage increased transfection efficiency but decreased cell viability.

One final caveat of electroporation in all its forms is the cellular damage inflicted by electrical shock, which reduces the starting pool of transgenic cells post-modification.(Z. Zhang et al., 2018) Nevertheless, electroporation represents an economical, relatively straightforward, and safe option for short-term GFP expression, and may be useful for standalone applications such as cell sorting.

3.4.3. Viral delivery

In recent years, researchers have expanded to other methods of GFP delivery, and viral delivery remains a popular choice. This method confers long-term, stable GFP expression due to integration of the transgene into the host cell genome. However, genomic integration also represents a safety concern due to possibility of insertion into a proto-oncogenic site.(Hamada et al., 2018) There is also evidence that virally modified cells can express immunogenic vector-encoded epitopes, prompting concerns that viral vectors may increase the immunogenicity of therapeutic cells.(Lamers et al., 2011) In addition, the full process of viral transduction can take up to a month to complete, rendering this method more cumbersome for the generation of GFP^+ cells.(Z. Zhang et al., 2018) However, average transduction efficiency using viral delivery is vastly superior to electroporation, with efficiency ranging from 30-80% in T cell subsets – though Boissel *et al.* reported 8-16% efficiency for peripheral blood cells.(Boissel et al., 2012; Z. Zhang et al., 2018) Chronic protein expression – which may persist for several months – renders viral delivery of GFP a relevant tool for *in vivo* experiments.(Noyan et al., 2017; Tenspolde et al., 2019)

3.4.4. Genome editing with CRISPR-Cas9

Arguably the most promising method of GFP delivery is that of Clustered Regularly Interspaced Short Palindromic Repeats (CRISPR) technology, an influential breakthrough in genetic engineering. CRISPR represents a reliable method of achieving highly stable and predictable gene expression because of its precise targeting of gene loci – unlike viral vector-based delivery, which incorporates genetic cargo into the host cell genome through semi-random integration and results in variable expression of GFP protein depending on the insertion site. Secondly, CRISPR editing is faster than viral delivery systems, thereby improving turnover times of transgenic cell production. Thirdly, CRISPR poses less of a biosafety risk than viral vector systems.(Odé et al., 2020) To give some examples of CRISPR application, Roth *et al.* described a platform for generating GFP expression through CRISPR-mediated insertion of a GFP fusion protein into the RAB11A locus of bulk T lymphocytes.(Roth et al., 2018) Using a similar approach, Eyquem *et al.* utilised CRISPR-Cas9 to deliver a CAR-GFP fusion gene into the TRAC locus of conventional T cells, generating CD19-specific CAR-T cells whose chimeric receptor expression could be easily analysed and quantified.(Eyquem et al., 2017)

3.5. Risks of GFP expression in mammalian cells

Transduction of GFP into human cells is known to increase their sensitivity to oxidative stress in comparison to transduction with surface markers.(Ganini et al., 2017; Goto et al., 2003) In murine studies, GFP has also been associated with enhanced immune response against adoptively transferred transgenic cells. An elegant experiment by Stripecke and colleagues demonstrated the immunogenic effects of GFP in murine models by injecting WT leukaemia cells of the BM185 line into BALB/c mice, while injecting BM185/EGFP cells into another cohort of BALB/c mice. The cohort receiving wtBM185 cells fully succumbed to leukaemia by 15 days, whereas only one of 12 mice receiving $eGFP^{+}$ cells experienced mortality, suggesting that the expression of GFP provoked an immune response against the transgenic leukaemia cells and

prevented tumour growth.(Stripecke et al., 1999) In a follow-up experiment, the group isolated splenocytes from mice receiving the BM185-EGFP infusion and restimulated them for five days with BM185/EGFP cells; the splenocytes were then tested for their ability to lyse the GFP-expressing cells and wtBM185 cells. The splenocytes from leukaemia-affected mice showed a significantly greater lysis response against BM185/EGFP cells than the unmodified counterparts, whereas in control assays using splenocytes from non-leukaemia mice, there was no significant difference in the cytotoxic response towards GFP^+ versus GFP^- cells.(Stripecke et al., 1999) While it is a possibility that the viral vectors used in the aforementioned study bore immunogenic potential themselves,(Lamers et al., 2011) the effects of GFP expression on the murine immune response warrant closer consideration of experimental results gained using GFP^+ cells.

Nevertheless, GFP^+ transgenic cells have endured as a gold standard for cell visualisation, quantification, and sorting across published studies. Other options for cell labelling are also not without risk – in particular, cytoplasmic and nucleic dyes are associated with cytotoxicity due to their interference with cellular structure and signalling mechanisms.(Progatzky et al., 2013) Therefore, in terms of limiting toxicity to therapeutic cells, GFP represents a safer option for cell labelling.

3.6. GFP expression in regulatory T cells

A number of investigations into the activity and therapeutic benefits of regulatory T cells have employed GFP as a reporter. The gold standard marker for Treg identification is its transcription factor FOXP3, but because it is intracellular, cell lysis must be performed prior to immunofluorescent staining and detection; this unfortunately prevents live cell sorting and downstream applications of $FOXP3^+$ cells. Surface-expressed GFP therefore becomes an invaluable tool for Treg sorting since it allows FACS to be performed on living cells, producing a highly pure Treg population which can then be further expanded *in vitro.*

GFP expression may be used as a proxy for expression of another Treg-associated marker when GFP is linked to a marker gene – for example, by using cells obtained from Foxp3^{GFP} transgenic mice (which co-express both genes under the same promoter), GFP expression is dependent on Foxp3 expression, and this has been used to monitor Treg phenotypic instability *in vivo*.(Addey et al., 2011) GFP can act as a quantifier of successful gene transduction in Tregs, such as CAR transduction, when co-expressed with the gene of interest.(Boardman et al., 2017)

GFP$^+$ Tregs are also commonly used to study the localisation and infiltration of adoptively transferred Tregs into target tissues within *in vivo* models of autoimmunity and transplantation; their presence may be confirmed with flow cytometry or cryosections combined with fluorescence microscopy, the latter providing direct visualisation of Treg interaction with the tissue.(Fransson et al., 2012; Hu et al., 2013; Pierini et al., 2017; Shao et al., 2019; Tischner et al., 2006)

Table 2. Varied applications of GFP expression in Tregs.

Author/Date	*In Vitro* or *In Vivo*?	Research Field	Generation Method of GFP$^+$ Tregs	Purpose of GFP	Data Generated from GFP Expression
(Tischner et al., 2006)	*In vivo*	Autoimmunity	GFP$^+$ transgenic rodents	Following the migration and expansion of Tregs and Tconvs in healthy vs. AT-EAE models	High infiltration of Tregs into the spinal cord after anti-CD28 JJ316 treatment in AT-EAE, but not healthy, rats
(Brusko et al., 2010)	*In vitro*	Cell engineering	Lentiviral transduction	Functional evaluation of GFP$^+$ TCR-Vβ12 transduced cells	13.2% of transduced Tregs were GFP$^+$Vβ12$^+$ by Day 9 of expansion, and this could be increased by antigen stimulation of the TCR
(Addey et al., 2011)	*In vivo*	Oncology	GFP$^+$ transgenic rodents	Studying the downregulation of Foxp3 in tumour microenvironments using Foxp3-	*Rag2*$^{-/-}$ mice with MB49 tumours showed significant loss of Foxp3$^+$ expression in Tregs

				dependent GFP expression	
(Eller et al., 2011)	*In vivo*	Autoimmunity	GFP^+ transgenic rodents	FACS and PCR-based detection of transferred Tregs in diabetic mice	Transferred Tregs were apoptotic by Day 14 post-transfer, but still attenuated disease symptoms
(D'Addio et al., 2011)	*In vitro & in vivo*	Foeto-maternal tolerance	GFP^+ transgenic rodents	Following the efficacy and fate of transferred Tregs in PDL1-blockade pregnant mice	*In vitro,* PDL1 blockade reduced conversion of $CD4^+Foxp3^-$ cells to $CD4^+Foxp3^+$; *in vivo,* adoptive transfer of Tregs increased foetal survival after PDL1 blockade
(Fransson et al., 2012)	*In vivo*	Autoimmunity	Lentiviral transduction	Studying the localisation of transferred CAR-Tregs in EAE models of MS	CAR-Tregs preferentially localised to the CNS (as seen in cryosections) via intranasal delivery
(P. Zhang et al., 2013)	*In vivo*	GvHD/marrow transplantation	GFP^+ transgenic rodents	FACS, and observing the fate and efficacy of iTregs in the context of GvHD mouse models	iTregs showed unstable Foxp3 expression compared to nTregs, but were still able to limit GvHD when combined with Rapamyin and IL-2
(Tauro et al., 2013)	*In vivo*	Autoimmunity	GFP^+ transgenic rodents	Following fate and senescence of iTregs during EAE treatment	iTregs isolated from EAE mice after 7 days showed up-regulation of KLRG1 compared to non-diseased mice, and $KLRG1^+$ cells showed enhanced death
(Hu et al., 2013)	*In vivo*	Transplantation	GFP^+ transgenic rodents	Studying Treg localisation and in kidney allograft models, while using FACS to confirm Treg depletion	Kidney allograft-infiltrating Tregs conferred spontaneous tolerance in an antigen-specific manner, which was conferred to skin grafts when kidney-tolerant Tregs were then transferred; Treg depletion ablated tolerance

(Sarkar et al., 2014)	*In vivo*	Haemophilia	GFP^+ transgenic rodents	Monitoring Treg-mediated suppression of antibody formation against therapeutic proteins for haemophilia	Tregs became undetectable after 2 weeks, but suppressive effects continued for over 2 months post-infusion
(Petzold et al., 2014)	*In vivo*	Cell origin	GFP^+ transgenic rodents	Used in combination with RFP to assess origins of Tregs in peripheral lymphoid organs	RFP^+GFP^- (extrathymic-derived) Tregs composed as much as 30% of Tregs in peripheral organs, and thymic-derived Tregs were greater at suppressing Tconvs than were extrathymic Tregs
(Xia et al., 2015)	*In vivo*	Ischaemia reperfusion injury	GFP^+ transgenic rodents	FACS, and studying the kinetics and effects of Tregs in the heart and spleen in post-myocardial infarction IRI	Tregs rapidly migrated to the heart but not the spleen after IRI, and *in vitro*-activated Tregs showed attenuated IRI compared to fresh Tregs
(Li et al., 2015)	*In vivo*	Allergy	GFP^+ transgenic rodents	Investigating the frequency of transferred Tregs in the lung and spleen in asthma models, and the effects of Treg CD39 expression	Treg frequency was reduced in the lung and spleen during airway inflammation, and also reduced in $CD39^{-/-}$ knockouts
(Delemarre et al., 2016)	*In vitro & in vivo*	GvHD/marrow transplantation	GFP^+ transgenic rodents	Assessing the survival and impacts of co-transferred Tregs on the success of HSCT	Tregs peaked in number 3 weeks post-infusion, then decreased rapidly; they reduced the production of proinflammatory cytokines but did not improve clinical outcomes
(Boardman et al., 2017)	*In vitro & in vivo*	Transplantation	Lentiviral transduction of CAR-GFP fusion protein	Sorting of CAR-Tregs and monitoring of transduction efficiency during a mouse model of allogeneic transplantation	7 days post-transduction, all GFP^+ Tregs were demonstrated to have detectable surface expression of the CAR

(Pierini et al., 2017)	*In vivo*	Transplantation	GFP^+ transgenic rodents	Studying abundance and localisation of transferred CAR-Tregs	CAR-Tregs home to and expand near allogeneic islet grafts
(Hoeppli et al., 2019)	*In vitro & in vivo*	Inflammation	Lentiviral transduction	Assessment of luciferase-GFP transduction efficiency, and cell purification	6 days post-transduction, efficiency was found to be 59.8%; Tregs were then purified to 98.1% for infusion into mouse models of intestinal inflammation
(Shao et al., 2019)	*In vivo*	Transplantation	GFP^+ transgenic rodents	Studying the localisation and effects of Tregs after sub-conjunctival injection into corneal allograft recipient mice	Tregs were detected in the ipsilateral cornea and DLNs 6 hours post-injection, based on GFP detection of cells via flow cytometry
(Sicard et al., 2020)	*In vivo*	Transplantation	GFP^+ transgenic rodents	Sorting of CAR-Tregs, and CAR-Treg survival/localisation post-infusion in the context of murine skin transplant models	Successful CAR transduction was between 65-75% of Tregs prior to infusion, and in sensitised mice, CARs were detectable in blood after 7 days with an average of 89% still GFP^+ ($Foxp3^+$)
(Jacob et al., 2021)	*In vivo*	Transplantation	Lentiviral transduction	Generation of an NIS-GFP fusion gene to allow for FACS and *ex vivo* tracking of Treg recruitment to skin allografts	NIS-GFP did not affect Treg marker expression (CD4, CD25, Foxp3, or CTLA-4), expansion, or suppressive capacity

As illustrated by the representative selection of publications, GFP^+ Tregs have been applied broadly across autoimmunity, inflammatory diseases, allergy, bone marrow transplantation, and solid organ transplantation, and many other fields where Tregs offer potential therapeutic benefit, and where GFP fluorescence aids in purification, tracking, and analysis of gene expression.

Overall, for the purpose of pre-clinical testing, GFP is regarded as an effective, accessible, and relatively simple method of inducing fluorescence in cells. Its value as a tool for live cell sorting and enrichment cannot be understated, and in combination with fluorescence microscopy it provides unique insights into cell-cell interactions within the tissue microenvironment. This makes it ideal for the study of regulatory T cells in both *in vitro* and pre-clinical *in vivo* models, particularly for the clinically relevant analysis of cell fate post-infusion.

4. Generation of GFP$^+$ human regulatory T cells

4.1. Generation of GFP$^+$ CD4$^+$ T cells as a proof of concept

CRISPR-Cas9 mediated gene delivery has been chosen as a method of stable introduction of GFP expression. In order to optimise the protocol, initially CRISPR was performed in bulk CD4$^+$ T cells derived from peripheral blood samples as proof of concept, due to the difficulty of isolating a high number of Tregs from blood for initial tests. The mechanism of CRISPR relies on a synthetic homology-directed repair template (HDRT) which consists of the gene insert flanked by a homology arm on either end, allowing neat incorporation of the gene into the host cell genome (Figure 3). The Cas9 enzyme is responsible for creating a double-stranded break at a precise locus with the aid of site-specific gRNA; the HDRT is subsequently incorporated into the break by the cell's own repair machinery in a process called Homology Directed Repair (HDR). Together, the homology arms of the HDRT and the gRNA confer extremely high target specificity, meaning that the gene insert can be directed to a locus of choice.

HDRTs targeting either CD4 or the housekeeping gene RAB11A were amplified with Agencourt AMPure XP beads (Beckmann Coulter, Cat: A63880) to attain sufficient concentration for CRISPR-Cas9-mediated editing. Bulk CD4$^+$ T cells were isolated from PBMCs using magnetic CD4 Microbeads. Sorted CD4$^+$ cells were either stimulated with CD3/CD28 Dynabeads™ or left unstimulated, and administered with 200 U/mL IL-2 for 3 days before electroporation with CRISPR-Cas9 elements and the HDRT.

Figure 3. CRISPR-Cas9-mediated gene insertion.

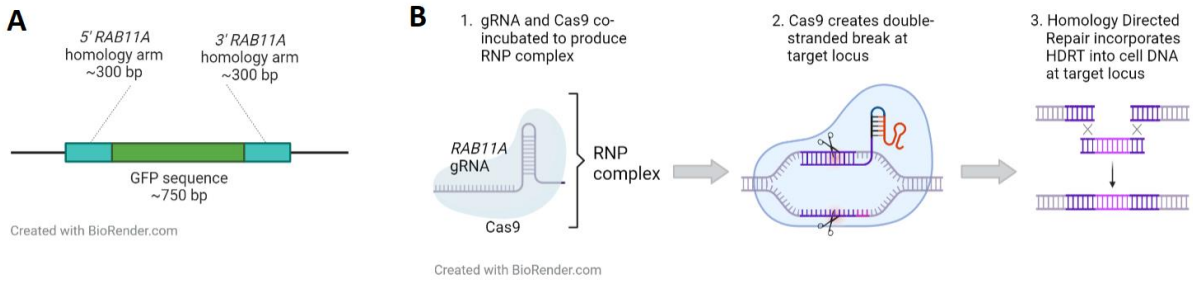


Figure 3. A) The insertion gene (GFP) flanked by two site-specific homology arms. B) CRISPR-Cas9 gene editing employs homology directed repair. The Cas9 enzyme and gRNA together form the ribonucleoprotein (RNP) complex which mediates the insertion of the HDRT into the host cell genome.

Samples were taken from wells at regular intervals starting from 1 day post-electroporation until Day 19 and analysed with flow cytometry. GFP expression was introduced into human $CD4^+$ T cells using CRISPR-Cas9 mediated HDR into either the RAB11A or CD4 locus with high efficiency (approximately 40% GFP^+ cells) and stable expression of the transgene, regardless of the locus (Figure 4).

Figure 4. GFP expression obtained using HDRTs targeting either RAB11A or CD4.

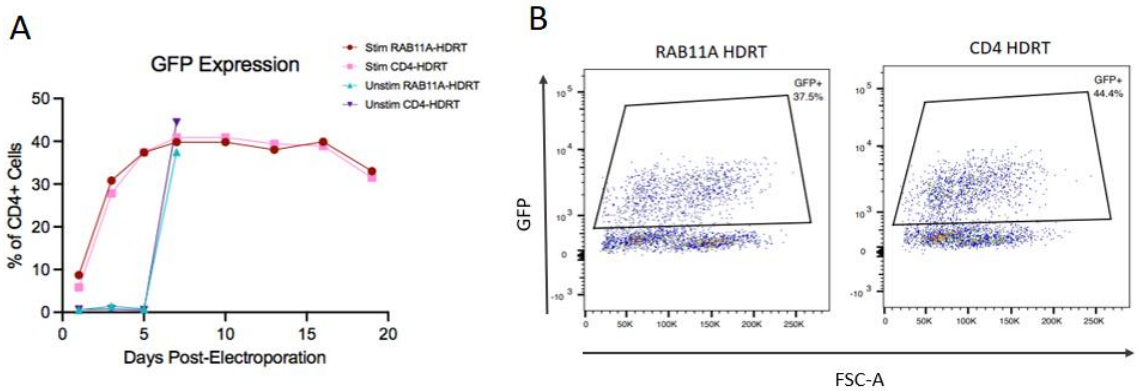


Figure 4. Comparison of GFP expression in $CD4^+$ T cells that underwent electroporation and CRISPR-Cas9 editing using a GFP HDRT targeted to either the RAB11A or the CD4 locus. A) GFP expression up to 19 days post-electroporation. Cells in the RAB11A and CD4 HDRT groups were further divided into those stimulated with CD3/CD28 Dynabeads™ post-electroporation, and those left unstimulated. B) GFP expression was similar at the same timepoint in stimulated $CD4^+$ T cells regardless of the HDRT target gene; the representative FACS plot was taken at Day 7 post-electroporation.

GFP was detected by flow cytometry (BD FACSCanto™ II) as early as 1 day post-electroporation, though expression rose drastically by Day 3 in the CD3/CD28-stimulated group (Figure 4A). Stimulated cells continued to express GFP at a consistent level (30-40%) until Day 16, whereupon GFP expression began to decrease but remain above 30%. The electroporation protocol (used here in conjunction with CRISPR-mediated GFP insertion) was modelled on the protocols of Zhang *et al.* (Zhang et al., 2018) and Roth *et al* (Roth et al., 2018); CRISPR editing was modelled on the protocol of Roth *et al.* (Roth et al., 2018). In their experiments, Roth and colleagues reported 33.7% GFP expression in $CD4^+$ T cells modified using RAB11A-GFP HDRT.(Roth et al., 2018) Therefore, the data presented in Figure 4 is highly consistent with previously reported GFP induction using the same method. This is highly encouraging as it demonstrates the efficacy of CRISPR-Cas9 in establishing long-term gene expression, which could not only be applied to GFP but to other genes of research interest. There was little difference in expression between different integration sites of the GFP sequence (Figure 4B).

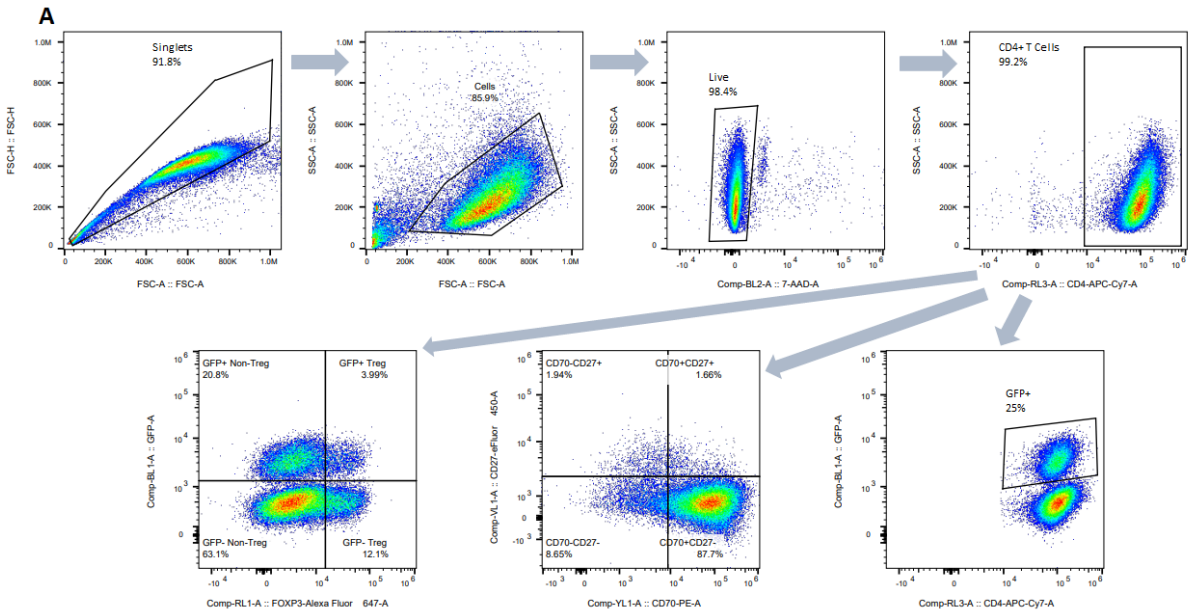
The unstimulated group of bulk $CD4^+$ cells took longer to achieve protein expression than the stimulated groups; expression rose sharply at Day 5, but flow cytometry could no longer be performed after this time point owning to the very small number of cells left in culture in the unstimulated group (Figure 4A).

4.2. Generation of GFP^+ human Tregs

Having demonstrated an efficient introduction of GFP into human $CD4^+$ T cells, a similar experiment was then performed using sorted $CD25^+CD127^{lo}/CD4^+$ human Tregs. This time, RAB11A alone was chosen as the target site for HDRT after considering the likelihood of ablating endogenous CD4 expression through targeting of the of the CD4-encoding gene if CD4-HDRT were used.(Muller et al., 2021) To investigate the effects of CRISPR-mediated GFP

insertion and expression on the suppressive capacity of human Tregs, $CD25^+$ cells were initially isolated from PBMCs using magnetic CD25 Microbeads before undergoing further sorting based on Treg marker expression in a BD FACSAria™ II. Tregs were expanded for 7 days (compared with 3 days for bulk $CD4^+$ cells) in the presence of CD3/CD28 Dynabeads™ and 1000 U/mL IL-2. Dynabeads were removed after 7 days and Tregs were prepared for electroporation as in 4.1, with one group receiving RAB11A-GFP HDRT via electroporation and one receiving electroporation without HDRT. A third group was left in continuous culture without electroporation. Tregs were re-stimulated with CD3/CD28 Dynabeads™ 36 hours post-electroporation. 7 days after electroporation (14 days total of culture), Tregs were analysed with flow cytometry to examine GFP expression across the three conditions of Tregs.

Figure 5. GFP expression in human Tregs 7 days post-electroporation.



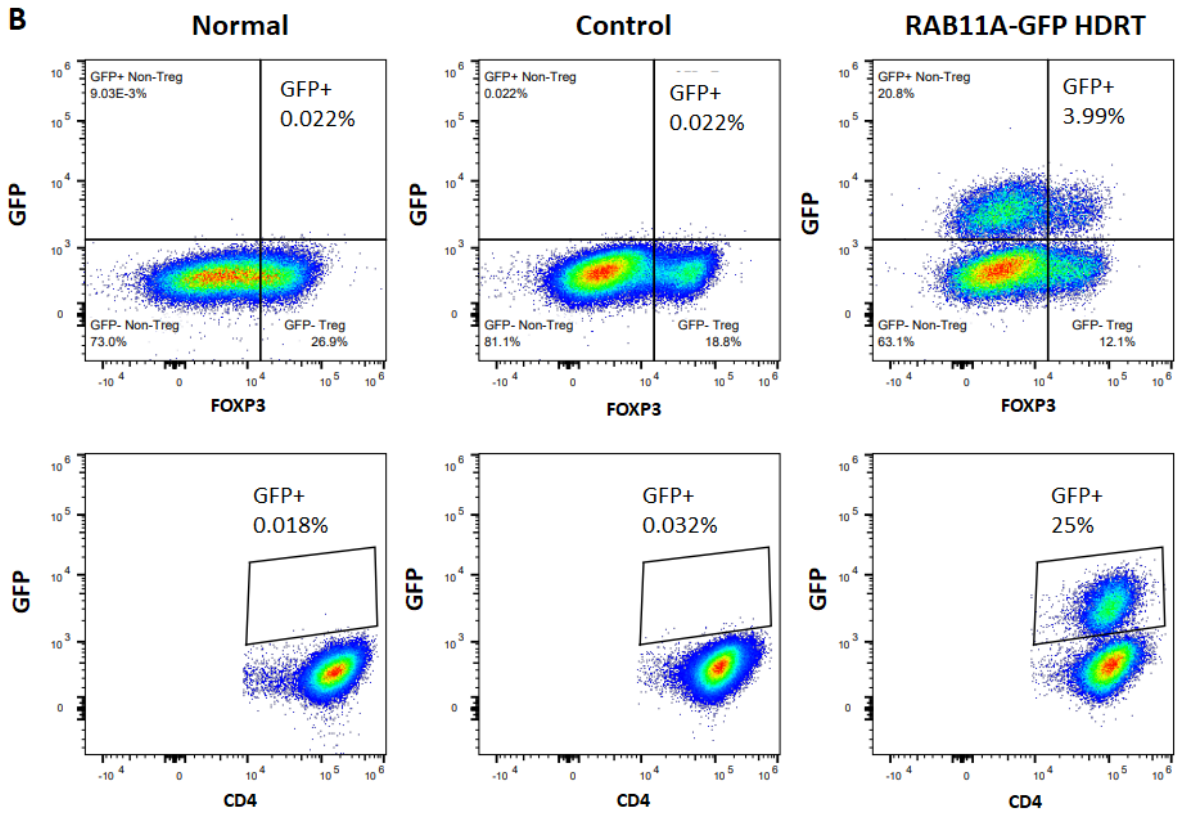


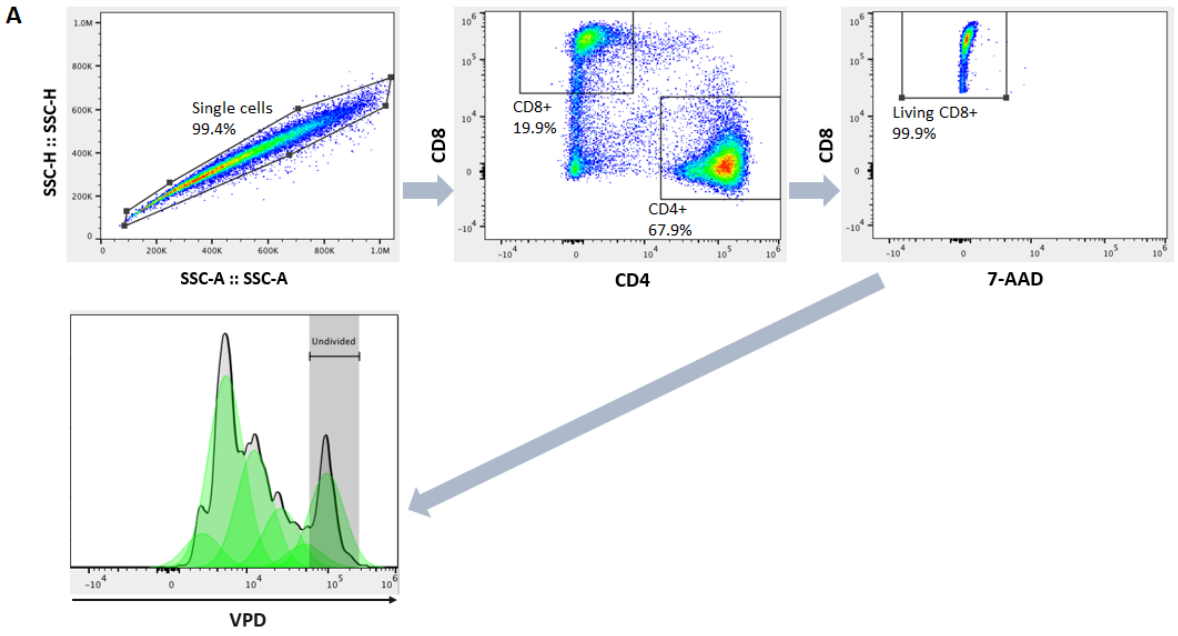
Figure 5. Sorted CD25^{+}CD127^{lo}/CD4^{+} human Tregs were expanded for 7 days before electroporation with RAB11A-GFP HDRT. Three days after electroporation, GFP expression was assessed with flow cytometry. A) Gating strategy represented using the GFP^{+} Tregs treatment group. B) GFP expression was analysed across the Normal Tregs group (no electroporation), Control Tregs group (electroporation, no HDRT, and the GFP^{+} Tregs group (electroporation with RAB11A-GFP HDRT). GFP expression was gated based on CD25^{+}CD127^{lo}/CD4^{+} Tregs and bulk CD4+ T cells (Figure 5B).

The sorting of CD25^{+}CD127^{lo}/CD4^{+} Tregs using Aria was unfortunately found to be sub-optimal, and a contaminating population of CD4^{+}CD25^{-} Tconvs was present during the electroporation stage. Consequently, the representation of Tregs in the treatment groups was low. However, a small population of GFP^{+} Tregs was generated (Figure 5B); moreover, GFP^{+} cells represented 25% of bulk CD4^{+} cells after 7 days of culture, which – although lower than what was attained in Figure 4 during the proof-of-concept experiments, is still an admirable level of editing efficiency and is consistent with CRISPR editing results in the literature.

4.3. Suppressive function of GFP^{+} human Tregs

Having demonstrated that human GFP-expressing Tregs can be generated, an *in vitro* suppression assay was used to test their function (despite the sub-optimal representation of Tregs in the total samples). The day after electroporation, the three treatment groups were cocultured with VPD-stained PBMCs for a further 3 days in ratios of 0:1 (no Tregs to PBMCs) to 1:64 Tregs to PBMCs, and analysed with flow cytometry to quantify the suppressive capacity of GFP$^+$ Tregs *versus* Normal Tregs on CD8$^+$ effector cells (Figure 6). GFP$^+$ Tregs (green) were compared to Control Tregs (blue) and to Normal Tregs (pink) to assess whether GFP induction, or electroporation alone, affected the suppressive capacity of human Tregs. The results were extremely encouraging, especially given the low proportion of true Tregs in the samples, illustrating maintenance of a powerful suppressive capacity.

Figure 6. Proliferation of CD8$^+$ effector cells when cocultured with Tregs.



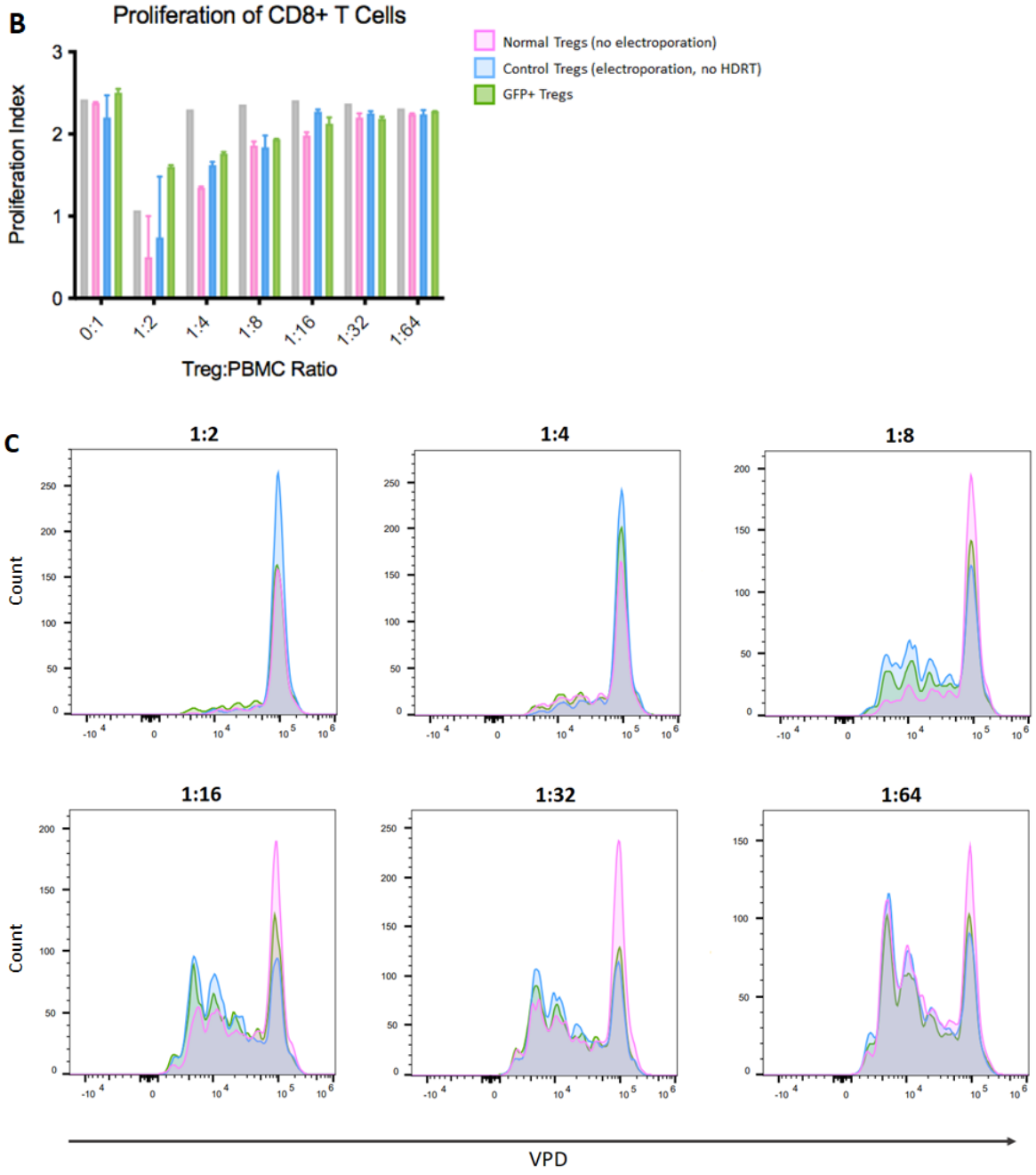


Figure 6. *In vitro* suppression assay testing the ability to inhibit CD8⁺ effector cell proliferation by: Normal Tregs (no electroporation, marked in pink), Control Tregs (electroporation, no HDRT, marked in blue), and GFP⁺ Tregs (marked in green). Cells were cocultured with VPD-stained PBMCs for 3 days before flow cytometry assessment. A) Gating strategy. B) Proliferation indexes for CD8⁺ cells treated with different Treg populations at different ratios. Error bars represent SEM. C) Example histograms of VPD dilution for different ratios of Tregs to PBMCs, illustrating effector cell proliferation.

GFP⁺ Tregs almost completely suppressed CD8⁺ T cell proliferation at a 1:2 ratio, and suppression decreased as expected as ratios moved towards 1:64. Both GFP⁺ Tregs and Control

(electroporated) Tregs exhibited a similar suppressive capacity to Normal (non-electroporated) cells, though this declined at a faster rate to Normal Tregs as ratios increased towards 1:64. Overall, the modified Tregs were extremely effective at suppressing effector cells in this assay.

4.4. Molecular changes upon suppression by GFP$^+$ human Tregs

Having demonstrated that GFP can be introduced into Tregs without affecting their i*n vitro* suppressive capacity (Figure 6), changes in gene expression within *in vitro* cultures were then investigated as a window into the suppressive mechanics of the cell. In this experiment, GFP$^+$ Tregs were compared to non-electroporated Tregs (Normal Tregs). Previously frozen GFP$^+$ Tregs and Normal Tregs (no electroporation) were thawed and cocultured for 3 days with PBMCs in differing ratios before analysis. All Treg treatments also received CD3/CD28 beads. Normal Tregs were obtained from the same donor as the GFP$^+$ Tregs.

Firstly, a positive control of stimulated PBMCs (PBMCs & beads) was compared to a negative control of unstimulated PBMCs (PBMCS only) (Figure 7A). Stimulated PBMCs demonstrated increased expression of certain chemokine and receptor genes, including *CCR2*, *CXCR6*, *IFNG*, and *IL17A*, as well as markers associated with T cell activation, such as *IL2RA* (encoding CD25), *CTLA4*, and *LAG3*. Interestingly, unstimulated PBMCs displayed higher relative expression of certain pro-inflammatory, mostly myeloid-related genes – including markers of innate immune cells (*CD14* and *CD163*), as well as mostly myeloid-related cytokines (such as *IL18*, *IL6*, *IL1A*) and chemokines (such as *CXCL8*, *CXCL9*, *CCL2*, and *CXCL10*). It is known that CD3/CD28 bead stimulation results in intense T cell proliferation and a resulting dilution of the myeloid marker signature on the stimulated PBMCs condition, and this is reflected in the gene expression results.

Next, the differential gene expression was compared between stimulated PBMCs (PBMCs & beads) and stimulated PBMCs cocultured with GFP^+ Tregs at a 1:1 ratio (Figure 7B). Similar to unstimulated PBMCs, the GFP^+ Tregs & PBMCs condition that was earlier demonstrated to be characterised by a significant reduction of T cell proliferation (Figure 6), displayed greater expression of myeoloid-associated genes (*CD163*, *MMP9*, *CCL2*, *CCL18*, *IL6*, *IL1A*, *CCR3*), resulting from a relative preservation of myeloid signature in the absence of T cell expansion. Notably, higher expression levels of the anti-inflammatory genes *TGFBI* and *LILRB4* were observed in the GFP^+ Treg treatment group.

Next, the differential gene expression was compared between stimulated PBMCs (PBMCs & beads) and stimulated PBMCs cocultured with non-electroporated Tregs (Normal Tregs & PBMCs) at a 1:1 ratio (Figure 7c). Similar to both the unstimulated PBMCs and the GFP^+ Treg treatment groups, Control Tregs demonstrated a higher expression of myeloid-related genes (*CD163*, *CCL13*, *CCL18*, *TLR4*) than stimulated PBMCs, indicating maintenance of myeloid signature when effector T cell proliferation is suppressed. Genes downregulated in the presence of Control Tregs included *IFNG*, *GZMB*, *IL13*, and *IL5*, which are associated with inflammation.

Figure 7. Differential gene expression between PBMC-only treatments and Tregs & PBMCs.

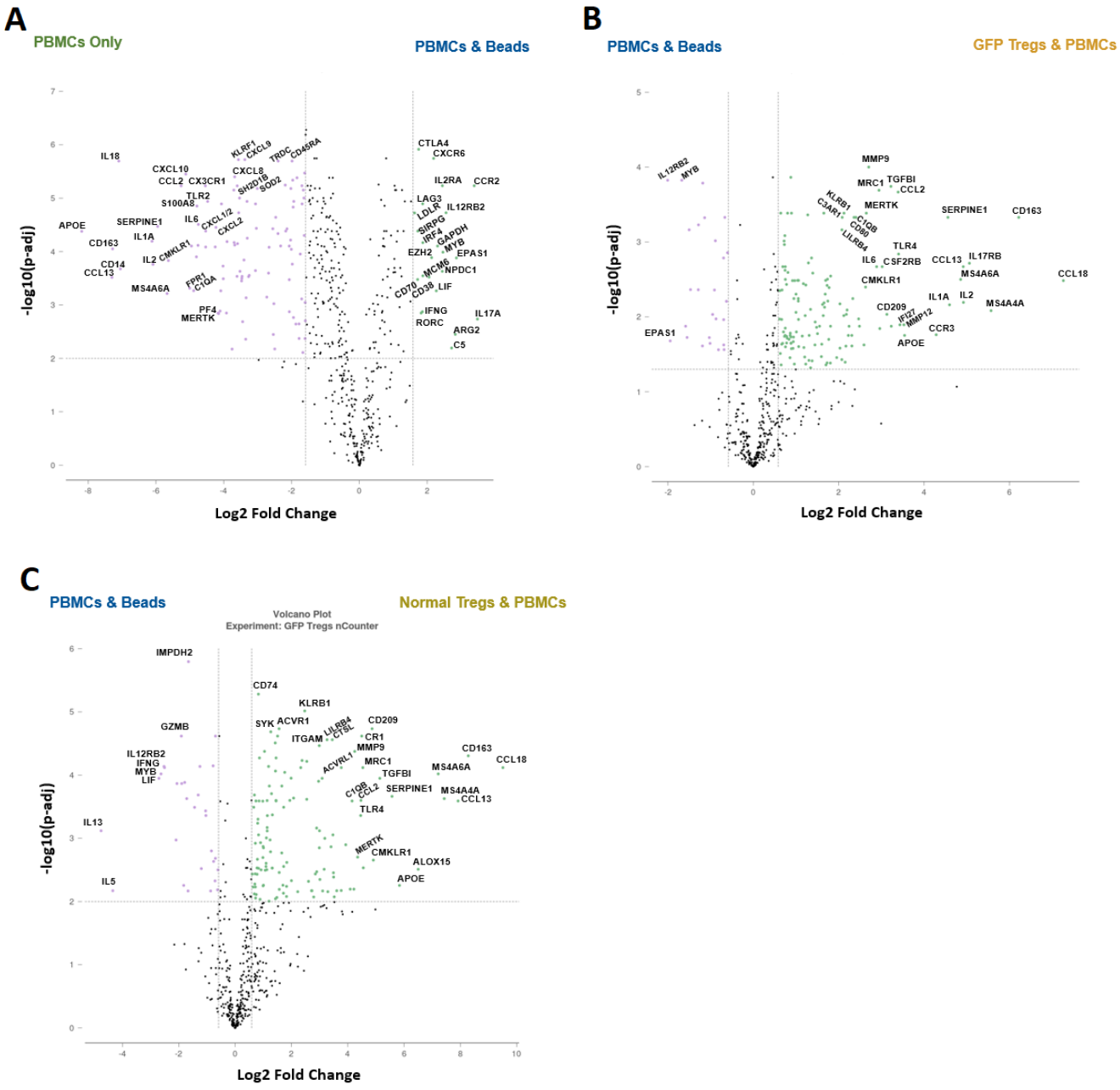


Figure 7. Volcano plots displaying normalised data from nCounter analysis of population-wide gene expression across treatment groups after a 3-day suppression assay, generated with Rosalind software. GFP⁺ Tregs received electroporation with RAB11A-GFP HDRT; Normal Tregs from the same donor did not undergo electroporation or receive HDRT or CRISPR components. A) Comparison of unstimulated (PBMCs Only) *versus* stimulated PBMCs (PBMCs & beads) conditions. B) Comparison of wells containing stimulated PBMCs (PBMCs & beads) *versus* suppressive conditions with GFP-expressing Tregs (GFP⁺ Tregs & PBMCs). C) Comparison of stimulated PBMCs (PBMC & beads) with a coculture of non-electroporated, non-transgenic Tregs and stimulated PBMCs (Normal Tregs & PBMCs).

Gene expression was then compared between both Treg-suppressed conditions, Control Tregs and GFP$^+$ Tregs, to examine if the GFP$^+$ Treg populations had a similar impact to the non-transgenic Tregs on gene expression *in vitro* (Figure 8). Indeed, in contrast to the comparisons depicted in Figure 7, only a few genes were significantly differentially expressed between both conditions. Treatments receiving GFP$^+$ Tregs (GFP$^+$ Tregs & PBMCs) had higher expression of *CD8*, *IL5*, *IL13*, and *IL17RB* when compared to the cocultures with Normal Tregs (Figure 8), possibly reflecting a trend towards slightly impaired suppression as observed in the suppression assay (Figure 6). However, overall, only a handful of genes were differentially expressed, suggesting comparable functional capacity of both Treg populations. This suggests that the combined stresses of electroporation, CRISPR-mediated gene insertion, and GFP expression do not drastically alter the phenotype of human Tregs.

Figure 8. Differential gene expression between GFP-expressing Tregs and Normal Tregs.

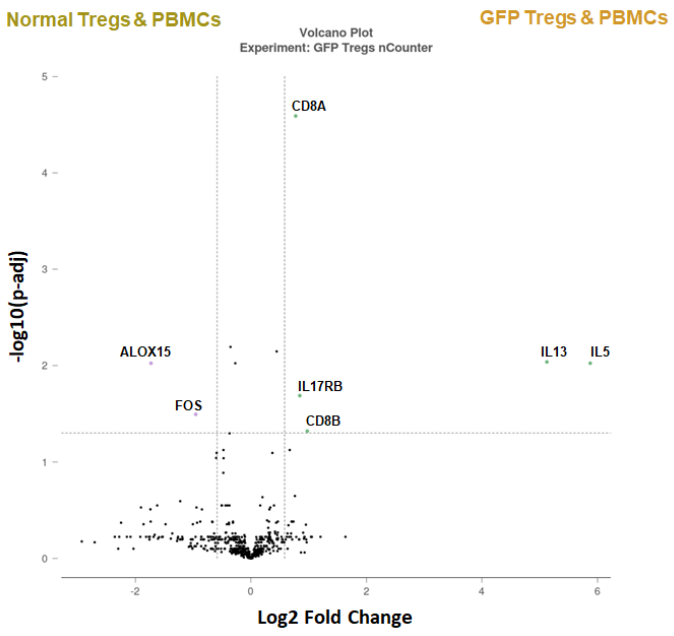


Figure 8. Few significant differences in gene expression were observed between GFP$^+$ Treg and Normal Treg treatment groups.

Looking at the expression of selected anti-inflammatory genes across all conditions, an increase in *IL10*, *IL10RA*, *CTLA4*, *LAG3*, *TGFBI*, *LILRB4*, and *FOXP3* was observed for both Treg-treated conditions compared to stimulated PBMCs only (Figure 9). For T cell-related genes, a decrease in expression of *GZMB*, *IFNG*, *CD8A*, *CD8B*, and *IL17F* was observed for both Treg-treated conditions compared to stimulated PBMCs only (Figure 10). For myeloid-related genes, a higher expression of markers of anti-inflammatory/alternatively activated macrophages *CD163* and *CD209* can be observed in both Treg-treated groups and the unstimulated control, mirrored by myeloid homing chemokines *CCL2*, *CCL13*, and *CCL18* (Figure 11).

Figure 9. Differential expression of anti-inflammatory genes between treatments.

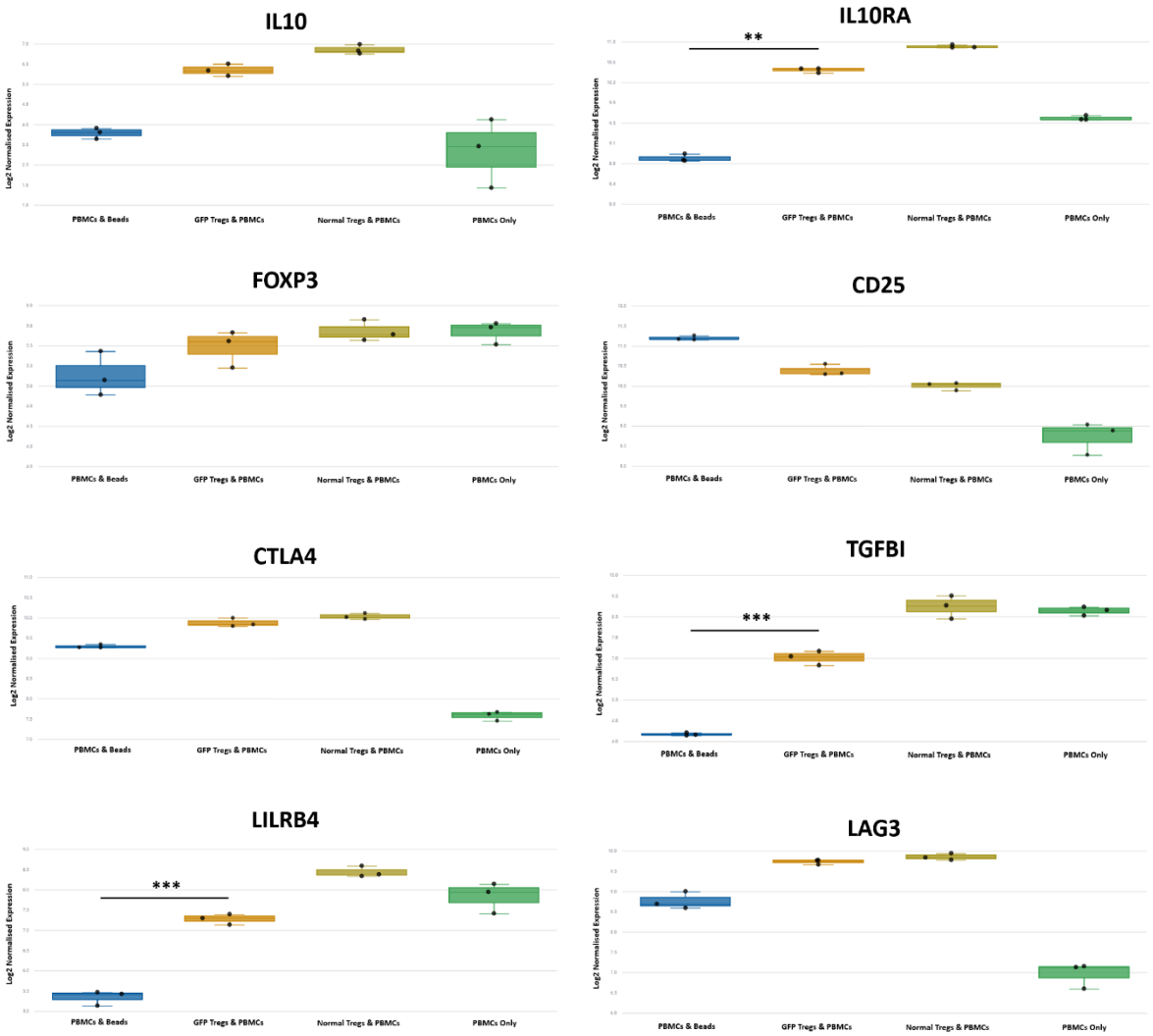


Figure 10. Differential expression of T cell-related genes between treatments.

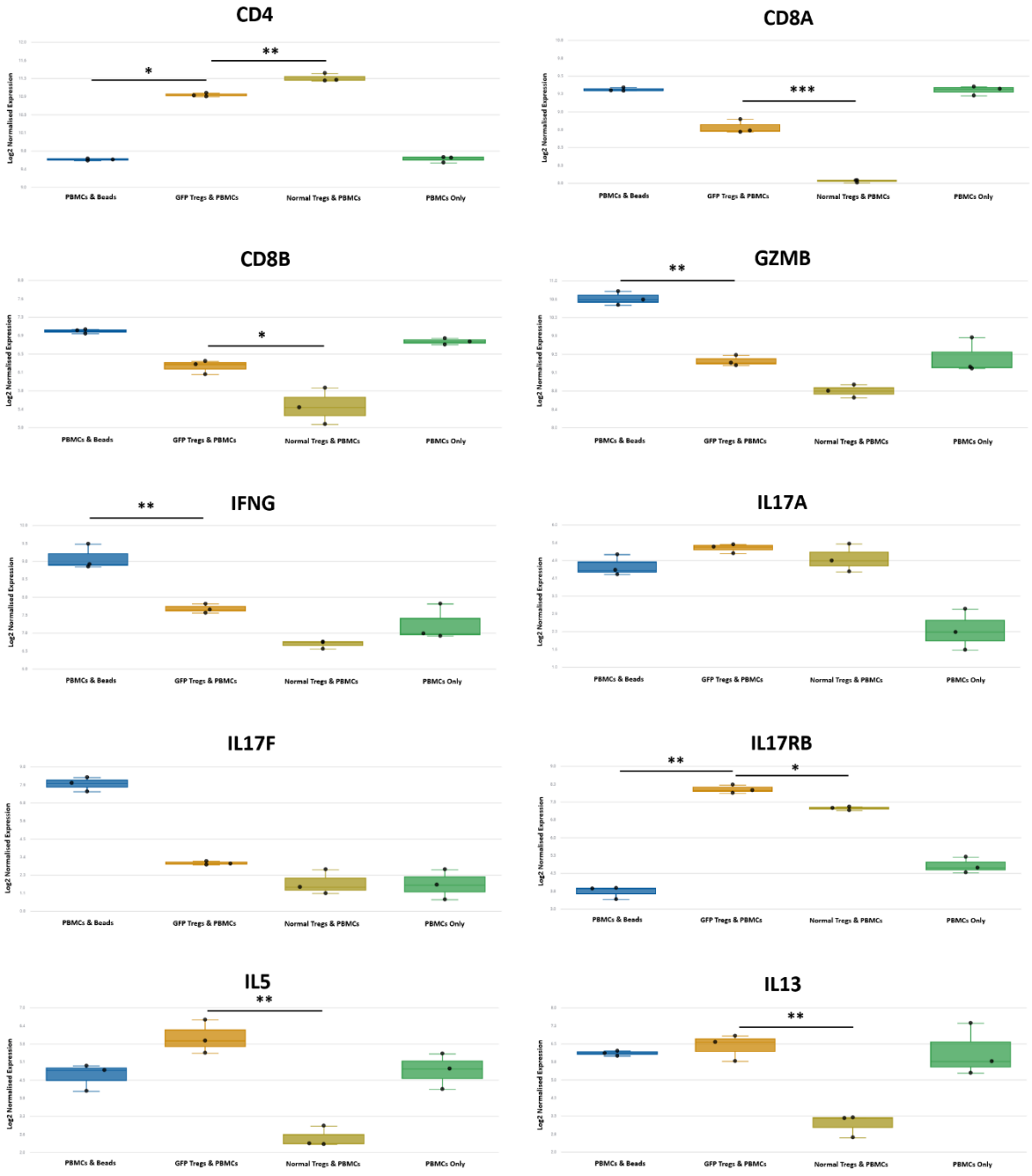
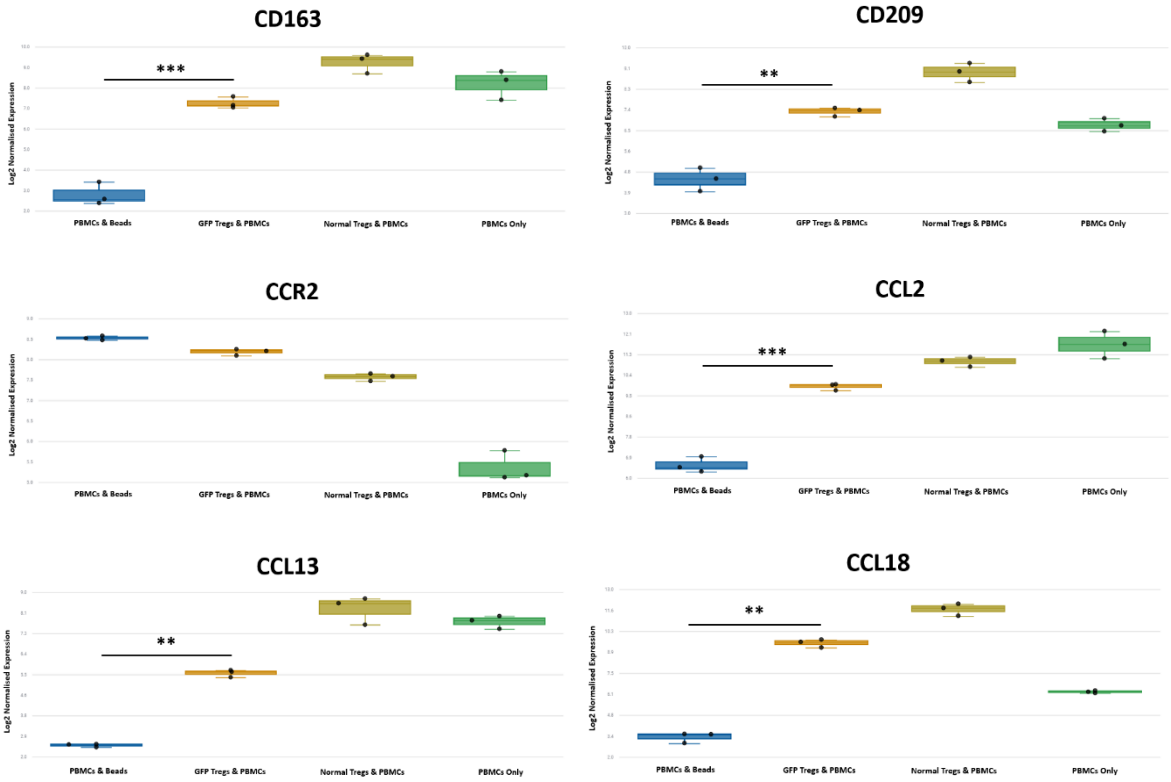


Figure 11. Differential expression of myeloid-related genes between treatments.



Figures 9-11. Box plots generated with Rosalind software showing differential expression of notable genes, based on nCounter analysis of population-wide gene expression across suppression assay treatment groups. N=3. Note that significance is based on adjusted p values. * < 0.05, ** < 0.01, *** < 0.001.

A heatmap was generated representing a computed distribution of different cell subtypes in the different culture conditions (Figure 12). These results echo previous observations in Figures 7-11. A low proportion of $CD8^+$ T cells and Th1 cells was observed in both Treg groups compared to the Treg-less groups which supports the notion of active tolerance. However, no pronounced enrichment in the Treg transcriptional signature in Treg-treated conditions was observed. As discussed previously, a clear downregulation of myeloid signatures (including macrophage, dendritic cell, and neutrophil signatures) was observed in the stimulated PBMCs group as compared to other treatment groups, most likely resulting from strong T cell activation and proliferation within this group.

Figure 12. Cell subtype representation across suppression assay treatment groups.

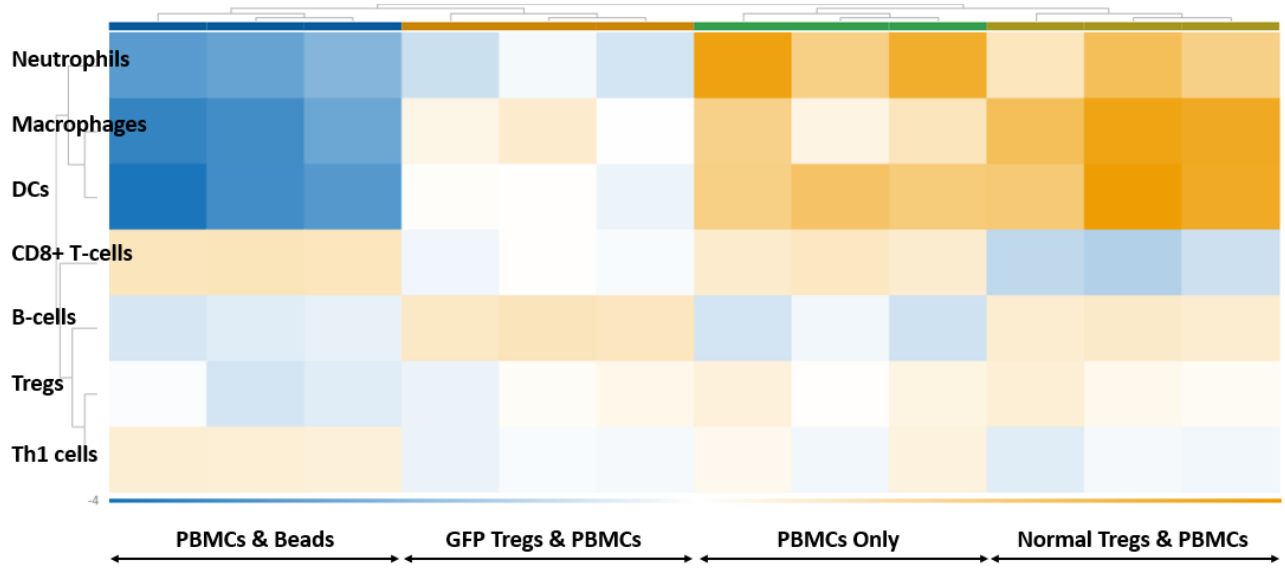


Figure 12. Heat map generated with Rosalind software displaying the representation of different cell subtypes across suppression assay treatment groups, based on marker expression.

Next, cytokine production by Tregs in cocultures with stimulated PBMCs (Figure 13A), or by Tregs in monocultures (Figure 13B), was assessed. As expected, unstimulated Tregs did not produce cytokines (Figure 13B – note that IL-2 was added to Treg-only cultures to ensure survival and must be disregarded in this analysis). Relatively high production of typical proinflammatory cytokines in the stimulated Treg conditions – in particular, IL-5, IL-6, IL-9, IL-13, IL-22, IFN-γ, and TNF-α – might seem surprising, but this has been routinely observed in previous experiments by our group. GFP^+ Tregs and Normal Tregs produced similar levels of IL-10.

When cytokine production was assessed in Treg cocultures with PBMCs (Figure 13A), efficient suppression of IL-2, IL-9, IL-17F, IL-22, IFN-γ, and TNF-α was observed for both populations of Tregs when compared to stimulated PBMC groups (PBMCs & beads). Note the

high readings of IL-10 in both the 1:1 GFP$^+$ Treg treatments and 1:1 Normal Treg treatments compared to the PBMCs (& beads) group, whereas the IL-10 levels in the 1:4 GFP$^+$ Treg and 1:4 Normal Treg wells were only slightly higher than those of the PBMCs (& beads) group. Th2-type cytokines IL-4, IL-5, IL-6, and IL-13, as well as Th17 cytokine IL-17A, seem to be increased in Treg conditions, especially with the GFP$^+$ Tregs.

Figure 13. Normalised Mean Fluorescence Intensity of cytokines in culture supernatant.

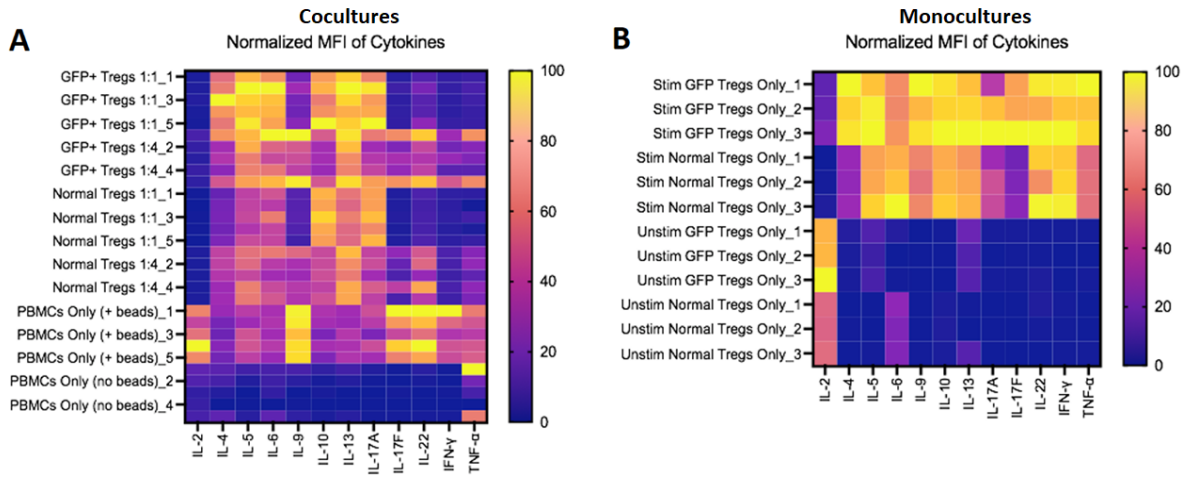


Figure 13. Heat map displaying the normalised MFI values of cytokines in supernatant between treatment groups. Raw data was obtained using the BioLegend™ Multi-Analyte Flow Assay Kit, Human Th Cytokine Panel (12-plex) and processed with BioLegend™ LEGENDplex™ software. Data normalisation and heat map generation were performed in GraphPad Prism Software. MFI values have been scaled from 0 to 100, with 0 representing the lowest expression within the sample range and 100 representing the highest. A) Cytokine production within cell monocultures – these were either stimulated with Dynabeads™ or left unstimulated. B) Cytokine production within suppression assay cocultures containing either GFP$^+$ Tregs & PBMCs, Normal Tregs & PBMCs, PBMCs only (& beads), or PBMCs only (no beads).

Discussion

Overall, the aim of the suppression assay was to investigate any differences in the functionality of CRISPR-Cas9 modified GFP$^+$ Tregs compared to unmodified "Normal" Tregs. The generation of GFP$^+$ Tregs was achieved through a process of electroporation and CRISPR editing, raising concern that electroporation would negatively affect Tregs as it creates temporary

perforations in the cell membrane, in addition to the stress caused by prolonged handling and transfer of cells between mediums during the process.

One caveat of this particular assay was the use of allogeneic target PBMCs, as opposed to autologous PBMCs derived from the same donor as the administered Tregs, due to its retrospective nature. It was therefore expected that some evidence of an allogeneic response would be evident within the treatment wells, leading to elevated production of proinflammatory cytokines and other proteins associated with immune activation. However, this does not detract from the main objective of the assay – to compare the functionality of CRISPR-modified GFP^+ Tregs with unmodified Tregs – and so the data still provides valuable insight into the impacts of genetic modification on Tregs, and particularly on their functionality in an inflammatory environment. Allogeneic Tregs have become an area of interest in the field of immunosuppression owing to the disadvantages of using of autologous cells, principally the interval between isolation from the patient and reinfusion. By contrast, allogeneic cells are envisaged as an "off the shelf" therapy that can be administered when needed, avoiding extended delays for treatment. They may also provide an option in cases where the patient (or animal model) is lymphodepleted or lymphopenic. The data presented here is therefore useful to gain an understanding of the immunological dynamics of allogeneic interaction and whether such Tregs can still exert an effective suppressive action over target cells.

From the data above, it is clear in the first instance that both Treg treatment groups exhibited upregulation of *IL10* and *IL10RA* – perhaps the most iconic cytokine (and its receptor) within the Treg repertoire of tolerogenic tools. Though the upregulation of *IL10* was not statistically significant in either Treg treatment group compared to the Treg-less PBMC groups, it was still several-fold higher. For *IL10RA*, the difference between GFP^+ Tregs and PBMCs & Beads was significant (p-adj = 0.00961). These results are encouraging as they point towards an

induction of Treg activation. Similarly, the anti-inflammatory genes *TGFBI* (p-adj = 0.000181) and *LILRB4* (p-adj = 0.000687) were upregulated in the GFP^+ Treg treatment group compared to PBMCs & Beads. However, it is especially noticeable in the cases of *TGFBI* and *LILRB4* that gene expression in the GFP^+ Treg treatment was reduced compared to Normal Treg treatment, though differences were statistically unsignificant; it appears that these pathways of suppression were less strongly induced by the GFP^+ Tregs, indicating either a reduced or altered functionality of the GFP^+ cells. This trend was also seen to a lesser extent with *IL10* and *IL10RA*, though again, the differences were not significant. This finding is not alarming given the overall upregulation of anti-inflammatory genes in the GFP^+ Treg treatment group, but it is an interesting observation that should be considered during future studies employing CRISPR-modified or GFP^+ Tregs.

CD8A and *CD8B* – markers of cytotoxic T-cells – were significantly higher in the GFP^+ Treg treatment group compared to the Normal Treg group (*CD8A* p-adj = 0.0000257; *CD8B* p-adj = 0.0477), suggesting that the GFP^+ Tregs were less capable of suppressing cytotoxic T cell expansion in an inflammatory setting. The GFP^+ Treg group also exhibited a slight but distinct increase in the expression levels of some proinflammatory genes compared to Normal Tregs, such as *IFNG* (unsignificant) and *IL17RB* (p-adj = 0.0205), also pointing to a reduction in suppressive capacity. Surprisingly, the GFP^+ Treg group showed significantly greater expression of *IL5* (p-adj = 0.00944) and *IL13* (p-adj = 0.00915) compared to the Normal Treg group – these proinflammatory genes are most commonly associated with Th2 cell activity. Since expression of *IL5* and *IL13* in GFP^+ Treg group was comparable to the expression levels in both Treg-less PBMC groups, it is likely that IL5- and IL13-producing cells were actively suppressed in the Normal Treg treatment group, supporting the notion that the modified Tregs were somewhat reduced in their suppressive capabilities.

FOXP3 is an essential marker of Treg identity as it encodes the transcription factor responsible for Treg development, function, and maintenance of phenotype; yet levels of *FOXP3* and *CD25* expression were similar across all four treatment groups, which is surprising considering that 100,000 additional regulatory cells were administered to each of the GFP^+ Treg and Normal Treg wells. Of course, the PBMC-Only groups would have also contained a proportion of Tregs (an estimated 5-10% of total PBMCs), but the levels of *FOXP3* and *CD25* reported by nCounter are underwhelming.(Cohen et al., 2002)

While the above figures provide valuable insight into the immunological environment of the assay treatment groups, and into the efficacy of genetically modified Tregs compared to unaltered Tregs, in some cases it is difficult to draw a conclusion. For example, *GZMB* encodes the cytolytic protein Granzyme B, which is secreted by cytotoxic cells during the proinflammatory response but is also produced by Tregs as a mechanism of tolerogenesis when directed against proinflammatory cells.(Schmidt et al., 2012) In addition, Granzyme B does not always have lytic activity when produced by $CD4^+$ T cells and has recently been implicated in T cell differentiation.(Hoek et al., 2021) Therefore, its presence (or lack thereof) could indicate either a pro- or anti-inflammatory milieu.

The results of the suppression assay demonstrate that GFP^+ Tregs are capable of mounting a suppressive response. These data also demonstrate a marginally weaker capacity for anti-inflammatory gene expression compared to their unmodified counterparts from the same donor. It is unknown at present whether the process of CRISPR editing – which places unnatural stress on the cells – affects their fitness and functionality in the long-term, and this result has not been presented in existing literature to the author's knowledge; yet there is some evidence that GFP can alter cell signalling through interference with the NF-κB pathway, and this may explain the reduced gene expression seen in the suppression assay.(Koelsch et al., 2013) Overall,

CRISPR-modified GFP^+ Tregs still possess an anti-inflammatory gene expression profile, which gives hope that they retain their functionality enough to retain their therapeutic benefits.

5. CAR-Tregs: a literature review

5.1. The clinical need for novel therapeutics in transplantation

While there is no doubt that current pharmacologic immunosuppressants offer prolonged survival and increased quality of life, they do pose significant risks to the patient. Organ toxicity is a major side effect of treatment with pharmacologic agents.(Fellström, 2001) Transplant recipients experience higher incidence of diabetes and cardiovascular disease, and while these diagnoses are strongly influenced by pre-transplantation comorbidities, they are also directly attributable to the use of immunosuppressive drugs.(Agarwal & Prasad, 2016; Miller, 2002) For example, up to 82% of renal transplant patients experience hypertension as a result of treatment with calcineurin inhibitors.(Miller, 2002; Weir et al., 2015) Together, the physiological impacts of immunosuppressive drugs elevate the risk of serious cardiovascular events such as cardiomyopathy, stroke, heart failure, and myocardial infarction.(Fellström, 2001) Organ toxicity in transplant recipients remains a major cause of allograft loss, patient morbidity, and mortality.

A major disadvantage of standard pharmacologic immunosuppressants is their non-specificity; their effects are often imposed on non-target tissues, resulting in toxicity towards otherwise healthy tissues. Ideally, immunosuppressive treatment should be directed to where it is needed, yet this is not the case for many standard drugs which act systemically to compromise the immune response. Long-term treatment with standard immunosuppressants increases the risk of cancer, in particular Kaposi sarcoma and squamous cell carcinoma, owing to the patient's reduced ability to detect and respond to abnormal cells.(Mittal & Colegio, 2017) Patients are also left vulnerable to fungal, mould, bacterial, and viral infections.(Fishman, 2007)

Because of the side effects of standard clinical-use immunosuppressants, there has been growing interest in producing novel cellular therapies to enhance safety towards transplant patients.

5.2. Regulatory T cells as novel therapeutic agents

Regulatory T cells, as discussed in Chapter 1, not only mediate tolerance towards self-antigens in healthy individuals, but they also limit the effector response in the event of allogeneic challenge; therefore, these cells are now under heavy investigation as a novel therapy in the fields of transplantation, autoimmune disease, and inflammatory disease.

Polyclonal Tregs – i.e. bulk Tregs bearing multiple TCR specificities – have been demonstrated in pre-clinical studies to be effective at reducing inflammatory conditions *in vivo*.(Edinger et al., 2003) The success in animal models has been such that polyclonal Tregs have advanced to clinical trials; the first in-human adoptive transfer studies gave evidence to support the use of polyclonal Tregs for the treatment of GvHD and autoimmune disease.(Bluestone et al., 2015; Chandran et al., 2017; Marek-Trzonkowska et al., 2014)

Regulatory T cells soon made their way to the transplant setting, and they have enjoyed safety and feasibility studies in the context of renal and liver transplant recipients.(Mathew et al., 2018; Sawitzki et al., 2020) The ONE Study, investigating the potential for polyclonal Tregs in renal transplant therapy, demonstrated the successful reduction in standard pharmacologic immunosuppression to Tacrolimus monotherapy after Treg infusion, and lower incidence of polyoma virus and cytomegalovirus compared to patients who did not receive Tregs.(Harden et al., 2021)

However, despite the promising suppressive capacity of polyclonal Tregs, there is also clinical evidence that these cell products are capable of conferring systemic immunosuppression on the recipient; as a result, patients have been reported in some trials to remain vulnerable to bacterial and fungal infections, toxoplasmosis, and adenoviral infection, sometimes resulting in mortality.(Di Ianni et al., 2011) This result been contradicted in a Phase

I trial by Mathew *et al.,* who reported no incidence of adverse events or opportunistic infection among renal transplant patients during a nearly two-year period post-infusion with Tregs.(Mathew et al., 2018) In an animal model in which polyclonal Tregs were administered to protect against GvHD, the infusion of therapeutic ratios of Tregs did not interfere with the ability to suppress tumour growth, suggesting maintenance of a functional immune system.(Edinger et al., 2003) However, because of varying reports pertaining to the effects of polyclonal Treg infusion on immunity, research efforts have shifted towards cells bearing antigen specificity in the hopes of generating localised, rather than systemic, suppression.

5.3. Engineered specificity for Tregs

While cell-based therapies circumvent many of the risks associated with pharmacologic drugs, it is possible the administration of polyclonal Tregs will cause long-term adverse effects such as cancer development and chronic toxicity in a similar manner. It has therefore become a major research interest to generate cellular therapies which are capable of localizing to specific tissues.

It has been frequently demonstrated that antigen-specific Tregs are more potent than their polyclonal counterparts and reducing inflammation and preventing allograft rejection.(Boardman et al., 2017; Sagoo et al., 2011) Yet there are many options for achieving antigen specificity in cell products. Sagoo *et al.* described a method of isolating and enriching alloantigen-activated Tregs through exposing a pool of polyclonal Tregs to an allogeneic stimulator. (Sagoo et al., 2011)

A very different approach has been to engineer specificity for an antigen of choice into a cellular product. Studies in the past have transduced TCRs of known specificity into $CD4^+$ cells, such as reported by Tsang *et al.* (Tsang et al., 2008) and Hull *et al.* (Hull et al., 2017). The former

presented the process of retroviral transduction of murine Tregs with TCR genes conferring indirect specificity to MHC-bound peptide, and reported the induction of indefinite graft survival in murine allograft recipients after treatment with the antigen-specific Tregs.(Tsang et al., 2008) Hull *et al.* generated human Tregs with specificity for islet cells using lentiviral transduction with TCR genes with antigen-specific suppression.(Hull et al., 2017) Others have combined CRISPR-mediated TCR insertion with simultaneous deletion of the endogenous TCR to prevent competition for surface expression, unwanted specificity, and early exhaustion.(Legut et al., 2018) However, while TCRs enable the targeting of intracellular antigens through processing and presentation on MHC molecules, their binding is restricted to MHC-presented antigens on the surface of antigen-presenting cells, which represents a major drawback.

5.4. Chimeric Antigen Receptors for engineered specificity

As mentioned in Chapter 1.2, the first chimeric antigen receptor was engineered in 1989 by Gross and colleagues.(Gross et al., 1989) The transgenic cells displayed MHC-independent, antigen-specific effector functions, including the ability to induce cytokine production in their target cells.

Although many researchers have focused on transducing recombinant TCRs into therapeutic cells as a means of conferring antigen specificity – and indeed, promising results have been reported from experimental models of type 1 diabetes and multiple sclerosis using this method (Hull et al., 2017; Kim et al., 2018) – the principal advantage of CARs is that, unlike TCRs, they do not rely on antigen presentation by MHCs for activation. The antibody-derived region enables CAR-expressing cells to bind any extracellular peptide, including MHCs themselves.

Second-generation CARs have drastically improved the longevity and proliferation of CAR-expressing cells.(Kowolik et al., 2006; Weinkove et al., 2019) The most commonly used domains are CD28 or 4-1BB (CD137), although CD27, OX40, ICOS (CD278), and CD40L have been used to a lesser extent. Third generations have an additional costimulatory domain to combine the advantages and overcome the limitations of individual domains; for example, a study by Ramos *et al.* found that the combination of CD28 and 4-1BB resulted in greater persistence and expansion compared to second-generation CARs with CD28 alone.(Ramos et al., 2018) Finally, fourth-generation CARs include a cytokine domain to further manipulate the immune environment, such as a proinflammatory cytokine domain to improve anti-tumour activity by CAR-expressing Tconvs. Irrespective of generation number, all CAR designs consist of a basic formula: an antigen-binding region (usually derived from an antibody), a transmembrane domain, and a CD3ζ chain at the intracellular tail to propagate the activation signal.

The concept of incorporating a modular receptor into Tregs for antigen-targeting was borrowed from existing technology in the field of cancer immunotherapy. For many years, researchers have been engineering CARs into conventional T cells in order to achieve targeted, enhanced tumour clearance. Not only does the inclusion of the CAR help to reduce aberrant binding in non-target tissues, it also increases the potency of the cell therapy by directing it to where it is needed. Early animal models of CAR-Tconvs elegantly showed the high therapeutic efficacy of CAR expression, and following on from the success of pre-clinical studies, these engineered cells progressed to clinical trials, where they produced significantly greater tumour clearance and incidence of complete remission compared to standard treatments.(Maude et al., 2018; Neelapu et al., 2017) Indeed, the novel CAR-Tconv therapy tisagenlecleucel achieved a complete remission rate of 93% in an early phase I/IIa trial of 75 cancer patients.(Maude et al., 2018) The field of immunosuppression has been slow to catch up with the technology, but

in 2016, the first publication examining the safety and efficacy of CAR-Tregs in a transplant model was published.(MacDonald et al., 2016) The study by MacDonald *et al.* developed an HLA-A2-specific CAR-Treg and found it to have antigen-specific suppressive functions, and importantly was superior to Tregs bearing an irrelevant specificity at preventing GvHD.(MacDonald et al., 2016) Soon afterwards, studies were conducted on HLA-A2-specific CAR-Tregs in the context of transplantation that illustrated the superiority of HLA-A2 CARs at preventing allograft rejection compared to polyclonal or non-HLA-A2-specific Tregs.(Boardman et al., 2017; Noyan et al., 2017)

Harking back to the distinct ability of CARs to bind MHC molecules, Human Leukocyte Antigens (HLAs) – the human equivalent of MHCs – expressed on the surface of nucleated cells have been identified as attractive targets for CAR-Tregs in the context of transplantation. Since, in genetically distinct individuals, there will be discrepancies between the HLA repertoire of the donor and recipient, it is possible to create a truly donor-specific cell product by targeting an HLA allele unique to the donor and avoid off-target binding on autologous organs.(Wright et al., 2022) Pre-clinical studies of antigen-specific Tregs have therefore focused on targeting these molecules. HLA-A2 is one of the most common HLA alleles across human populations, implicating that a large number of patients can be treated with a single CAR bearing this specificity.(Ikhtiar et al., 2018; Luo et al., 2002; Saito et al., 2016; Sanchez-Mazas et al., 2017) Indeed, murine models of allogeneic solid organ transplantation involving CAR-Tregs have invariably utilized HLA-A2-specific CARs.(Boardman et al., 2017; MacDonald et al., 2016; Noyan et al., 2017; Sicard et al., 2020) As the field of CAR-Treg therapy expands, other common HLA antigens will be explored as potential targets in order to cover the different haplotypes present across human populations.

The MHC-unrestricted CAR is able to bind to MHC molecules directly, meaning that HLAs can function as the target antigen. This is extremely relevant in the context of allogeneic transplantation, as the inevitable discrepancies between the MHC allelic repertoire of the

allogeneic donor organ and the transplant recipient – even in well-matched transplants – provide the opportunity for highly specific targeting of the donor organ. CARs have the unique ability to recognise and bind MHC antigens themselves without the need for antigen presentation, meaning that this technology is ideal for delivering localised cell therapy based on the MHC expression of the organ. Prior to the development of CARs, this would not have been possible to such as extent with other methods of engineered specificity.

Overall, CARs are synthetic constructs composed of individual segments that may be added or subtracted, derived from different sources, or substituted to suit the requirements of the application. Below is a representative summary of different applications of CAR-Tregs to illustrate the variety of research uses.

Table 2. Designs and applications of CAR-Tregs.

Author/Date	Insertion Method	Research Field	Antigen Target	CAR Design Features	Results of CAR$^+$ Tregs
(Elinav et al., 2008)	Retroviral transduction	Inflammation	2,4,6-trinitrophenol (TNP)	CD28 domain, FcRγ intracellular tail	In a murine model of colitis, transferred CAR-Tregs reduced colitis symptoms in an antigen-specific, dose-dependent manner
(Fransson et al., 2012)	Lentiviral transduction	Autoimmunity	Myelin oligo-dendrocyte glycoprotein (MOG)	CD28 domain, CD3ζ intracellular tail	CAR-Tregs localised to the CNS after intra-nasal delivery, and significantly suppressed Tconv proliferation & proinflammatory cytokine production
(MacDonald et al., 2016)	Lentiviral transduction	GvHD/marrow transplantation	HLA-A2	CD28 domain, CD3ζ intracellular tail	CAR stimulation achieved greater expansion and activation (CD69) vs TCR; CAR-Tregs maintained

					FOXP3$^+$ levels and preferentially interacted with HLA-A2$^+$ cells
(Boardman et al., 2017)	Lentiviral transduction	Transplantation	HLA-A2	CD28 domain, CD3ζ intracellular tail, eGFP tag, cMyc tag	HLA-A2 CAR-Tregs were more potent suppressors of HLA-A2$^+$ cells than HLA-A2$^-$ cells, and reduced damage of skin allografts in mice compared to polyclonal CAR-Tregs
(Pierini et al., 2017)	Transient transfection	Transplantation, GvHD/marrow transplantation	FITC	"mAbCAR" design with FITC-targeting CAR bound to FITC-conjugated monoclonal antibody. CD28 domain, CD3ζ intracellular tail, FLAG	Allowed efficient, modular use of CARs with monoclonal antibodies, and allowed antigen-specific Treg localisation and tolerance induction
(Yoon et al., 2017)	Retroviral transduction	Haemophilia	FVIII	CD28 domain, CD3ζ intracellular tail, GFP tag	FVIII CAR-Tregs strongly proliferated in the presence of FVIII compared to polyclonal Tregs, and can exert bystander suppression
(Noyan et al., 2017)	Retroviral transduction	Transplantation	HLA-A2	CD28 domain, CD3ζ intracellular tail, ΔLNGFR tag	CAR-Tregs reduced swelling, and improved graft survival in skin allografts in mice compared to polyclonal CAR-Tregs – even up to 40 days of graft survival without other immune-suppression
(Skuljec et al., 2017)	Transfection	Allergy	Carcino-embryonic antigen (CEA)	CD28 domain, CD3ζ intracellular tail	CAR-Tregs localised to CEA$^+$ organs (especially lungs and spleen) but not CEA$^-$ organs in mice, and reduced inflammation and mucus production compared to polyclonal Tregs

(Zhang et al., 2018)	Retroviral transduction	Haemophilia	FVIII	CD28 domain, CD3ζ intracellular tail	CAR-Tregs significantly prevented anti-FVIII Ab production by B cells *in vitro* and *in vivo*
(Tenspolde et al., 2019)	Retroviral transduction	Autoimmunity	Insulin	CD28 domain, CD3ζ intracellular tail, Foxp3, Thy1.1 tag	CAR-Tregs were as suppressive as polyclonal Tregs; they did not prevent diabetes in NOD/Ltj mice but did persist for up to 17 weeks in the spleen
(Imura et al., 2020)	Retroviral transduction	Autoimmunity	CD19	CD28 domain, CD3ζ intracellular tail, Venus tag	CAR-Tregs significantly inhibited B cell proliferation and Ab production compared to polyclonal Tregs; this was largely dependent on TGF-β production
(Pohl et al., 2020)	Retroviral transduction	Haemophilia	FVIII-specific memory B cells	FVIII-A2 chain binding region, CD28 domain, CD3ζ intracellular tail, ZsGreen	An antigen fragment could be used as binding region to bind anti-FVIII antibody-producing B cells, thereby suppressing formation of polyclonal anti-FVIIIAb secreting cells.
(Sicard et al., 2020)	Retroviral transduction	Transplantation	HLA-A2	Myc tag, CD28 domain, CD3ζ intracellular tail	CARs caused antigen-specific immunosuppressi on but required CAR-mediated antigen binding for persistence
(Martin et al., 2021)	Lentiviral transduction	GvHD/marrow transplantation	HLA-A2	CD28 domain, CD3ζ intracellular tail, hFOXP3	Both $CD4^+CD25^+$ and CD4+25- cells were engineered to express Foxp3 using the CAR; CAR-Tregs produced less proinflammatory cytokine than polyclonal Tregs,

					and reduced GvHD severity in mice
(Lee et al., 2022)	Retroviral transduction	Transplantation	C4d	CD28 domain, CD3ζ intracellular tail	When transferred into murine recipients of ABO-incompatible heart allografts, CAR-Tregs infiltrated the graft and improved graft survival
(Schreeb et al., 2022)	Lentiviral vector	Transplantation	HLA-A2	CD28 domain, CD3ζ intracellular tail	First proposed in-human trial of CAR-Tregs; results unpublished

A wide range of studies encompassing transplantation, allergy, haemophilia, and autoimmune disease have employed CAR-Tregs in recent years. Perhaps it is due to the phenomenal success of CAR-Tconvs in experimental cancer therapy that researchers have been inspired to apply the technology to other areas of immunology. In the representative selection of literature describing CAR-Treg generation in Table 2, CAR designs are generally of the "second-generation", i.e. they contain only one costimulatory domain, and CD28 is by far the most popular choice. Some designs include a FACS-detectable tag such as cMyc, for which the cells require antibody staining prior to flow cytometry. Retroviral transduction is extremely well represented as a transduction method, possibly due to the reputation of viral delivery systems as having long-term, stable gene expression, which is highly suitable for long-term studies wishing to investigate the kinetics, localisation, and persistence of CAR-Tregs *in vivo* to assess their clinical relevance. As can be seen in the table, CAR-Tregs form an extremely recent branch of Treg engineering, but their popularity is exploding as researchers increasingly seek alternatives to traditional pharmacologic immunosuppressants.

6. Construction of a third-generation CAR specific for HLA-A2

As discussed in the previous chapter, the use of CAR-Tregs over polyclonal expanded Tregs can be beneficial in transplantation; research has demonstrated their higher expansion rate upon antigen stimulation and their superior potency at preventing allograft rejection.(Boardman et al., 2017; Noyan et al., 2017; Skuljec et al., 2017; Yoon et al., 2017) In a murine model, it was found that an infusion of CAR-Tregs could maintain allograft survival for 40 days without concurrent immunosuppressive drugs.(Noyan et al., 2017) Additionally, they have shown preferential, antigen-specific homing to their target organ which supports the use of CAR therapy as a means of avoiding systemic immunosuppression.(Fransson et al., 2012; Skuljec et al., 2017)

Third-generation CARs have been demonstrated to be superior to second-generation CARs in terms of persistence and therapeutic efficacy in conventional T cells, owing to the fact that the presence of two costimulatory domains counteracts the pitfalls of each individual costimulatory domain and combines the advantages of each; as previously mentioned, a study by Ramos *et al.* found that by combining the domains CD28 and 4-1BB within the same CAR, transgenic cells showed greater expansion and persistence.(Ramos et al., 2018) There have, however, been no published examples of third-generation CARs in Tregs to date.

CD28 is by far the most commonly selected domain for CARs and was therefore deemed to be a reliable choice; the inclusion of CD28 is known to confer a high proliferation rate in the host cells. However, its high intracellular activation signal results in faster onset of exhaustion and reduced persistence.(Guedan et al., 2018; Salter et al., 2018) CD28 is particularly favoured in CAR designs for Tregs, perhaps because it promotes a high level of IL-10 secretion and overall suppressive capacity when expressed by Tregs.(Boroughs et al., 2019)

CD27, on the other hand, is far less extensively used although it holds promise as a costimulatory domain as demonstrated by Song *et al.,* who reported that human T cells bearing a

CD27 domain showed greater persistence compared to those bearing a CD28 domain.(Song et al., 2012) As persistence is reduced in CD28 CARs, inclusion of CD27 with CD28 might theoretically compensate for this while conferring the superior suppressive capacity, cytokine production, and cellular expansion of CD28 CARs.(Boroughs et al., 2019; Song et al., 2012) Therefore, a CD28-CD27 CAR was expected to produce transgenic Tregs with superior longevity and suppressive function.

In this chapter, a third-generation CAR was developed with specificity for HLA-A2. HLA-A2 was selected as the target for the CAR design as it is a major antigen of interest in transplantation. Discrepancies between the HLA haplotypes of donor organs and recipient patients means that targeting Tregs to a "non-self" HLA molecule promotes high specificity for the donor organ and reduces systemic immunosuppression. Moreover, HLA-A2 has been the standard target antigen for models of allogeneic solid organ transplantation in CAR-Treg studies.(Boardman et al., 2017; MacDonald et al., 2016; Noyan et al., 2017; Sicard et al., 2020)

A Myc tag was also incorporated into the CAR design as an independent means of testing CAR expression, although the CAR would be later incorporated into an eGFP plasmid.

6.1. Isolation of BB7.2 scFV sequence from hybridomas

To confer suitable specificity to the CAR construct, a BB7.2 hybridoma line with specificity for HLA-A2 was expanded for 14 days. Hybridomas were then harvested, frozen as dry pellets, and subsequently underwent RNA extraction to obtain genomic material using the RNeasy Mini Kit. RNA was then converted to DNA via reverse transcription using the High-Capacity cDNA Reverse Transcription Kit.

A selection of putative primers was tested in different combinations by PCR to identify the most likely candidates for complete isolation of the heavy and light chains of the BB7.2 variable

regions (Figure 14). Based on the fluorescence of the gel bands, the optimal combinations were used to produce the light and heavy chain BB7.2 sequences.

Figure 14. Identification of correct primer combinations for BB7.2 chain amplification.

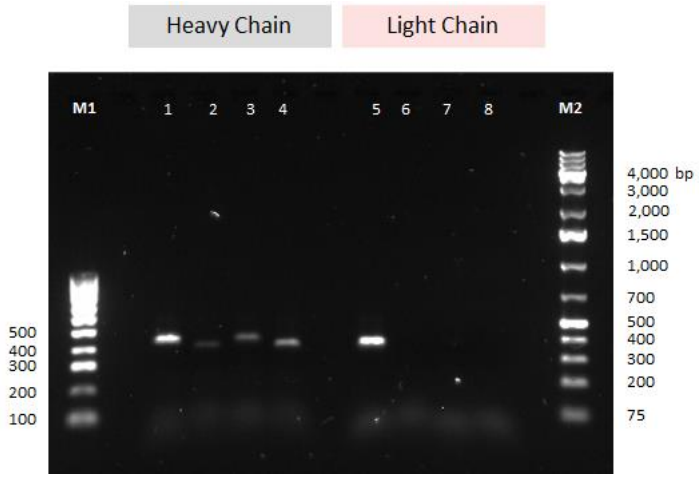


Figure 14. PCR-mediated trials of putative forward primers for the heavy and light chains of BB7.2 anti-HLA-A2 monoclonal antibody, using hybridoma-derived DNA as the PCR template. Different PCR conditions were tested (data not shown) and the optimal conditions were confirmed: DNA denaturation at 96°C, annealing at 67°C, and extension at 72°C. Pooled primers were initially tested (data not shown) before four promising candidates from the light and heavy chain groups were selected for individual PCRs with the reverse primers. After PCR amplification, samples were loaded onto a 1.2% agarose TAE gel alongside HyperLadder™ 100bp (annotated as M1) and GeneRuler 1 kb DNA Ladder (annotated as M2). Numbers 1-4 on the electrophoresis gel represent the results of PCRs of forward primers DLP85, DLP90, DLP93, DLP94 in combination with the reverse primer DLP95 (Heavy Chain); numbers 5-8 represent the results of PCRs of forward primers DLP96, DLP99, DLP100, DLP103 in combination with the reverse primer DLP106. Visible bands are the result of binding and amplification with primers, leading to the selection of successful primers for isolation of the full BB7.2 scFv chains.

After screening of putative primers, it was determined that the combination of DLP85/DLP95 for the heavy chain, and DLP96/DLP106 for the light chain, were the optimal candidates for producing full-length light and heavy chain BB7.2 fragments for sequencing. PCR products were cloned and sent for Sanger sequencing, and the nucleotide sequence for each was obtained.

6.2. Construction of the HLA-A2-specific CAR

The sequences of the light and heavy chains were used to construct the scFv antigen-binding region of the CAR. Additional components of the CAR were chosen either for a specific therapeutic or research purpose (e.g. CD28 and CD27 costimulatory domains, and the Myc tag), or – for structural components – because of their prevalence in previous CAR designs.

Figure 15. Design of the CAR construct.

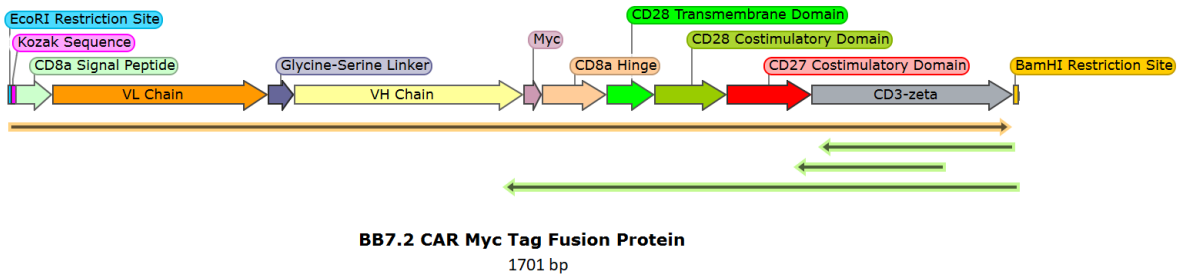


Figure 15. Image obtained with SnapGene software, © 2021 Insightful Science. The complete CAR was designed using SnapGene software, and sequences for other components were obtained through freely available published sources listed in Chapter 2.4.

The CAR sequence was sent for synthesis off-site with the Invitrogen GeneArt Gene Synthesis service. A pMK cloning vector was selected as the backbone with kanamycin resistance for screening.

6.3. Insertion of the CAR into a pIRES2-eGFP expression plasmid

Following synthesis of the CAR construct within a pMK vector, the CAR-pMK plasmid DNA was transformed into OneShot® chemically competent bacterial cells for amplification, with kanamycin as a selection antibiotic. The plasmid was purified and digested with EcoRI-HF and BamHI-HF high-fidelity enzymes for 3 hours at 37°C to release the CAR construct from the pMK backbone.

The restriction digest was repeated using the same enzymes for a pIRES2-eGFP-ND26 expression vector and this was briefly treated for 30 minutes with CIAP to reduce self-ligation later on. Digestion products were run through gel electrophoresis to separate the DNA fragments. The CAR fragment and the pIRES2-eGFP backbone were identified on their respective gels (Figure 16A); the gel bands were excised and processed using the Wizard® SV Gel and PCR Clean-up System to obtain eluted DNA.

To incorporate the CAR sequence into the pIRES2-eGFP-ND26 expression plasmid, the digested CAR fragment and the digested pIRES2-eGFP were combined in a ligation reaction at room temperature for 16 hours. This was then transformed into competent cells and plasmids were later purified. The plasmids were then run on a gel to confirm successful ligation (5 repeats corresponding to 5 selected bacterial colonies on the agar plate following transformation) (Figure 16B). Owing to the lack of colonies on the ligation control plates (CAR alone, and pIRES vector alone) it was unfortunately not possible to run these controls on the gel. However, the presence of a single band of the correct estimated size confirmed that ligation had succeeded.

Figure 16. Gel electrophoresis verification of restriction digests and ligation.

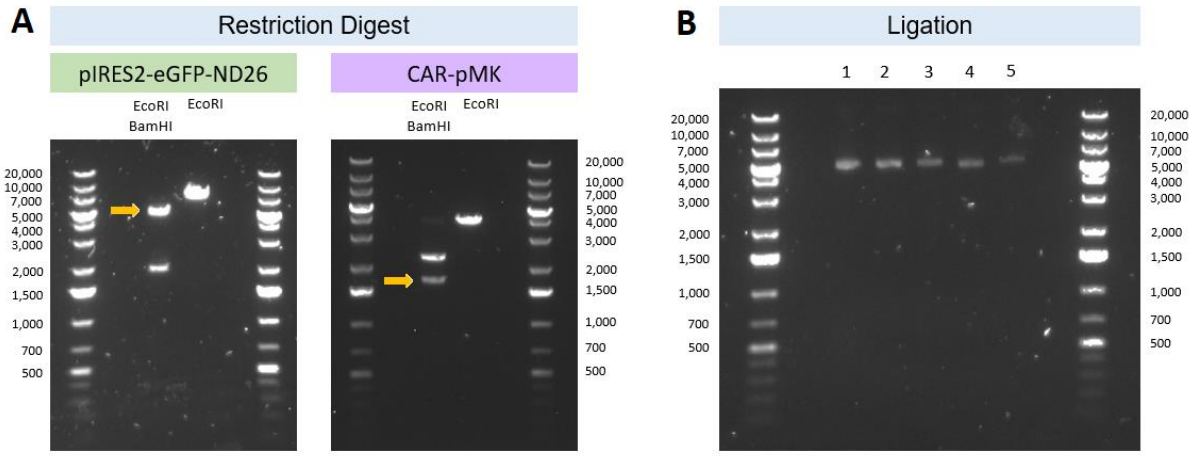


Figure 16. Restriction digests of piRES2-eGFP-ND26 fluorescent expression plasmid and CAR-pMK cloning plasmid, followed by transfer of the CAR sequence into the expression plasmid. A) pIRES2-eGFP-ND26 expression plasmid and CAR-pMK cloning plasmid were each incubated with the restriction enzymes EcoRI and BamHI in the presence of rCutSmart™ Buffer for 3 hours at 37°C; both enzymes corresponded to restriction sites on the plasmid, resulting in a linearized pIRES2-eGFP backbone and a separate irrelevant DNA fragment for the expression vector digest, and a purified CAR sequence and an irrelevant pMK backbone for the CAR digest. A control with EcoRI only (no BamHI) was performed simultaneously to illustrate the incomplete excision of DNA between the two restriction sites. pIRES-eGFP was further incubated in 1 U/µL Calf Intestinal Alkaline Phosphatase after digestion to prevent self-ligation. The upper-left gel band in Figure A – pIRES-eGFP-ND26 – contained purified, fully digested pIRES-eGFP (~5000 bp). The bottom-left gel band in Figure A – CAR-pMK – contained purified BB7.2 CAR (~1700 bp). These gel bands were excised, and DNA was eluted using the Wizard® SV Gel and PCR Clean-up System. B) After DNA elution, the pIRES-eGFP and CAR fragments were combined in a ligase reaction using T4 ligase in T4 Ligase Buffer at room temperature for 16 hours. Putative ligated plasmids were transformed into competent cells for amplification, and were later isolated using the Qiagen Plasmid Mini Kit. Purified ligated pIRES2-eGFP-CAR plasmids were then loaded onto 1.0% agarose TAE gels for verification.

Figure 17. Schematic diagram of the restriction digest and ligation procedure.

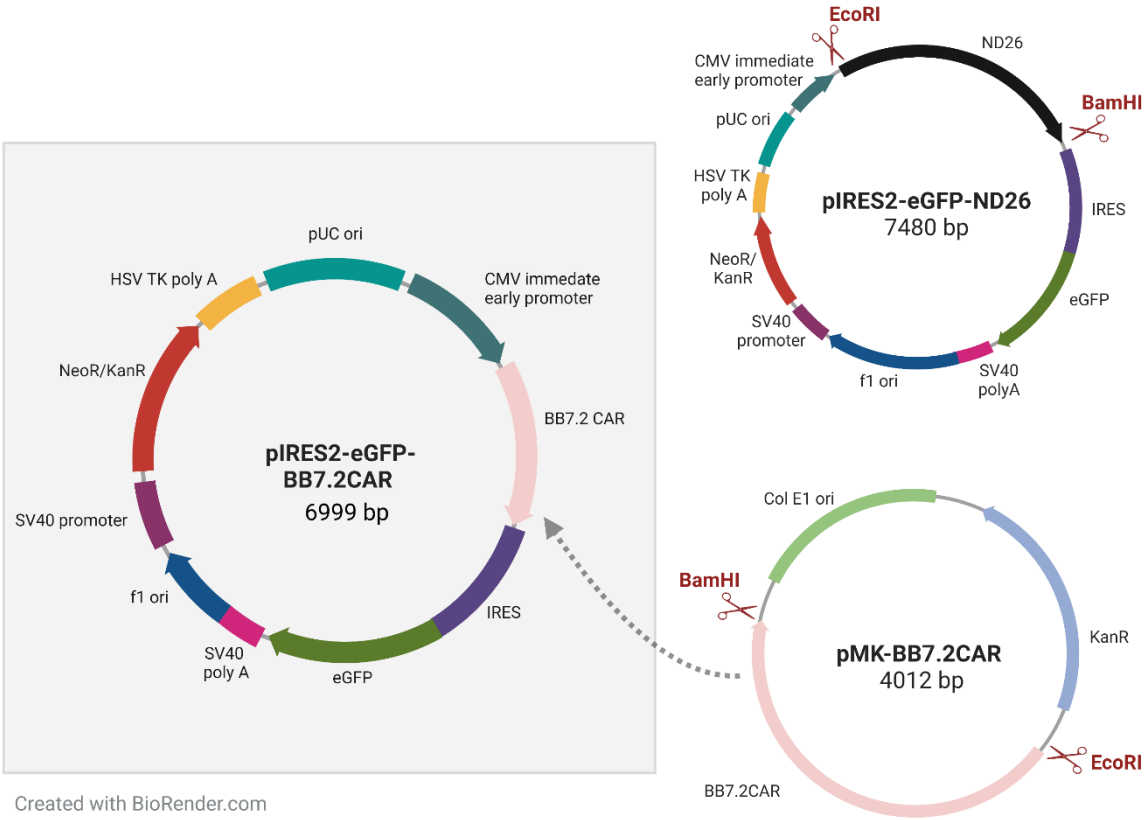


Figure 17. Following digest with EcoRI and BamHI, the BB7.2 CAR is transferred to the pIRES2-eGFP expression vector to produce a new plasmid encoding the CAR and GFP, which can be co-expressed in a host cell using an IRES.

Discussion

The final product was an expression vector suitable for human cells, bearing eGFP for convenient sorting and *in vivo* localisation, and importantly containing a third-generation CAR with specificity for HLA-A2. This construct holds potential for investigating the effects of a third-generation CAR on Treg functionality, which has not yet been explored in the literature. It also represents a potentially valuable tool for experimental models of allogeneic transplantation.

When the study was initiated, it was envisaged that the CAR would be tested against HLA-A2 tetramers to provide confirmation of target binding, and subsequently tested against HLA-$A2^+$ and HLA-$A2^-$ human cells to prove their efficacy in culture. It was also envisaged that the CAR would ultimately be introduced into human Tregs using CRISPR-Cas9, using the same protocol that was optimised during the GFP experiments in this thesis. However, owing to a combination of extended periods of optimising experiments and the resulting shortage of time, and the disruption to research caused by the COVID-19 pandemic, this stage was never reached. However, these tests of the HLA-A2 CAR would be the next stage in confirming the suitability of the BB7.2 CAR construct for use in transplantation research.

7. Conclusions and future directions

7.1. GFP expression as a research tool

In this thesis, I have put forward the argument for GFP expression as an invaluable tool for research through a detailed literature review. I have also discussed the potential implications of GFP insertion and expression on the behaviour of cells. The suppression assays presented in Chapters 2.5.4. and 2.5.5. support the argument that GFP insertion does not deleteriously affect the functionality of Tregs, and that Tregs receiving GFP HDRT subsequently show a gene expression profile consistent with unmodified Tregs (Figures 8 and 9). PBMCs cultures receiving GFP^+ Treg treatment showed in a marginal increase in proinflammatory gene expression compared to treatment with unmodified Normal Tregs, specifically *CD8*, *IL5*, *IL13*, and *IL17RB* (Figures 8 and 10), which was reflected in a slightly inferior suppressive capacity of GFP^+ Tregs as observed from VPD staining of a separate coculture assay (Figure 6), yet many anti-inflammatory genes classically associated with Treg phenotype were similar between both Treg groups, notably *FOXP3*, *CD25*, *CTLA4,* and *IL10* (Figure 9).

The levels of IL-10 protein in coculture supernatant were similar between GFP^+ and unmodified Tregs, showing that the production of anti-inflammatory cytokine was not impaired in genetically modified GFP^+ Tregs (Figure 13). This is extremely reassuring as IL-10 represents a major mechanism of suppression for Tregs.

In addition, a lower $CD8^+$ cell marker signature was observed in PBMC cultures receiving Tregs – both GFP^+ and unmodified – compared to PBMCs alone, consistent with the VPD results presented in Figure 6 showing an inhibitory effect of both Treg groups on the proliferation of effector $CD8^+$ T cells. Of major interest, GFP^+ Tregs exerted potent suppression of effector $CD8^+$ cells when cocultured at ratios of 1:2 and 1:4, despite the impure population of Tregs after Aria sorting before electroporation (Figures 6B and 6C); suppression was

comparable to that of unmodified Tregs as observed by the VPD staining and proliferation indexes (Figures 6B and 6C).

It appears that CRISPR-mediated GFP expression results in a *marginal* decrease in Treg suppressive capacity but does not hinder their cytokine production or their ability to inhibit the proliferation of effector $CD8^+$ T cells *in vitro*. Overall, the data presented suggests that GFP expression represents a valuable tool for cell labelling and does not drastically alter the phenotype of regulatory T cells. Maintenance of phenotypic behaviour following GFP modification renders these cells a reliable tool for *in vitro* studies.

It would be extremely interesting to test these GFP^+ Tregs in an *in vivo* humanized mouse model to assess, A) Treg homing to the allograft compared with homing to autologous immune and non-immune organs; B) whether infiltrated Tregs inside the allograft represent the descendants of adoptively transferred Tregs, or whether they are induced *in vivo*.

As per the original intention of this thesis, it would be equally interesting to see whether CRISPR-mediated insertion of the BB7.2 CAR into human Tregs, as was initially planned, would display similar editing efficiency as GFP (considering the difference in size), and importantly whether CAR expression would alter the phenotype of Tregs. This remains for future studies.

7.2. Third-generation Chimeric Antigen Receptor expression in human Tregs

The development of a third-generation CAR for expression in Tregs represents a novel achievement as this has not been done previously – at least not in published literature. Although experiments for this thesis did not reach the point of introducing the CAR construct to human Tregs, this would be the next step of research.

As discussed in the previous chapters, the distinct ability of CARs to bind MHC molecules renders them unique in the world of synthetic receptors. Human Leukocyte Antigens (HLAs) – the human equivalent of MHCs – expressed on the surface of nucleated cells have been identified as attractive targets for CAR-Tregs in context of transplantation. HLA-A2 is the most common allele across human populations, implicating that a large number of patients could be treated with a single CAR bearing this specificity.(Ikhtiar et al., 2018; Luo et al., 2002; Saito et al., 2016; Zhou et al., 2015) Murine models of allogeneic solid organ transplantation involving CAR-Tregs have invariably utilized HLA-A2-specific CARs.(Boardman et al., 2017; MacDonald et al., 2016; Noyan et al., 2017; Sicard et al., 2020)

The CAR design presented in this thesis incorporates two costimulatory domains: CD28, known for inducing high cell proliferation and higher activation; and CD27, known to improve the persistence of CAR-expressing cells. Future experiments should seek to compare the anti-inflammatory function, as well as cell proliferation and persistence, of this third-generation CAR in human Tregs compared to a CAR bearing only one of these domains, to verify the effects of combining these two domains in one construct.

As with GFP-expressing Tregs, it would be extremely interesting to examine BB7.2CAR-expressing Tregs in humanized mouse models to observe the kinetics and therapeutic effects of these CARs *in vivo*, which could hold great significance for the clinical application of CAR-Tregs in the future.

8. Appendices

8.1. Complete sequence of the BB7.2-specific CD28-CD27 CAR

GAATTCACCACCATGGCGCTGCCGGTGACCGCGCTGCTGCTGCCGCTGGCGCTGCTGCTGCATGCGGCGC
GCCCGGATGTTTTGATGACCCAAACTCCACTCTCCCTGCCTGTCAGTCTTGGAGATCAAGTCTCCATCTCTT
GCAGATCTAGTCAGAGCATTGTACATAGTAATGGAAACACCTATTTAGAATGGTACCTGCAGAAACCAGGC
CAGTCTCCAAAGCTCCTGATCTACAAAGTTTCCAACCGATTTTCTGGGGTCCCAGACAGGTTCAGTGGCA
GTGGATCAGGGACAGATTTCACACTCAAGATCAGCAGAGTGGAGGCTGAGGATCTGGGAGTTTATTACT
GCTTTCAAGGTTCACATGTTCCTCGGACGTTCGGTGGAGGCACCAAGCTGGAAATCAAACGGGCTGATG
CTGCACCAACTGTACCAGGCGGCGGCGGCAGCGGCGGCGGCGGCAGCGGCGGCGGCGGCAGCCAGGT
GCAGCTGAAGCAGTCTGGACCTGAGCTGGTGAAGCCTGGGGCCTCAGTGAAGATGTCCTGCAAGGCTTC
TGGCTACACCTTCACAAGCTACCATATACAGTGGGTGAAGCAGAGGCCTGGACAGGGACTTGAGTGGATT
GGATGGATTTATCCTGGAGATGGTAGTACTCAGTACAATGAGAAGTTCAAGGGCAAGACCACACTGACTG
CAGACAAATCCTCCAGCACAGCCTACATGTTGCTCAGCAGCCTGACCTCTGAGGACTCTGCGATCTATTTC
TGTGCAAGGGAGGGGACCTACTATGCTATGGACTACTGGGGTCAAGGAACCTCAGTCACCGTCTCCTCAG
CCAAAACGACACCCCCATCTGACTATCCACTGGAACAGAAACTGATTAGCGAAGAAGATCTGCCGACCCC
GGCGCCGACCATTGCGAGCCAGCCGCTGAGCCTGCGCCCGGAAGCGTGCCGCCCGGCGGCGGGCGGC
GCGGTGCATACCCGCGGCCTGGATTTTGCGTGCGATTTTTGGGTGCTGGTGGTGGTGGGCGGCGTGCTG
GCGTGCTATAGCCTGCTGGTGACCGTGGCGTTTATTATTTTTTGGGTGCGCAGCAAACGCAGCCGCGGCG
GCCATAGCGATTATATGAACATGACCCCGCGCCGCCCGGGCCCGACCCGCAAACATTATCCGTATGCGCCG
CCGCGCGATTTTGCGGCGTATCGCAGCCAGAGGAGGAAGTACAGGAGCAACAAGGGCGAGAGCCCCGT
GGAGCCCGCCGAGCCCTGCAGGTACAGCTGCCCCAGGGAGGAGGAGGGCAGCACCATCCCCATCCAGG
AGGACTACAGGAAGCCCGAGCCCGCCTGCAGCCCCCGCGTGAAATTTAGCCGCAGCGCGGATGCGCCG
GCGTATAAACAGGGCCAGAACCAGCTGTATAACGAACTGAACCTGGGCCGCCGCGAAGAATATGATGTGC
TGGATAAACGCCGCGGCCGCGATCCGGAAATGGGCGGCAAACCGCGCCGCAAAAACCCGCAGGAAGGC
CTGTATAACGAACTGCAGAAAGATAAAATGGCGGAAGCGTATAGCGAAATTGGCATGAAAGGCGAACGC
CGCCGCGGCAAAGGCCATGATGGCCTGTATCAGGGCCTGAGCACCGCGACCAAAGATACCTATGATGCGC
TGCATATGCAGGCGCTGCCGCCGCGCTAAGGATCC

Appendix Table 1. Full sequence of the CD28-CD27-BB7.2-CAR, including EcoRI restriction site (GAATTC, position 1-6 bp), Kozak sequence (ACCACC, position 7-12 bp), CD8α extracellular signal peptide (ATGGCGCTGCCGGTGACCGCGCTGCTGCTGCCGCTGGCGCTGCTGCTGCATGCGGCGCGCCCG, position 13-75 bp), and BamHI restriction site (GGATCC, position 1696-1701 bp). The construct is 1701 bp in total.

8.2. Impact of COVID-19 on this thesis

The COVID pandemic had a significant effect on the research conducted for this thesis and the resulting data that could be obtained from practical experiments. However, I have decided to present the data that was acquired during my studentship as I believe it holds significance for the field of Treg immunotherapy and provides a stepping stone for further progression in research towards allograft-specific immunotherapy in transplantation.

9. Bibliography

Addey, C., White, M., Dou, L., Coe, D., Dyson, J., & Chai, J.-G. (2011). Functional Plasticity of Antigen-Specific Regulatory T Cells in Context of Tumor. *The Journal of Immunology*, *186*(8), 4557–4564. https://doi.org/10.4049/JIMMUNOL.1003797

Agarwal, A., & Prasad, G. V. R. (2016). Post-transplant dyslipidemia: Mechanisms, diagnosis and management. *World Journal of Transplantation*, *6*(1), 125–134. https://doi.org/10.5500/wjt.v6.i1.125

Akkaya, B., Oya, Y., Akkaya, M., Al Souz, J., Holstein, A. H., Kamenyeva, O., Kabat, J., Matsumura, R., Dorward, D. W., Glass, D. D., & Shevach, E. M. (2019). Regulatory T cells mediate specific suppression by depleting peptide–MHC class II from dendritic cells. *Nature Immunology 2019 20:2*, *20*(2), 218–231. https://doi.org/10.1038/s41590-018-0280-2

Andersson, J., Tran, D. Q., Pesu, M., Davidson, T. S., Ramsey, H., O'Shea, J. J., & Shevach, E. M. (2008). CD4+FoxP3+ regulatory T cells confer infectious tolerance in a TGF-β–dependent manner. *Journal of Experimental Medicine*, *205*(9), 1975–1981. https://doi.org/10.1084/JEM.20080308

Bedoya, F., Ghassemi, S., June, C. H., Levine, B. L., Melenhorst, J. J., Milone, M. C., Powell, D. J. J., & Zheng, Z. (n.d.). *US10273300B2 - Methods of making chimeric antigen receptor-expressing cells - Google Patents*. Retrieved October 7, 2022, from https://patents.google.com/patent/US10273300B2/en

Bluestone, J. A., Buckner, J. H., Fitch, M., Gitelman, S. E., Gupta, S., Hellerstein, M. K., Herold, K. C., Lares, A., Lee, M. R., Li, K., Liu, W., Long, S. A., Masiello, L. M., Nguyen, V., Putnam, A. L., Rieck, M., Sayre, P. H., & Tang, Q. (2015). Type 1 diabetes immunotherapy using polyclonal regulatory T cells. *Science Translational Medicine*, *7*(315). https://doi.org/10.1126/SCITRANSLMED.AAD4134/SUPPL_FILE/7-315RA189_SM.PDF

Boardman, D. A., Philippeos, C., Fruhwirth, G. O., Ibrahim, M. A. A., Hannen, R. F., Cooper, D., Marelli-Berg, F. M., Watt, F. M., Lechler, R. I., Maher, J., Smyth, L. A., & Lombardi, G. (2017).

Expression of a Chimeric Antigen Receptor Specific for Donor HLA Class I Enhances the Potency of Human Regulatory T Cells in Preventing Human Skin Transplant Rejection. *American Journal of Transplantation*, *17*(4), 931–943. https://doi.org/10.1111/ajt.14185

Boissel, L., Betancur, M., Lu, W., Wels, W. S., Marino, T., Van Etten, R. A., & Klingemann, H. (2012). Comparison of mRNA and lentiviral based transfection of natural killer cells with chimeric antigen receptors recognizing lymphoid antigens. *Leukemia and Lymphoma*, *53*(5), 958–965. https://doi.org/10.3109/10428194.2011.634048/SUPPL_FILE/DISCLOSURE.ZIP

Boroughs, A. C., Larson, R. C., Choi, B. D., Bouffard, A. A., Riley, L. S., Schiferle, E., Kulkarni, A. S., Cetrulo, C. L., Ting, D., Blazar, B. R., Demehri, S., & Maus, M. V. (2019). Chimeric antigen receptor costimulation domains modulate human regulatory T cell function. *JCI Insight*, *4*(8). https://doi.org/10.1172/jci.insight.126194

Brogdon, J., Gill, S., June, C. H., Kalos, M. D., Loew, A., & Scholler, J. (n.d.). *Effective targeting of primary human leukemia using anti-cd123 chimeric antigen receptor engineered t cells - Patent US-2017183415-A1 - PubChem*. Retrieved October 7, 2022, from https://pubchem.ncbi.nlm.nih.gov/patent/US-2017183415-A1

Brusko, T. M., Koya, R. C., Zhu, S., Lee, M. R., Putnam, A. L., McClymont, S. A., Nishimura, M. I., Han, S., Chang, L. J., Atkinson, M. A., Ribas, A., & Bluestone, J. A. (2010). Human Antigen-Specific Regulatory T Cells Generated by T Cell Receptor Gene Transfer. *PLOS ONE*, *5*(7), e11726. https://doi.org/10.1371/JOURNAL.PONE.0011726

Chandran, S., Tang, Q., Sarwal, M., Laszik, Z. G., Putnam, A. L., Lee, K., Leung, J., Nguyen, V., Sigdel, T., Tavares, E. C., Yang, J. Y. C., Hellerstein, M., Fitch, M., Bluestone, J. A., & Vincenti, F. (2017). Polyclonal Regulatory T Cell Therapy for Control of Inflammation in Kidney Transplants. *American Journal of Transplantation*, *17*(11), 2945–2954. https://doi.org/10.1111/AJT.14415

Chang, S. H., Kim, T. J., Kim, Y., Han, S. S., Lee, S. K., Sim, J. H., Kim, Y. J., Lee, S. J., Rhyu, I. J., Nam, K. H., Mohan, C., & Kim, H. R. (2019). Impacts of GFP-FoxP3+ regulatory T cells on lupus hallmarks differ by genetic background and type of GFP knock-in.

Https://Doi.Org/10.1080/08916934.2019.1657098, *52*(5–6), 199–207. https://doi.org/10.1080/08916934.2019.1657098

Chen, K. Y., Liu, J., & Ren, E. C. (2012). Structural and functional distinctiveness of HLA-A2 allelic variants. In *Immunologic Research* (Vol. 53, Issues 1–3, pp. 182–190). https://doi.org/10.1007/s12026-012-8295-5

Cohen, J. L., Trenado, A., Vasey, D., Klatzmann, D., & Salomon, B. L. (2002). CD4+CD25+ Immunoregulatory T Cells New Therapeutics for Graft-Versus-Host Disease. *Journal of Experimental Medicine*, *196*(3), 401–406. https://doi.org/10.1084/JEM.20020090

D'Addio, F., Riella, L. V., Mfarrej, B. G., Chabtini, L., Adams, L. T., Yeung, M., Yagita, H., Azuma, M., Sayegh, M. H., & Guleria, I. (2011). The Link between the PDL1 Costimulatory Pathway and Th17 in Fetomaternal Tolerance. *The Journal of Immunology*, *187*(9), 4530–4541. https://doi.org/10.4049/JIMMUNOL.1002031

Dai, Y., Li, J., Li, J., Dai, G., Mu, H., Wu, Q., Hu, K., & Cao, Q. (2007). Skin epithelial cells in mice from umbilical cord blood mesenchymal stem cells. *Burns*, *33*(4), 418–428. https://doi.org/10.1016/J.BURNS.2006.08.028

Delemarre, E. M., Van Den Broek, T., Mijnheer, G., Meerding, J., Wehrens, E. J., Olek, S., Boes, M., Van Herwijnen, M. J. C., Broere, F., Van Royen, A. V., Wulffraat, N. M., Prakken, B. J., Spierings, E., & Van Wijk, F. (2016). Autologous stem cell transplantation aids autoimmune patients by functional renewal and TCR diversification of regulatory T cells. *Blood*, *127*(1), 91–101. https://doi.org/10.1182/BLOOD-2015-06-649145

Deuse, T., Hu, X., Gravina, A., Wang, D., Tediashvili, G., De, C., Thayer, W. O., Wahl, A., Garcia, J. V., Reichenspurner, H., Davis, M. M., Lanier, L. L., & Schrepfer, S. (2019). Hypoimmunogenic derivatives of induced pluripotent stem cells evade immune rejection in fully immunocompetent allogeneic recipients. *Nature Biotechnology 2019 37:3*, *37*(3), 252–258. https://doi.org/10.1038/s41587-019-0016-3

Di Ianni, M., Falzetti, F., Carotti, A., Terenzi, A., Castellino, F., Bonifacio, E., Del Papa, B., Zei, T.,

Iacucci Ostini, R., Cecchini, D., Aloisi, T., Perruccio, K., Ruggeri, L., Balucani, C., Pierini, A., Sportoletti, P., Aristei, C., Falini, B., Reisner, Y., … Martelli, M. F. (2011). Tregs prevent GVHD and promote immune reconstitution in HLA-haploidentical transplantation. *Blood*, *117*(14), 3921–3928. https://doi.org/10.1182/BLOOD-2010-10-311894

Edinger, M., Hoffmann, P., Ermann, J., Drago, K., Garrison Fathman, C., Strober, S., & Negrin, R. S. (2003). *CD4 + CD25 + regulatory T cells preserve graft-versus-tumor activity while inhibiting graft-versus-host disease after bone marrow transplantation*. https://doi.org/10.1038/nm915

Elinav, E., Waks, T., & Eshhar, Z. (2008). Redirection of Regulatory T Cells With Predetermined Specificity for the Treatment of Experimental Colitis in Mice. *Gastroenterology*, *134*(7), 2014–2024. https://doi.org/10.1053/J.GASTRO.2008.02.060

Eller, K., Kirsch, A., Wolf, A. M., Sopper, S., Tagwerker, A., Stanzl, U., Wolf, D., Patsch, W., Rosenkranz, A. R., & Eller, P. (2011). Potential Role of Regulatory T Cells in Reversing Obesity-Linked Insulin Resistance and Diabetic Nephropathy. *Diabetes*, *60*(11), 2954–2962. https://doi.org/10.2337/DB11-0358

Eyquem, J., Mansilla-Soto, J., Giavridis, T., Van Der Stegen, S. J. C., Hamieh, M., Cunanan, K. M., Odak, A., Gönen, M., & Sadelain, M. (2017). Targeting a CAR to the TRAC locus with CRISPR/Cas9 enhances tumour rejection. *Nature 2017 543:7643*, *543*(7643), 113–117. https://doi.org/10.1038/nature21405

Fellström, B. (2001). Risk factors for and management of post-transplantation cardiovascular disease. *BioDrugs*, *15*(4), 261–278. https://doi.org/10.2165/00063030-200115040-00006/FIGURES/TAB2

Field, E. H., Matesic, D., Rigby, S., Fehr, T., Rouse, T., & Gao, Q. (2001). CD4+CD25+ regulatory cells in acquired MHC tolerance. *Immunological Reviews*, *182*(1), 99–112. https://doi.org/10.1034/J.1600-065X.2001.1820108.X

Fishman, J. A. (2007). Infection in solid-organ transplant recipients. *The New England Journal of*

Medicine, *357*(25), 2601–2614. https://doi.org/10.1056/NEJMRA064928

Fransson, M., Piras, E., Burman, J., Nilsson, B., Essand, M., Lu, B. F., Harris, R. A., Magnusson, P. U., Brittebo, E., & Loskog, A. S. I. (2012). CAR/FoxP3-engineered T regulatory cells target the CNS and suppress EAE upon intranasal delivery. *Journal of Neuroinflammation*, *9*(1), 1–12. https://doi.org/10.1186/1742-2094-9-112/FIGURES/6

Galetto, R. (2015a). *Cd123 specific chimeric antigen receptors for cancer immunotherapy*.

Galetto, R. (2015b). *Bcma (cd269) specific chimeric antigen receptors for cancer immunotherapy*. https://doi.org/10.1158/1078-0432.CCR-12-2422

Ganini, D., Leinisch, F., Kumar, A., Jiang, J. J., Tokar, E. J., Malone, C. C., Petrovich, R. M., & Mason, R. P. (2017). Fluorescent proteins such as eGFP lead to catalytic oxidative stress in cells. *Redox Biology*, *12*, 462–468. https://doi.org/10.1016/J.REDOX.2017.03.002

Goto, H., Yang, B., Petersen, D., Pepper, K. A., Alfaro, P. A., Kohn, D. B., & Reynolds, C. P. (2003). Transduction of green fluorescent protein increased oxidative stress and enhanced sensitivity to cytotoxic drugs in neuroblastoma cell lines. *Molecular Cancer Therapeutics*, *2*(9), 911–917. http://intl-mct.aacrjournals.org/cgi/content/full/2/9/911

Gross, G., Waks, T., & Eshhar, Z. (1989). Expression of immunoglobulin-T-cell receptor chimeric molecules as functional receptors with antibody-type specificity. *Proceedings of the National Academy of Sciences*, *86*(24), 10024–10028. https://doi.org/10.1073/PNAS.86.24.10024

Grossman, W. J., Verbsky, J. W., Barchet, W., Colonna, M., Atkinson, J. P., & Ley, T. J. (2004). Human T Regulatory Cells Can Use the Perforin Pathway to Cause Autologous Target Cell Death. *Immunity*, *21*(4), 589–601. https://doi.org/10.1016/J.IMMUNI.2004.09.002

Guedan, S., Posey, A. D., Shaw, C., Wing, A., Da, T., Patel, P. R., McGettigan, S. E., Casado-Medrano, V., Kawalekar, O. U., Uribe-Herranz, M., Song, D., Melenhorst, J. J., Lacey, S. F., Scholler, J., Keith, B., Young, R. M., & June, C. H. (2018). Enhancing CAR T cell persistence through ICOS and 4-1BB costimulation. *JCI Insight*, *3*(1). https://doi.org/10.1172/JCI.INSIGHT.96976

Hadjantonakis, A. K., & Nagy, A. (2000). The color of mice: in the light of GFP-variant reporters.

Histochemistry and Cell Biology 2000 115:1, *115*(1), 49–58. https://doi.org/10.1007/S004180000233

Hakamata, Y., Tahara, K., Uchida, H., Sakuma, Y., Nakamura, M., Kume, A., Murakami, T., Takahashi, M., Takahashi, R., Hirabayashi, M., Ueda, M., Miyoshi, I., Kasai, N., & Kobayashi, E. (2001). Green Fluorescent Protein-Transgenic Rat: A Tool for Organ Transplantation Research. *Biochemical and Biophysical Research Communications*, *286*(4), 779–785. https://doi.org/10.1006/BBRC.2001.5452

Hamada, M., Nishio, N., Okuno, Y., Suzuki, S., Kawashima, N., Muramatsu, H., Tsubota, S., Wilson, M. H., Morita, D., Kataoka, S., Ichikawa, D., Murakami, N., Taniguchi, R., Suzuki, K., Kojima, D., Sekiya, Y., Nishikawa, E., Narita, A., Hama, A., … Takahashi, Y. (2018). Integration Mapping of piggyBac-Mediated CD19 Chimeric Antigen Receptor T Cells Analyzed by Novel Tagmentation-Assisted PCR. *EBioMedicine*, *34*, 18–26. https://doi.org/10.1016/J.EBIOM.2018.07.008

Harden, P. N., Game, D. S., Sawitzki, B., Van der Net, J. B., Hester, J., Bushell, A., Issa, F., Brook, M. O., Alzhrani, A., Schlickeiser, S., Scotta, C., Petchey, W., Streitz, M., Blancho, G., Tang, Q., Markmann, J., Lechler, R. I., Roberts, I. S. D., Friend, P. J., … Lombardi, G. (2021). Feasibility, long-term safety, and immune monitoring of regulatory T cell therapy in living donor kidney transplant recipients. *American Journal of Transplantation*, *21*(4), 1603–1611. https://doi.org/10.1111/AJT.16395

Hayden, P. J., Sirait, T., Koster, L., Snowden, J. A., & Yakoub-Agha, I. (2019). An international survey on the management of patients receiving CAR T-cell therapy for haematological malignancies on behalf of the Chronic Malignancies Working Party of EBMT. *Current Research in Translational Medicine*, *67*(3), 79–88. https://doi.org/10.1016/J.RETRAM.2019.05.002

Hoek, K. L., Greer, M. J., McClanahan, K. G., Nazmi, A., Piazuelo, M. B., Singh, K., Wilson, K. T., & Olivares-Villagómez, D. (2021). Granzyme B prevents aberrant IL-17 production and intestinal pathogenicity in CD4+ T cells. *Mucosal Immunology 2021 14:5*, *14*(5), 1088–1099.

https://doi.org/10.1038/s41385-021-00427-1

Hoeppli, R. E., MacDonald, K. N., Leclair, P., Fung, V. C. W., Mojibian, M., Gillies, J., Rahavi, S. M. R., Campbell, A. I. M., Gandhi, S. K., Pesenacker, A. M., Reid, G., Lim, C. J., & Levings, M. K. (2019). Tailoring the homing capacity of human Tregs for directed migration to sites of Th1-inflammation or intestinal regions. *American Journal of Transplantation : Official Journal of the American Society of Transplantation and the American Society of Transplant Surgeons*, *19*(1), 62–76. https://doi.org/10.1111/AJT.14936

Hoffman, R. M. (2018). Visualization of GFP-Expressing Tumors and Metastasis In Vivo. *Https://Doi.Org/10.2144/01305bi01*, *30*(5), 1016–1026. https://doi.org/10.2144/01305BI01

Hori, S., Nomura, T., & Sakaguchi, S. (2003). Control of regulatory T cell development by the transcription factor Foxp3. *Science (New York, N.Y.)*, *299*(5609), 981–985. https://doi.org/10.1126/SCIENCE.1079490

Horwitz, D. A., Gray, J. D., & Zheng, S. G. (2002). The potential of human regulatory T cells generated ex vivo as a treatment for lupus and other chronic inflammatory diseases. *Arthritis Research*, *4*(4), 241–246. https://doi.org/10.1186/AR414/FIGURES/2

Hu, M., Wang, C., Zhang, G. Y., Saito, M., Wang, Y. M., Fernandez, M. A., Wang, Y., Wu, H., Hawthorne, W. J., Jones, C., O'Connell, P. J., Sparwasser, T., Bishop, G. A., Sharland, A. F., & Alexander, S. I. (2013). Infiltrating Foxp3+ Regulatory T Cells From Spontaneously Tolerant Kidney Allografts Demonstrate Donor-Specific Tolerance. *American Journal of Transplantation*, *13*(11), 2819–2830. https://doi.org/10.1111/AJT.12445

Hull, C. M., Nickolay, L. E., Estorninho, M., Richardson, M. W., Riley, J. L., Peakman, M., Maher, J., & Tree, T. I. M. (2017). Generation of human islet-specific regulatory T cells by TCR gene transfer. *Journal of Autoimmunity*, *79*, 63–73. https://doi.org/10.1016/J.JAUT.2017.01.001

Ikhtiar, A. M., Jazairi, B., Khansa, I., & Othman, A. (2018). HLA class i alleles frequencies in the Syrian population. *BMC Research Notes*, *11*(1), 1–8. https://doi.org/10.1186/S13104-018-3427-1/TABLES/4

Imura, Y., Ando, M., Kondo, T., Ito, M., & Yoshimura, A. (2020). CD19-targeted CAR regulatory T cells suppress B cell pathology without GvHD. *JCI Insight*, *5*(14). https://doi.org/10.1172/JCI.INSIGHT.136185

Issa, F., Hester, J., Goto, R., Nadig, S. N., Goodacre, T. E., & Wood, K. (2010). Ex vivo-expanded human regulatory T cells prevent the rejection of skin allografts in a humanized mouse model. *Transplantation*, *90*(12), 1321–1327. https://doi.org/10.1097/TP.0B013E3181FF8772

Jacob, J., Nadkarni, S., Volpe, A., Peng, Q., Tung, S. L., Hannen, R. F., Mohseni, Y. R., Scotta, C., Marelli-Berg, F. M., Lechler, R. I., Smyth, L. A., Fruhwirth, G. O., & Lombardi, G. (2021). Spatiotemporal in vivo tracking of polyclonal human regulatory T cells (Tregs) reveals a role for innate immune cells in Treg transplant recruitment. *Molecular Therapy. Methods & Clinical Development*, *20*, 324. https://doi.org/10.1016/J.OMTM.2020.12.003

Jones, S. C., Murphy, G. F., & Korngold, R. (2003). Post-hematopoietic cell transplantation control of graft-versus-host disease by donor CD4+25+ T cells to allow an effective graft-versus-leukemia response. *Biology of Blood and Marrow Transplantation*, *9*(4), 243–256. https://doi.org/10.1053/BBMT.2003.50027

Kaeuferle, T., Deisenberger, L., Jablonowski, L., Stief, T. A., Blaeschke, F., Willier, S., & Feuchtinger, T. (2020). CRISPR-Cas9-Mediated Glucocorticoid Resistance in Virus-Specific T Cells for Adoptive T Cell Therapy Posttransplantation. *Molecular Therapy*, *28*(9), 1965–1973. https://doi.org/10.1016/J.YMTHE.2020.06.002

Kim, Y. C., Zhang, A. H., Yoon, J., Culp, W. E., Lees, J. R., Wucherpfennig, K. W., & Scott, D. W. (2018). Engineered MBP-specific human Tregs ameliorate MOG-induced EAE through IL-2-triggered inhibition of effector T cells. *Journal of Autoimmunity*, *92*, 77–86. https://doi.org/10.1016/J.JAUT.2018.05.003

Koelsch, K. A., Wang, Y. J., Maier-Moore, J. S., Sawalha, A. H., & Wren, J. D. (2013). GFP Affects Human T Cell Activation and Cytokine Production following In Vitro Stimulation. *PLOS ONE*, *8*(4), e50068. https://doi.org/10.1371/JOURNAL.PONE.0050068

Kowolik, C. M., Topp, M. S., Gonzalez, S., Pfeiffer, T., Olivares, S., Gonzalez, N., Smith, D. D., Forman, S. J., Jensen, M. C., & Cooper, L. J. N. (2006). CD28 Costimulation Provided through a CD19-Specific Chimeric Antigen Receptor Enhances In vivo Persistence and Antitumor Efficacy of Adoptively Transferred T Cells. *Cancer Research*, *66*(22), 10995–11004. https://doi.org/10.1158/0008-5472.CAN-06-0160

Lamers, C. H. J., Willemsen, R., Van Elzakker, P., Van Steenbergen-Langeveld, S., Broertjes, M., Oosterwijk-Wakka, J., Oosterwijk, E., Sleijfer, S., Debets, R., & Gratama, J. W. (2011). Immune responses to transgene and retroviral vector in patients treated with ex vivo–engineered T cells. *Blood*, *117*(1), 72–82. https://doi.org/10.1182/BLOOD-2010-07-294520

Lee, S. K., Han, J., Piao, H., Shin, N., Jang, J. Y., Yan, J. J., Kim, H., Chung, J., & Yang, J. (2022). Anti-C4d chimeric antigen receptor regulatory T cells suppressed allograft rejection in ABO-incompatible heart transplantation. *Genes & Diseases*, *9*(1), 1–4. https://doi.org/10.1016/J.GENDIS.2021.07.001

Legut, M., Dolton, G., Mian, A. A., Ottmann, O. G., & Sewell, A. K. (2018). CRISPR-mediated TCR replacement generates superior anticancer transgenic T cells. *Blood*, *131*(3), 311–322. https://doi.org/10.1182/BLOOD-2017-05-787598

Li, P., Gao, Y., Cao, J., Wang, W., Chen, Y., Zhang, G., Robson, S. C., Wu, Y., & Yang, J. (2015). CD39+ regulatory T cells attenuate allergic airway inflammation. *Clinical & Experimental Allergy*, *45*(6), 1126–1137. https://doi.org/10.1111/CEA.12521

Lippincott-Schwartz, J., & Patterson, G. H. (2003). Development and use of fluorescent protein markers in living cells. *Science*, *300*(5616), 87–91. https://doi.org/10.1126/SCIENCE.1082520/SUPPL_FILE/LIPPINCOTTSCHWARTZ.SOM.PDF

Luo, M., Embree, J., Ramdahin, S., Ndinya-Achola, J., Njenga, S., Bwayo, J. B., Pan, S., Mao, X., Cheang, M., Stuart, T., Brunham, R. C., & Plummer, F. A. (2002). HLA-A and HLA-B in Kenya, Africa: </br>Allele frequencies and identification of </br>HLA-B*1567 and HLA-B*4426. *Tissue Antigens*, *59*(5), 370–380. https://doi.org/10.1034/J.1399-0039.2002.590503.X

MacDonald, K. G., Hoeppli, R. E., Huang, Q., Gillies, J., Luciani, D. S., Orban, P. C., Broady, R., & Levings, M. K. (2016). Alloantigen-specific regulatory T cells generated with a chimeric antigen receptor. *Journal of Clinical Investigation*, *126*(4), 1413–1424. https://doi.org/10.1172/JCI82771

Marek-Trzonkowska, N., Myśliwiec, M., Dobyszuk, A., Grabowska, M., Derkowska, I., Juścińska, J., Owczuk, R., Szadkowska, A., Witkowski, P., Młynarski, W., Jarosz-Chobot, P., Bossowski, A., Siebert, J., & Trzonkowski, P. (2014). Therapy of type 1 diabetes with CD4+CD25highCD127-regulatory T cells prolongs survival of pancreatic islets — Results of one year follow-up. *Clinical Immunology*, *153*(1), 23–30. https://doi.org/10.1016/J.CLIM.2014.03.016

Martin, A., Daris, M., Johnston, J. A., & Cui, J. (2021). HLA-A*02:01-directed chimeric antigen receptor/forkhead box P3-engineered CD4+ T cells adopt a regulatory phenotype and suppress established graft-versus-host disease. *Cytotherapy*, *23*(2), 131–136. https://doi.org/10.1016/j.jcyt.2020.10.002

Mathew, J. M., H-Voss, J., LeFever, A., Konieczna, I., Stratton, C., He, J., Huang, X., Gallon, L., Skaro, A., Ansari, M. J., & Leventhal, J. R. (2018). A Phase I Clinical Trial with Ex Vivo Expanded Recipient Regulatory T cells in Living Donor Kidney Transplants. *Scientific Reports 2018 8:1*, *8*(1), 1–12. https://doi.org/10.1038/s41598-018-25574-7

Maude, S. L., Laetsch, T. W., Buechner, J., Rives, S., Boyer, M., Bittencourt, H., Bader, P., Verneris, M. R., Stefanski, H. E., Myers, G. D., Qayed, M., De Moerloose, B., Hiramatsu, H., Schlis, K., Davis, K. L., Martin, P. L., Nemecek, E. R., Yanik, G. A., Peters, C., … Grupp, S. A. (2018). Tisagenlecleucel in Children and Young Adults with B-Cell Lymphoblastic Leukemia. *New England Journal of Medicine*, *378*(5), 439–448. https://doi.org/10.1056/NEJMOA1709866/SUPPL_FILE/NEJMOA1709866_DISCLOSURES.PDF

McGuinness, R. P., Ge, Y., Patel, S. D., Kashmiri, S. V. S., Lee, H. S., Hand, P. H., Schlom, J., Finer, M. H., & McArthur, J. G. (2004). Anti-Tumor Activity of Human T Cells Expressing the CC49-zeta Chimeric Immune Receptor. *Https://Home.Liebertpub.Com/Hum*, *10*(2), 165–173.

https://doi.org/10.1089/10430349950018968

Mellor, A. L., Munn, D., Chandler, P., Keskin, D., Johnson, T., Marshall, B., Jhaver, K., & Baban, B. (2003). Tryptophan catabolism and T cell responses. *Advances in Experimental Medicine and Biology*, *527*, 27–35. https://doi.org/10.1007/978-1-4615-0135-0_3

Miller, L. W. (2002). Cardiovascular Toxicities of Immunosuppressive Agents. *American Journal of Transplantation*, *2*(9), 807–818. https://doi.org/10.1034/J.1600-6143.2002.20902.X

Mittal, A., & Colegio, O. R. (2017). Skin Cancers in Organ Transplant Recipients. *American Journal of Transplantation*, *17*(10), 2509–2530. https://doi.org/10.1111/AJT.14382

Moreb, J. S., & Chang, L.-J. (2015). *Car based immunotherapy*.

Mothe, A. J., Kulbatski, I., Van Bendegem, R. L., Lee, L., Kobayashi, E., Keating, A., & Tator, C. H. (2005). Analysis of green fluorescent protein expression in transgenic rats for tracking transplanted neural stem/progenitor cells. *Journal of Histochemistry and Cytochemistry*, *53*(10), 1215–1226. https://doi.org/10.1369/JHC.5A6639.2005/ASSET/IMAGES/LARGE/10.1369_JHC.5A6639.2005-FIG2.JPEG

Müller, T., Uherek, C., Maki, G., Chow, K. U., Schimpf, A., Klingemann, H. G., Tonn, T., & Wels, W. S. (2008). Expression of a CD20-specific chimeric antigen receptor enhances cytotoxic activity of NK cells and overcomes NK-resistance of lymphoma and leukemia cells. *Cancer Immunology, Immunotherapy*, *57*(3), 411–423. https://doi.org/10.1007/S00262-007-0383-3/FIGURES/7

Muller, Y. D., Ferreira, L. M. R., Ronin, E., Ho, P., Nguyen, V., Faleo, G., Zhou, Y., Lee, K., Leung, K. K., Skartsis, N., Kaul, A. M., Mulder, A., Claas, F. H. J., Wells, J. A., Bluestone, J. A., & Tang, Q. (2021). Precision Engineering of an Anti-HLA-A2 Chimeric Antigen Receptor in Regulatory T Cells for Transplant Immune Tolerance. *Frontiers in Immunology*, *12*, 3717. https://doi.org/10.3389/FIMMU.2021.686439/BIBTEX

Nakamura, K., Kitani, A., & Strober, W. (2001). Cell Contact–Dependent Immunosuppression by

Cd4+Cd25+Regulatory T Cells Is Mediated by Cell Surface–Bound Transforming Growth Factor β. *Journal of Experimental Medicine*, *194*(5), 629–644. https://doi.org/10.1084/JEM.194.5.629

Neelapu, S. S., Locke, F. L., Bartlett, N. L., Lekakis, L. J., Miklos, D. B., Jacobson, C. A., Braunschweig, I., Oluwole, O. O., Siddiqi, T., Lin, Y., Timmerman, J. M., Stiff, P. J., Friedberg, J. W., Flinn, I. W., Goy, A., Hill, B. T., Smith, M. R., Deol, A., Farooq, U., … Go, W. Y. (2017). Axicabtagene Ciloleucel CAR T-Cell Therapy in Refractory Large B-Cell Lymphoma. *New England Journal of Medicine*, *377*(26), 2531–2544. https://doi.org/10.1056/NEJMOA1707447/SUPPL_FILE/NEJMOA1707447_DISCLOSURES.PDF

Norrman, K., Fischer, Y., Bonnamy, B., Sand, F. W., Ravassard, P., & Semb, H. (2010). Quantitative Comparison of Constitutive Promoters in Human ES cells. *PLOS ONE*, *5*(8), e12413. https://doi.org/10.1371/JOURNAL.PONE.0012413

Noyan, F., Zimmermann, K., Hardtke-Wolenski, M., Knoefel, A., Schulde, E., Geffers, R., Hust, M., Huehn, J., Galla, M., Morgan, M., Jokuszies, A., Manns, M. P., & Jaeckel, E. (2017). Prevention of Allograft Rejection by Use of Regulatory T Cells With an MHC-Specific Chimeric Antigen Receptor. *American Journal of Transplantation*, *17*(4), 917–930. https://doi.org/10.1111/ajt.14175

Odé, Z., Condori, J., Peterson, N., Zhou, S., & Krenciute, G. (2020). CRISPR-Mediated Non-Viral Site-Specific Gene Integration and Expression in T Cells: Protocol and Application for T-Cell Therapy. *Cancers 2020, Vol. 12, Page 1704*, *12*(6), 1704. https://doi.org/10.3390/CANCERS12061704

Okabe, M., Ikawa, M., Kominami, K., Nakanishi, T., & Nishimune, Y. (1997). 'Green mice' as a source of ubiquitous green cells. *FEBS Letters*, *407*(3), 313–319. https://doi.org/10.1016/S0014-5793(97)00313-X

Onishi, Y., Fehervari, Z., Yamaguchi, T., & Sakaguchi, S. (2008). Foxp3+ natural regulatory T cells preferentially form aggregates on dendritic cells in vitro and actively inhibit their maturation.

Proceedings of the National Academy of Sciences of the United States of America, *105*(29), 10113–10118. https://doi.org/10.1073/PNAS.0711106105/SUPPL_FILE/0711106105SI.PDF

Pandiyan, P., Zheng, L., Ishihara, S., Reed, J., & Lenardo, M. J. (2007). CD4+CD25+Foxp3+ regulatory T cells induce cytokine deprivation–mediated apoptosis of effector CD4+ T cells. *Nature Immunology 2007 8:12*, *8*(12), 1353–1362. https://doi.org/10.1038/ni1536

Perez-Cunningham, J., Boyer, S. W., Landon, M., & Forsberg, E. C. (2016). Hematopoietic stem cell-specific GFP-expressing transgenic mice generated by genetic excision of a pan-hematopoietic reporter gene. *Experimental Hematology*, *44*(8), 755-764.e1. https://doi.org/10.1016/J.EXPHEM.2016.05.002

Petzold, C., Steinbronn, N., Gereke, M., Strasser, R. H., Sparwasser, T., Bruder, D., Geffers, R., Schallenberg, S., & Kretschmer, K. (2014). Fluorochrome-based definition of naturally occurring Foxp3+ regulatory T cells of intra- and extrathymic origin. *European Journal of Immunology*, *44*(12), 3632–3645. https://doi.org/10.1002/EJI.201444750

Piccirillo, C. A., Tritt, M., Sgouroudis, E., Albanese, A., Pyzik, M., & Hay, V. (2005). Control of Type 1 Autoimmune Diabetes by Naturally Occurring CD4+CD25+ Regulatory T Lymphocytes in Neonatal NOD Mice. *Annals of the New York Academy of Sciences*, *1051*(1), 72–87. https://doi.org/10.1196/ANNALS.1361.048

Pierini, A., Iliopoulou, B. P., Peiris, H., Pérez-Cruz, M., Baker, J., Hsu, K., Gu, X., Zheng, P. P., Erkers, T., Tang, S. W., Strober, W., Alvarez, M., Ring, A., Velardi, A., Negrin, R. S., Kim, S. K., & Meyer, E. H. (2017). T cells expressing chimeric antigen receptor promote immune tolerance. *JCI Insight*, *2*(20). https://doi.org/10.1172/JCI.INSIGHT.92865

Pohl, A. D. P., Venkatesha, S. H., Zhang, A. H., & Scott, D. W. (2020). Suppression of FVIII-Specific Memory B Cells by Chimeric BAR Receptor-Engineered Natural Regulatory T Cells. *Frontiers in Immunology*, *11*, 693. https://doi.org/10.3389/FIMMU.2020.00693/BIBTEX

Progatzky, F., Dallman, M. J., & Celso, C. Lo. (2013). From seeing to believing: labelling strategies for in vivo cell-tracking experiments. *Interface Focus*, *3*(3).

https://doi.org/10.1098/RSFS.2013.0001

Ramos, C. A., Rouce, R., Robertson, C. S., Reyna, A., Narala, N., Vyas, G., Mehta, B., Zhang, H., Dakhova, O., Carrum, G., Kamble, R. T., Gee, A. P., Mei, Z., Wu, M. F., Liu, H., Grilley, B., Rooney, C. M., Heslop, H. E., Brenner, M. K., … Dotti, G. (2018). In Vivo Fate and Activity of Second- versus Third-Generation CD19-Specific CAR-T Cells in B Cell Non-Hodgkin's Lymphomas. *Molecular Therapy*, *26*(12), 2727–2737. https://doi.org/10.1016/j.ymthe.2018.09.009

Rondon, I., Roell, M., & Bedinger, D. (2009). *Novel triple tag sequence and methods of use thereof*.

Roth, T. L., Puig-Saus, C., Yu, R., Shifrut, E., Carnevale, J., Li, P. J., Hiatt, J., Saco, J., Krystofinski, P., Li, H., Tobin, V., Nguyen, D. N., Lee, M. R., Putnam, A. L., Ferris, A. L., Chen, J. W., Schickel, J. N., Pellerin, L., Carmody, D., … Marson, A. (2018). Reprogramming human T cell function and specificity with non-viral genome targeting. *Nature 2018 559:7714*, *559*(7714), 405–409. https://doi.org/10.1038/s41586-018-0326-5

Sagoo, P., Ali, N., Garg, G., Nestle, F. O., Lechler, R. I., & Lombardi, G. (2011). Human regulatory T cells with alloantigen specificity are more potent inhibitors of alloimmune skin graft damage than polyclonal regulatory T cells. *Science Translational Medicine*, *3*(83). https://doi.org/10.1126/SCITRANSLMED.3002076

Saito, P. K., Yamakawa, R. H., Noguti, E. N., Bedendo, G. B., Júnior, W. V. da S., Yamada, S. S., & Borelli, S. D. (2016). HLA-A, HLA-B, and HLA-DRB1 Allele and Haplotype Frequencies in Renal Transplant Candidates in a Population in Southern Brazil. *Journal of Clinical Laboratory Analysis*, *30*(3), 258–265. https://doi.org/10.1002/JCLA.21846

Saito, P. K., Yamakawa, R. H., Noguti, E. N., Bedendo, G. B., Veríssimo Da Silva, W., Ergio, S. ´, Yamada, S., & Donizete Borelli, S. (n.d.). *HLA-A, HLA-B, and HLA-DRB1 Allele and Haplotype Frequencies in Renal Transplant Candidates in a Population in Southern Brazil*. https://doi.org/10.1002/jcla.21846

Sakaguchi, S., Sakaguchi, N., Asano, M., Itoh, M., & Toda, M. (1995). *Immunologic self-tolerance*

maintained by activated T cells expressing IL-2 receptor alpha-chains (CD25). Breakdown of a single mechanism of self-tolerance causes various autoimmune diseases. http://www.jimmunol.org/content/155/3/1151

Salter, A. I., Ivey, R. G., Kennedy, J. J., Voillet, V., Rajan, A., Alderman, E. J., Voytovich, U. J., Lin, C., Sommermeyer, D., Liu, L., Whiteaker, J. R., Gottardo, R., Paulovich, A. G., & Riddell, S. R. (2018). Phosphoproteomic analysis of chimeric antigen receptor signaling reveals kinetic and quantitative differences that affect cell function. *Science Signaling*, *11*(544). https://doi.org/10.1126/SCISIGNAL.AAT6753/SUPPL_FILE/AAT6753_TABLE_S5.XLSX

Sanchez-Mazas, A., Nunes, J. M., Middleton, D., Sauter, J., Buhler, S., McCabe, A., Hofmann, J., Baier, D. M., Schmidt, A. H., Nicoloso, G., Andreani, M., Grubic, Z., Tiercy, J. M., & Fleischhauer, K. (2017). Common and well-documented HLA alleles over all of Europe and within European sub-regions: A catalogue from the European Federation for Immunogenetics. *HLA*, *89*(2), 104–113. https://doi.org/10.1111/TAN.12956

Sarkar, D., Biswas, M., Liao, G., Seay, H. R., Perrin, G. Q., Markusic, D. M., Hoffman, B. E., Brusko, T. M., Terhorst, C., & Herzog, R. W. (2014). Ex vivo expanded autologous polyclonal regulatory T cells suppress inhibitor formation in hemophilia. *Molecular Therapy - Methods & Clinical Development*, *1*, 14030. https://doi.org/10.1038/MTM.2014.30

Sawitzki, B., Harden, P. N., Reinke, P., Moreau, A., Hutchinson, J. A., Game, D. S., Tang, Q., Guinan, E. C., Battaglia, M., Burlingham, W. J., Roberts, I. S. D., Streitz, M., Josien, R., Böger, C. A., Scottà, C., Markmann, J. F., Hester, J. L., Juerchott, K., Braudeau, C., … Geissler, E. K. (2020). Regulatory cell therapy in kidney transplantation (The ONE Study): a harmonised design and analysis of seven non-randomised, single-arm, phase 1/2A trials. *The Lancet*, *395*(10237), 1627–1639. https://doi.org/10.1016/S0140-6736(20)30167-7

Schaefer, B. C., Schaefer, M. L., Kappler, J. W., Marrack, P., & Kedl, R. M. (2001). Observation of Antigen-Dependent CD8+ T-Cell/ Dendritic Cell Interactions in Vivo. *Cellular Immunology*, *214*(2), 110–122. https://doi.org/10.1006/CIMM.2001.1895

Schmidt, A., Oberle, N., & Krammer, P. H. (2012). Molecular mechanisms oftreg-mediatedt cell suppression. *Frontiers in Immunology*, *3*(MAR), 51. https://doi.org/10.3389/FIMMU.2012.00051/BIBTEX

Schreeb, K., Culme-Seymour, E., Ridha, E., Dumont, C., Atkinson, G., Hsu, B., & Reinke, P. (2022). Study Design: Human Leukocyte Antigen Class I Molecule A∗02-Chimeric Antigen Receptor Regulatory T Cells in Renal Transplantation. *Kidney International Reports*, *7*(6), 1258–1267. https://doi.org/10.1016/j.ekir.2022.03.030

Shao, C., Chen, Y., Nakao, T., Amouzegar, A., Yin, J., Tahvildari, M., Lužnik, Z., Chauhan, S. K., & Dana, R. (2019). Local Delivery of Regulatory T Cells Promotes Corneal Allograft Survival. *Transplantation*, *103*(1), 182–190. https://doi.org/10.1097/TP.0000000000002442

Shi, L., Mai, S., Israels, S., Browne, K., Trapani, J. A., & Greenberg, A. H. (1997). Granzyme B (GraB) Autonomously Crosses the Cell Membrane and Perforin Initiates Apoptosis and GraB Nuclear Localization. *Journal of Experimental Medicine*, *185*(5), 855–866. https://doi.org/10.1084/JEM.185.5.855

Sicard, A., Lamarche, C., Speck, M., Wong, M., Rosado-Sánchez, I., Blois, M., Glaichenhaus, N., Mojibian, M., & Levings, M. K. (2020). Donor-specific chimeric antigen receptor Tregs limit rejection in naive but not sensitized allograft recipients. *American Journal of Transplantation*, *20*(6), 1562–1573. https://doi.org/10.1111/AJT.15787

Skuljec, J., Chmielewski, M., Happle, C., Habener, A., Busse, M., Abken, H., & Hansen, G. (2017). Chimeric antigen receptor-redirected regulatory T cells suppress experimental allergic airway inflammation, a model of asthma. *Frontiers in Immunology*, *8*(SEP), 1125. https://doi.org/10.3389/FIMMU.2017.01125/BIBTEX

Soboleski, M. R., Oaks, J., & Halford, W. P. (2005). Green fluorescent protein is a quantitative reporter of gene expression in individual eukaryotic cells. *The FASEB Journal*, *19*(3), 1–20. https://doi.org/10.1096/FJ.04-3180FJE

Song, D. G., Ye, Q., Poussin, M., Harms, G. M., Figini, M., & Powell, D. J. (2012). CD27 costimulation

augments the survival and antitumor activity of redirected human T cells in vivo. *Blood*, *119*(3), 696–706. https://doi.org/10.1182/BLOOD-2011-03-344275

Stripecke, R., Del Carmen Villacres, M., Skelton, D. C., Satake, N., Halene, S., & Kohn, D. B. (1999). Immune response to green fluorescent protein: implications for gene therapy. *Gene Therapy 1999 6:7*, *6*(7), 1305–1312. https://doi.org/10.1038/sj.gt.3300951

Tan, Y., Abdulreda, M. H., Cruz-Guilloty, F., Cutrufello, N., Shishido, A., Martinez, R. E., Duffort, S., Xia, X., Echegaray-Mendez, J., Levy, R. B., Berggren, P. O., & Perez, V. L. (2013). Role of T Cell Recruitment and Chemokine-Regulated Intra-Graft T Cell Motility Patterns in Corneal Allograft Rejection. *American Journal of Transplantation*, *13*(6), 1461–1473. https://doi.org/10.1111/AJT.12228

Tauro, S., Nguyen, P., Li, B., & Geiger, T. L. (2013). Diversification and senescence of Foxp3+ regulatory T cells during experimental autoimmune encephalomyelitis. *European Journal of Immunology*, *43*(5), 1195–1207. https://doi.org/10.1002/EJI.201242881

Tenspolde, M., Zimmermann, K., Weber, L. C., Hapke, M., Lieber, M., Dywicki, J., Frenzel, A., Hust, M., Galla, M., Buitrago-Molina, L. E., Manns, M. P., Jaeckel, E., & Hardtke-Wolenski, M. (2019). Regulatory T cells engineered with a novel insulin-specific chimeric antigen receptor as a candidate immunotherapy for type 1 diabetes. *Journal of Autoimmunity*, *103*, 102289. https://doi.org/10.1016/J.JAUT.2019.05.017

Tischner, D., Weishaupt, A., Van Den Brandt, J., Müller, N., Beyersdorf, N., Ip, C. W., Toyka, K. V., Hünig, T., Gold, R., Kerkau, T., & Reichardt, H. M. (2006). Polyclonal expansion of regulatory T cells interferes with effector cell migration in a model of multiple sclerosis. *Brain*, *129*(10), 2635–2647. https://doi.org/10.1093/BRAIN/AWL213

Tsang, J. Y. S., Tanriver, Y., Jiang, S., Xue, S. A., Ratnasothy, K., Chen, D., Stauss, H. J., Bucy, R. P., Lombardi, G., & Lechler, R. (2008). Conferring indirect allospecificity on CD4+CD25+ Tregs by TCR gene transfer favors transplantation tolerance in mice. *The Journal of Clinical Investigation*, *118*(11), 3619–3628. https://doi.org/10.1172/JCI33185

Wang Xiuli, & Forman Stephen J. (2015). *CS1 targeted chimeric antigen receptor-modified T cells*.

Weinkove, R., George, P., Dasyam, N., & McLellan, A. D. (2019). Selecting costimulatory domains for chimeric antigen receptors: functional and clinical considerations. *Clinical & Translational Immunology*, *8*(5), e1049. https://doi.org/10.1002/CTI2.1049

Weir, M. R., Burgess, E. D., Cooper, J. E., Fenves, A. Z., Goldsmith, D., McKay, D., Mehrotra, A., Mitsnefes, M. M., Sica, D. A., & Taler, S. J. (2015). Assessment and Management of Hypertension in Transplant Patients. *Journal of the American Society of Nephrology*, *26*(6), 1248–1260. https://doi.org/10.1681/ASN.2014080834

Wright, G. P., Notley, C. A., Xue, S. A., Bendle, G. M., Holler, A., Schumacher, T. N., Ehrenstein, M. R., & Stauss, H. J. (2009). Adoptive therapy with redirected primary regulatory T cells results in antigen-specific suppression of arthritis. *Proceedings of the National Academy of Sciences of the United States of America*, *106*(45), 19078–19083. https://doi.org/10.1073/PNAS.0907396106/SUPPL_FILE/0907396106SI.PDF

Wright, S., Hennessy, C., Hester, J., & Issa, F. (2022). Chimeric Antigen Receptors and Regulatory T Cells: The Potential for HLA-Specific Immunosuppression in Transplantation. *Engineering*, *10*, 30–43. https://doi.org/10.1016/J.ENG.2021.10.018

Wu, D. C., Hester, J., Nadig, S. N., Zhang, W., Trzonkowski, P., Gray, D., Hughes, S., Johnson, P., & Wood, K. J. (2013). Ex vivo expanded human regulatory T cells can prolong survival of a human islet allograft in a humanized mouse model. *Transplantation*, *96*(8), 707–716. https://doi.org/10.1097/TP.0B013E31829FA271

Xia, N., Jiao, J., Tang, T. T., Lv, B. J., Lu, Y. Z., Wang, K. J., Zhu, Z. F., Mao, X. B., Nie, S. F., Wang, Q., Tu, X., Xiao, H., Liao, Y. H., Shi, G. P., & Cheng, X. (2015). Activated regulatory T-cells attenuate myocardial ischaemia/reperfusion injury through a CD39-dependent mechanism. *Clinical Science*, *128*(10), 679–693. https://doi.org/10.1042/CS20140672

Yang, M., Baranov, E., Jiang, P., Sun, F. X., Li, X. M., Li, L., Hasegawa, S., Bouvet, M., Al-Tuwaijri, M., Chishima, T., Shimada, H., Moossa, A. R., Penman, S., & Hoffman, R. M. (2000). Whole-body

optical imaging of green fluorescent protein-expressing tumors and metastases. *Proceedings of the National Academy of Sciences of the United States of America*, *97*(3), 1206–1211. https://doi.org/10.1073/PNAS.97.3.1206/ASSET/84D7A2F6-D681-4E5C-A7EB-CCCDB06F72DC/ASSETS/GRAPHIC/PQ0205158006.JPEG

Yang, M., Jiang, P., & Hoffman, R. M. (2007). Whole-Body Subcellular Multicolor Imaging of Tumor-Host Interaction and Drug Response in Real Time. *Cancer Research*, *67*(11), 5195–5200. https://doi.org/10.1158/0008-5472.CAN-06-4590

Ye, K., Jin, S., & Schultz, J. S. (2004). Genetically Engineered Fluorescent Cell Marker for Labeling CD34+ Hematopoietic Stem Cells. *Biotechnology Progress*, *20*(2), 561–565. https://doi.org/10.1021/BP0342452

Yoon, J., Schmidt, A., Zhang, A. H., Königs, C., Kim, Y. C., & Scott, D. W. (2017). FVIII-specific human chimeric antigen receptor T-regulatory cells suppress T- and B-cell responses to FVIII. *Blood*, *129*(2), 238–245. https://doi.org/10.1182/BLOOD-2016-07-727834

Yu, Y. A., Oberg, K., Wang, G., & Szalay, A. A. (2003). Visualization of molecular and cellular events with green fluorescent proteins in developing embryos: a review. *Luminescence*, *18*(1), 1–18. https://doi.org/10.1002/BIO.701

Zhang, A.-H., Yoon, J., Kim, Y. C., & Scott, D. W. (2018). Targeting Antigen-Specific B Cells Using Antigen-Expressing Transduced Regulatory T Cells. *The Journal of Immunology*, *201*(5), 1434–1441. https://doi.org/10.4049/JIMMUNOL.1701800/-/DCSUPPLEMENTAL

Zhang, P., Tey, S.-K., Koyama, M., Kuns, R. D., Olver, S. D., Lineburg, K. E., Lor, M., Teal, B. E., Raffelt, N. C., Raju, J., Leveque, L., Markey, K. A., Varelias, A., Clouston, A. D., Lane, S. W., MacDonald, K. P. A., & Hill, G. R. (2013). Induced Regulatory T Cells Promote Tolerance When Stabilized by Rapamycin and IL-2 In Vivo. *The Journal of Immunology*, *191*(10), 5291–5303. https://doi.org/10.4049/JIMMUNOL.1301181

Zhang, Z., Qiu, S., Zhang, X., & Chen, W. (2018). Optimized DNA electroporation for primary human T cell engineering. *BMC Biotechnology*, *18*(1), 1–9. https://doi.org/10.1186/S12896-

018-0419-0/FIGURES/5

Zhao, D. M., Thornton, A. M., DiPaolo, R. J., & Shevach, E. M. (2006). Activated CD4+CD25+ T cells selectively kill B lymphocytes. *Blood*, *107*(10), 3925–3932. https://doi.org/10.1182/BLOOD-2005-11-4502

Zhao, Y., Zheng, Z., Cohen, C. J., Gattinoni, L., Palmer, D. C., Restifo, N. P., Rosenberg, S. A., & Morgan, R. A. (2006). High-Efficiency Transfection of Primary Human and Mouse T Lymphocytes Using RNA Electroporation. *Molecular Therapy*, *13*(1), 151–159. https://doi.org/10.1016/J.YMTHE.2005.07.688

Zhou, X.-Y., Zhu, F.-M., Li, J.-P., Mao, W., Zhang, D.-M., Liu, M.-L., Hei, A.-L., Dai, D.-P., Jiang, P., Shan, X.-Y., Zhang, B.-W., Zhu, C.-F., Shen, J., Deng, Z.-H., Wang, Z.-L., Yu, W.-J., Chen, Q., Qiao, Y.-H., Zhu, X.-M., … Cai, J.-P. (2015). High-Resolution Analyses of Human Leukocyte Antigens Allele and Haplotype Frequencies Based on 169,995 Volunteers from the China Bone Marrow Donor Registry Program. *PLOS ONE*, *10*(9), e0139485. https://doi.org/10.1371/journal.pone.0139485